การสังเคราะห์ พิสูจน์โครงสร้างและพอลิเมอไรเซชันของ
3,4-เอทิลีนไดออกซีไทโอฟีนที่มีการแทนที่ที่เอทิลีนบริดจ์

นายจิรศักดิ์ ชาพรมมา

SYNTHESIS, CHARACTERIZATION AND POLYMERIZATION OF
3,4-ETHYLENEDIOXYTHIOPHENE SUBSTITUTED AT ETHYLENE BRIDGE

Mr. Jirasak Chapromma

A Thesis Submitted in Partial Fulfillment of the Requirements
for the Degree of Master of Science Program in Chemistry
Department of Chemistry
Faculty of Science
Chulalongkorn University
Academic Year 2009

Thesis Title   SYNTHESIS, CHARACTERIZATION AND
                   POLYMERIZATION OF 3,4-ETHYLENEDIOXY
                   THIOPHENE SUBSTITUTED AT ETHYLENE BRIDGE

By   Mr. Jirasak Chapromma

Field of Study   Chemistry

Thesis Advisor   Assistant Professor Yongsak Sritana-anant, Ph.D.

Accepted by the Faculty of Science, Chulalongkorn University in Partial
Fulfillment of the Requirements for the Master's Degree

…………………………………………Dean of the Faculty of Science
(Professor Supot Hannongbua, Dr.rer.nat.)

THESIS COMMITTEE

………………………………………….. Chairman
(Assistant Professor Warinthorn Chavasiri, Ph.D.)

……………………………………….……. Thesis Advisor
(Assistant Professor Yongsak Sritana-anant, Ph.D.)

……………………………………….. Examiner
(Sumrit Wacharasindhu, Ph.D.)

……………………………………….. External Examiner
(Assistant Professor Ekasith Somsook, Ph.D.)

จิรศักดิ์ ชาพรมมา : การสังเคราะห์ พิสูจน์โครงสร้างและพอลิเมอไรเซชันของ
3,4-เอทิลีนไดออกซีไทโอฟีน ที่มีการแทนที่ที่เอทิลีนบริดจ์. (SYNTHESIS,
CHARACTERIZATION AND POLYMERIZATION OF 3,4-ETHYLENE
DIOXTHIOPHENE SUBSTITUTED AT ETHYLENE BRIDGE) อ.ที่ปรึกษา
วิทยานิพนธ์หลัก : ผู้ช่วยศาสตราจารย์ ดร.ยงศักดิ์ ศรีธนาอนันต์, 155 หน้า.

งานวิจัยนี้เป็นการสังเคราะห์ 3,4-เอทิลีนไดออกซีไทโอฟีน ที่มีการแทนที่ที่เอทิลีนบริดจ์
และอนุพันธ์ที่เกี่ยวข้องอื่นๆ ด้วยหลากหลายวิธี การสังเคราะห์ 3,4-ไดแอลคอกซีไทโอฟีน-2,5-ได
คาร์บอกซีเลต ชนิดใหม่ ด้วยปฏิกิริยา ดับเบิ้ล วิลเลียมสันอีเทอริฟิเคชันกับแอลคิลเฮไลด์ชนิด
ต่างๆ ได้ปริมาณของผลิตภัณฑ์ ต่างๆ กันออกไป หลังจากทำปฏิกิริยาดีคาร์บอกซีเลชัน พบว่าได้
สารชนิดใหม่ที่สามารถใช้เป็นมอนอเมอร์ได้ คือ ไวนิลอีดอท ปฏิกิริยาเฮโลจิเนชันด้วยเอ็นโบรโม
ซัคซินิไมด์ (เอ็นบีเอส) และ เอ็นคลอโรซัคซินิไมด์ (เอ็นซีเอส) กับอนุพันธ์ของไทโอฟีนชนิดต่างๆ
ได้ผลิตภัณฑ์ในปริมาณมากระหว่าง 80-99% ปฏิกิริยาทรานส์อีเทอริฟิเคชันของ 3,4-ไดเมทอกซี
ไทโอฟีน กับ ทรานส์-1,2-ไซโคลเฮกเซนไดออล ได้ผลิตภัณฑ์ 3,4-ไซโคลเฮกซิลีนไดออกซีไทโอฟีน
(ซีดอท) ถึง 86% ปฏิกิริยาพอลิเมอไรเซชันแบบเชื่อมต่อทางเคมีของซีดอทจะให้ผลิตภัณฑ์พอลิ
(3,4-ไซโคลเฮกซิลีนไดออกซีไทโอฟีน) (พีซีดอท) ในปริมาณ 69% ในขณะที่ใช้ 2,5-ไดโบรโม-3,4-
ไซโคลเฮกซิลีนไดออกซีไทโอฟีน สามารถเกิดปฏิกิริยาพอลิเมอไรเซชันแบบเฟสของแข็งได้พีซีดอท
เช่นเดียวกัน และวิเคราะห์โครงสร้างของพอลิเมอร์ด้วยเทคนิคเอ็นเอ็มอาร์ เอฟที-ไออาร์ เอสอีเอ็ม
ยูวี-วิซิเบิ้ล เอ็กซ์อาร์ดี มัลดิทอฟเอ็มเอส ทีจีเอ ดีเอสซีและเครื่องวัดการนำไฟฟ้าแบบโฟร์พ้อยท์
โพรบ พบว่าพีซีดอทที่ได้จากพอลิเมอไรเซชันแบบเฟสของแข็งที่อุณหภูมิ 120 องศาเซลเซียส เป็น
เวลา 24 ชั่วโมง แล้วเก็บไว้ที่อุณหภูมิห้องอีกเป็นเวลา 14 วัน จะมีค่าการนำไฟฟ้าสูงสุด คือ 131
ซีเมนส์ต่อเซนติเมตร

ภาควิชา........เคมี............ ลายมือชื่อนิสิต............................
สาขาวิชา........เคมี............ ลายมือชื่ออ.ที่ปรึกษาวิทยานิพนธ์หลัก............................
ปีการศึกษา........2552............

5072590123   : MAJOR CHEMISTRY

KEYWORDS : 3,4-ETHYLENEDIOXYTHIOPHENE / 3,4-DIALKOXY THIOPHENE / SOLID-STATE POLYMERIZATION / CONDUCTING POLYMER

JIRASAK CHAPROMMA : SYNTHESIS, CHARACTERIZATION AND POLYMERIZATION OF 3,4-ETHYLENEDIOXYTHIOPHENE SUBSTITUTED AT ETHYLENE BRIDGE. THESIS ADVISOR : ASST. PROF. YONGSAK SRITANA-ANANT, 155 pp.

Various routes to synthesis of EDOT substituted at ethylene bridge and other related derivatives have been attempted. Synthesis of new diethyl 3,4-dialkoxythiophene-2,5-dicarboxylate derivatives using double Williamson etherifications of the corresponding alkyl halides yielded the desired thiophene dicarboxylate precursors in range of yields. Decarboxylation obtained a new potential monomer (Vinyl-EDOT). Halogenation of various thiophene derivatives with N-bromosuccinimide (NBS) or N-chlorosuccinimide (NCS) have been accomplished in excellent yields (80-99%). Transetherification of 3,4-dimethoxy-thiophene with $trans$-1,2-cyclohexanediol to obtain 3,4-cyclohexylenedioxy-thiophene (CDOT) in good yield (86%). This monomer was subjected to oxidative polymerization to give poly(3,4-cyclohexylenedioxythiophene) (PCDOT) in 69%. 2,5-Dibromo-3,4-cyclohexylenedioxythiophene (DBCDOT) could be polymerized in solid state which also gave the polymer PCDOT. Characterizations of the resulting polymer were performed by NMR, FT-IR, SEM, UV-Vis, XRD, MALDI-TOF MS, TGA, DSC and Four-point-probe conductometer. Solid-state polymerized PCDOT heated at 120 ºC for 24 hours and stored at room temperature for 14 days gave the best value of conductivity up to 131 S/cm.

Department : ....CHEMISTRY.......   Student's Signature ....

Field of Study : ....CHEMISTRY.......   Advisor's Signature ....

Academic Year :..........2009.............

ACKNOWLEDGEMENTS

CONTENTS

Page

LIST OF FIGURES

Figure **Page**

LIST OF TABLES

LIST OF SCHEMES

LIST OF ABBREVIATIONS

^{13}C-NMR : carbon-13 nuclear magnetic resonance spectroscopy

^{1}H-NMR : proton nuclear magnetic resonance spectroscopy

AlCl$_3$: anhydrous aluminum chloride

cm : centimeter

cm^{-1} : unit of wavenumber (IR)

CH$_3$COOH : acetic acid

CDOT : 3,4-(cyclohexyliden-1,2-dioxy)thiophene or

3,4-cyclohexylenedioxythiophene

d : doublet (NMR), day (s)

DBCDOT : 2,5-dibromo-3,4-(cyclohexyliden-1,2-dioxy)thiophene or

2,5-dibromo-3,4-cyclohexylenedioxythiophene

DBEDOT : 2,5-dibromo-3,4-ethylenedioxythiophene

DBDMT : 2,5-dibromo-3,4-dimethoxythiophene

DMT : 3,4-dimethoxythiophene

EDOT : 3,4-ethylenedioxythiophene

DMF : *N,N*-dimethylformamide

DMSO-d_6 : hexadeuterated dimethyl sulfoxide

DSC : differential scanning calorimetry

DTG : derivative thermal gravimetric analysis

equiv : equivalent (s)

EtOAc : ethyl acetate

EtOH : ethanol

eV : electron volt

FeCl$_3$: anhydrous ferric chloride

GPC : gel permeation chromatography

g : gram (s)

HH : head to head

h : hour (s)

HT : head to tail

HCl	: hydrochloric acid
HOMO	: highest occupied molecular orbital
Hz	: hertz (s)
IR	: infrared spectroscopy
J	: coupling constant
LED	: light emitting diode
LUMO	: lowest unoccupied molecular orbital
M	: molar (s)
m	: multiplet (NMR)
MeOH	: methanol
min	: minute
mg	: milligram (s)
mL	: milliliter (s)
mmol	: millimole (s)
M_n	: number average molecular weight
mM	: millimolar
m.p.	: melting point
m/z	: mass per charge ratio (s)
MALDI-TOF	: matrix assisted laser desorption ionisation time-of-flight mass spectrometry
MS	: mass spectrometry
NaOH	: sodium hydroxide
NBS	: *N*-bromosuccinimide
NCS	: *N*-chlorosuccinimide
nm	: nanometer (s)
ºC	: degree Celsius
ppm	: parts per million (unit of chemical shift)
PCDOT	: poly(3,4-(cyclohexyliden-1,2-dioxy)thiophene) or poly(3,4-cyclohexylenedioxythiophene)
PDMT	: poly(3,4-dimethoxythiophene)
P3AT	: poly(3-alkylthiophene)
P3HT	: poly(3-hexylthiophene)

PT	: polythiophene
q	: quartet (NMR)
RT, rt	: room temperature
s	: singlet (NMR)
st	: stretching vibration (IR)
S	: siemen
SEM	: scanning electron micrographs
SSP	: solid-state polymerization
PTSA	: *p*-toluenesulfonic acid
T_c	: crystallization temperature
TGA	: thermogravimetric analysis
T_m	: melting temperature
TT	: tail to tail
t	: triplet (NMR)
TLC	: thin layer chromatography
UV-Vis	: ultra-violet and visible spectroscopy
δ	: chemical shift
λ_{max}	: maximum wavelength
XRD	: X-ray powder diffraction

CHAPTER I

INTRODUCTION

1.1 A Brief History

The initial focused study of conjugated polymers originated since the discovery of conductivity in polyacetylene with an order of 10^{-5} S/cm by Hatano and coworkers [1]. The high levels of conductivity in polymers was first observed in 1977 when Shirakawa, MacDiarmid and Heeger discovered that oxidation with halogen vapor made polyacetylene films 10^9 times more conductive than they were originally [2]. This discovery was awarded the Nobel Prize in Chemistry in 2000 "for the discovery and development of electrically conductive polymers". An important step in the development of conjugated poly(heterocycles) occurred in 1979 when Diaz and coworkers obtained polypyrrole (PPy) as a free standing film by oxidative electropolymerization of pyrrole [3].

Conducting polymers have unique properties that are interesting for this new technology [4]. They not only have the electronic properties of a semiconductor but also the mechanical flexibility and ease of production of plastics. Moreover, conjugated polymers are good materials to be employed in the fabrication of electronic devices because their properties can be fine-tuned by external parameters during chemical synthesis within a certain band width.

Thiophene was a target compound as a potential precursor for polymer synthesis. Indeed, in the field of conjugated polymers, polythiophenes and their derivatives have received significant attention for their unique electrical properties, ability to exhibit environmental stabilities, the ease of derivatization and ability to be polymerized by various methods. Other polymers such as polypyrrole, polyaniline and poly(*p*-phenylene) **(Figure 1.1)** were prepared but they do not have good stability or conductivity **(Table 1.1)**.

polyacetylene
(PA)

poly(*p*-phenylene)
(PPP)

Polyaniline
(PANI)

poly(*p*-phenylene vinylene)
(PPV)

polypyrole
(PPy)

polythiophene
(PT)

Poly(3-hexylthiophene)
(P3HT)

Poly(3,4-ethylenedioxythiophene)
(PEDOT)
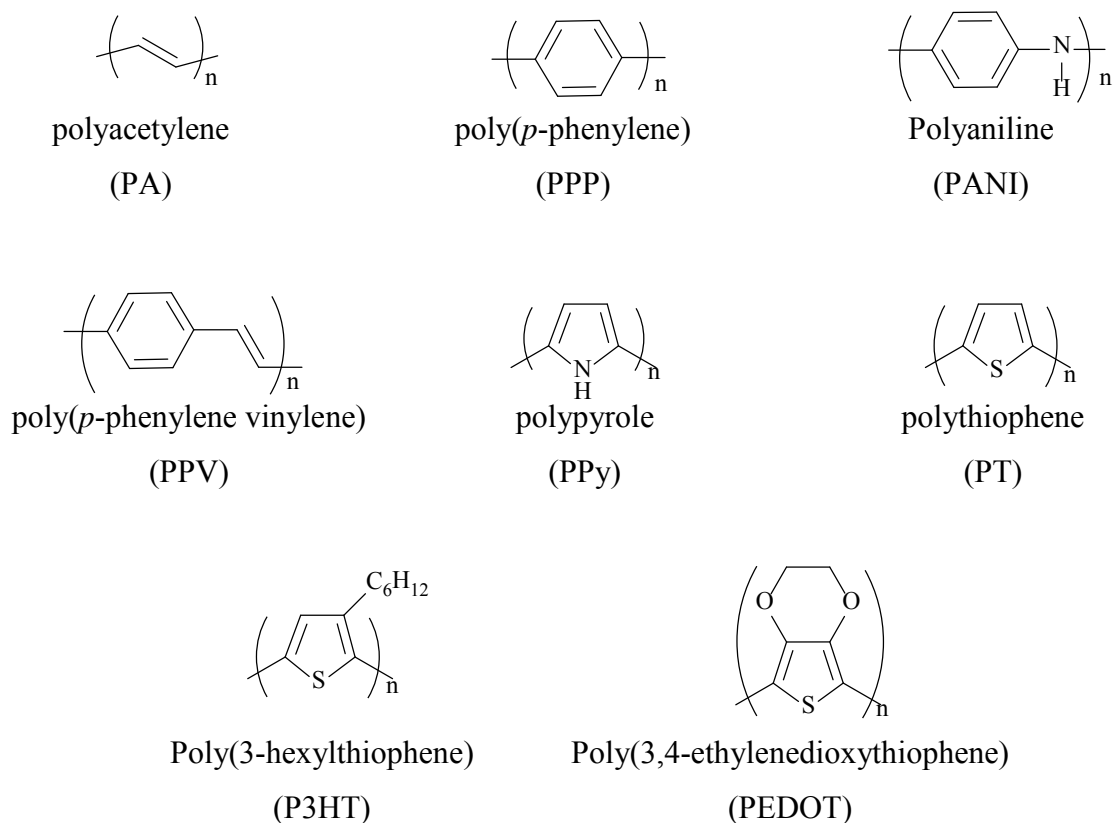
Figure 1.1 Structure of some conjugated polymers [5].

Table 1.1 Stability and processing attributes of some conducting polymers

Polymer	Conductivity (S/cm)	Stability (doped state)	Processing Possibility
Polyacetylene	10^3-10^5	poor	limited
Poly(*p*-phenylene)	1000	poor	limited
poly(*p*-phenylene vinylene)	1000	poor	limited
Polypyrroles	100	fair	good
Polythiophenes	100	good	excellent
Polyaniline	10	good	good

1.2 Applications of organic conducting polymers

According to the attractive and tunable properties of organic conducting polymers, this facilitates the use of conducting polymers in many applications such as:

- **Applications utilizing the inherent conductivity of polymer**

  Antistatic coating (metal and polymer), microelectronic devices, stealth material for providing a minimum radar profile for military aircrafts and naval vessels

- **Electrochemical switching, energy storage and conversion**

  New rechargeable battery, redox supercapacitors

- **Polymer photovoltaics (light-induce charge separation)**

- **Display technologies**

  Light emitting diode (LED), flat panel displays

- **Electromechanical actuators**

  Artificial muscles, windows wipers in spacecrafts, rehabilitation gloves electronic Braille screen, bionic ears for deaf patients.

- **Separation technologies**

  Novel smart-membrane, selective molecular recognition

- **Cellular communication**

  Growth and control of biological cell cultures

- **Controlled release devices**

  Ideal host for the controlled release of chemical substances

- **Corrosion protection**

  New-generation Corrosion protective coatings

1.3 Organic *versus* Inorganic Semiconductors

Organic materials offer several major advantages over their inorganic and traditional counterparts. Some potential benefits are:

• *Low weight*. The densities of molecular materials and polymers are much lower than those of traditional metals (1-2 g/cm^3 compared to 3-10 g/cm^3). In modern electronic equipment, such as cellular phones and portable computers, the weight of the battery constitutes 50 % or more of the total weight.

• *Low cost*. Traditional semiconductors are extremely sensitive to impurities and must be produced, handled and assembled in high-tech clean rooms. Organic materials, on the other hand, may be synthesized in relatively unsophisticated laboratories and are much more tolerant to contaminations. A square centimeter layer of silicon costs about \$1, while organic thin-films of the same size have been produced for as little as 1 cent. Prices are assumed to diminish even further, with increasing production.

• *Tunability*. The art of organic chemistry offers an infinite amount of chemical modifications of the active materials, which may be fine-tuned to suit each desired application.

• *Flexibility*. Inorganic semiconductors are terribly stiff and therefore useless for flexible devices. Many organic semiconductors are on the other hand quite flexible, making devices such as plastic color displays realizable.

• *Solubility/Processability*. Many molecular materials are soluble in common organic solvents and can therefore be applied onto the desired substrates by simple evaporation.

1.4 Conjugated polymers

Polymers are long chain molecules which are utilized mostly as in plastics such as polystyrene and polyethylene. In general, polymers are considered good insulators. However, conjugated polymers are classified as organic semiconductors [6]. They contain a backbone consisting of alternating single and double bonds between carbon-carbon or carbon-nitrogen atoms. Eventhough conjugated polymers are known as linear or rigid rods, they are not completely straight and flat, but twisted along their backbones [7]. Polymer chains consist of sp^2-hybridized carbons and p-electrons. These p-electrons form a delocalized π-system, which gives rise to the semiconducting properties. At present, conducting polymers are used in wide range of areas such as thin film transistors [8], sensors [9-11], light emitting diodes [12] and electrochromic windows or multichromic displays [13, 14].
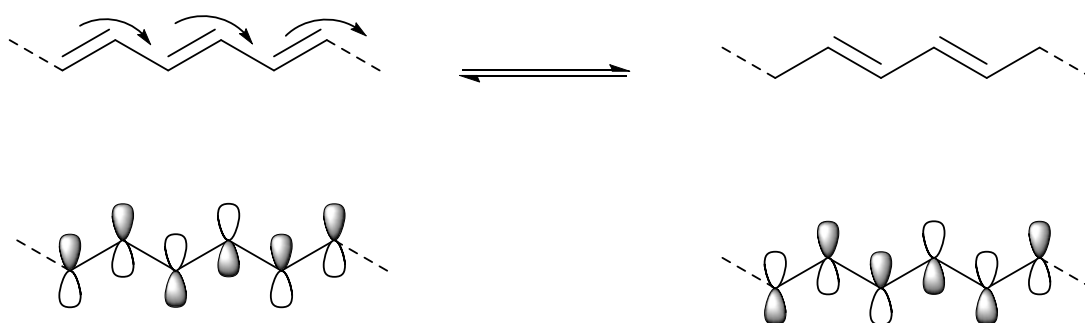
Figure 1.2 The delocalized π system of conjugated polymers

1.5 Band Theory

By linking a string of π aromatic molecules together, conjugated systems can be created such that the HOMO and LUMO of these extended systems merge into continuous bands that can be modeled as semiconductors. By taking the $E_{1/2}$ values for oxidation for thiophene oligomers and their onset of absorption from UV-Vis experiments, a plot of the position of the HOMO and LUMO can be analyzed as shown in Figure 1.3 [15, 16]. Thiophene oxidizes at 2.07 V vs SCE and has a HOMO-LUMO separation of 5.0 eV based on UV-Vis experiments. Addition of a second

thiophene ring to create bithiophene extends the conjugation and results in a lowering of both the energy gap and oxidation potential to 3.5 eV and 1.31 V, respectively [17]. Terthiophene has an oxidation potential of 1.05 V and an energy gap of 3.0 eV [18]. The oxidation of quaterthiophene occurs at 0.95 V, and its energy gap is 2.8 eV [19]. As the π-system is extended further to sexithiophene, the values approach a saturation point with oxidation occuring at 0.83 V and an energy gap of 2.5 eV. Further extension leads to intractable solids and, at this point, the addition of thiophene units results in properties that are "polythiophene-like." Polythiophene oxidizes at 0.7 V, and its energy gap is 2.0 eV.
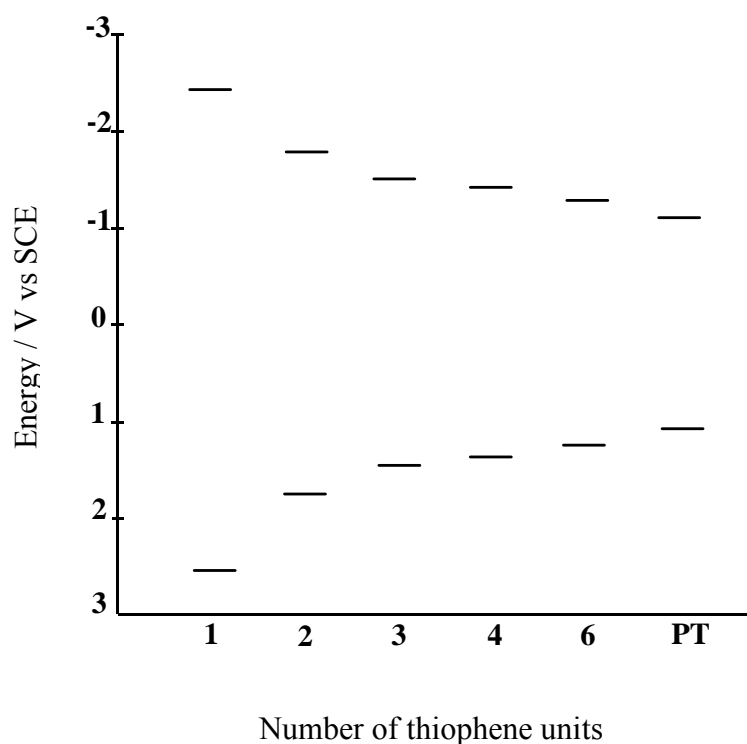
Figure 1.3 Band diagram of thiophene.

1.6 Conductivity

When a known voltage is applied over a resistor, conductivity is defined by Ohm's Law:

$$U = R\,I \qquad\qquad (1)$$

U is the drop of potential (unit Volts, V), R is the proportionality constant resistance (measured in Ohms, Ω) and I is the current (unit Amperes, A). Ohm's Law is empirical and, obviously, linear. Not all materials obey Ohm's Law, *i.e.* they exhibit non-linear behavior. This non-linearity is the foundation of all semiconductor devices, such as field-effect transistors and light-emitting diodes.

In Ohmic materials, the resistance R is proportional to the length of the resistor l (unit meters, m) and inversely proportional to the cross-section area of the resistor A (measured in square-meters, m^2) according to:

$$R = \rho\, l\, /\, A \qquad\qquad (2)$$

Here, ρ is the resistivity (SI unit Ωm – the unit Ωcm is, however, used more frequently) of the material. The inverse of the resistivity is the conductivity σ (unit Sm^{-1} or Scm^{-1}), where Ω^{-1} is the conductance (unit Siemens, S). Conductivity σ is proportional to the number of charge carriers and how fast they can move in the material (mobility μ - unit cm^2/Vs) (e is the charge of an electron, $\sim 1.6 \times 10^{-19}$ C):

$$\sigma = n\, \mu\, e \qquad\qquad (3)$$

For materials that do not obey Ohm's Law, such as electrolyte solutions and semiconductors, an extra term must be added to equation 3 to correct for the presence of positive charges (holes or cations). Conductivity is temperature dependent. While the conductivity in metallic materials increase with decreasing temperature, the opposite is true for semiconductors. Actually, this behavior is measured when one wishes to determine whether a specific material is a conductor or a semiconductor.

1.7 What makes material conduct electricity?

Any given material may be placed in one of the three categories depicted in **Figure 1.4** [20]. The valence band is defined as the total sum of all HOMOs, and is therefore lower in energy, in accordance with the Aufbau principle. The conduction band is made up of LUMOs and is consequently higher in energy.

a. Insulator   b. Semiconductor   c. Conductor
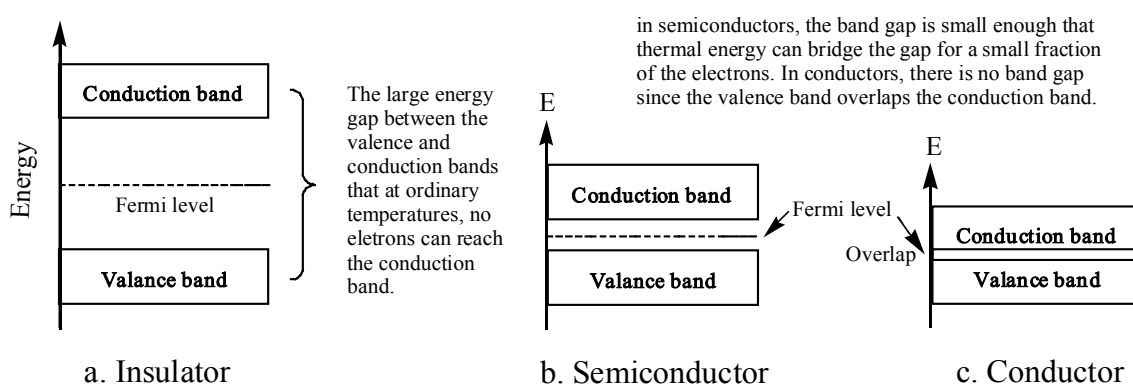
Figure 1.4 Simple band picture explaining the difference between an insulator, a semiconductor, and a metal [20].

As stated before, common molecular compounds are insulators (category a). The band gap in these materials is too wide (over 3-4 eV) for any excitation of charge carriers to occur. The reason for this wide bandgap in insulators is that the valence band is made up of bonding orbitals, which are completely filled, while the conduction band is constructed of anti-bonding orbitals of much higher energy. If a charge is injected into an insulator, it has no energetically favorable way to travel within the material. Electric current is, by definition, the uniform motion of charges. For this reason, the insulating material does not conduct electricity.

Semiconductors (category b) have a narrow bandgap (under 3 eV), which allows some excitation of charge carriers to the conduction band. Since the overlap between the two bands is not very efficient, semiconductors usually have conductivities much lower than true metallic conductors. When the temperature of a

semiconductor is lowered, the probability of thermal excitation to the conduction band is diminished, which explains why conductivity of semiconductors decrease with decreasing temperature. Anisotropy is very common among semiconductors. Semiconductors often have relatively high mobilites μ, but their conductivities are limited by the low number of charge carriers n.

Metallic conductors (category c), have either an incomplete valence band (as in the figure), which is the case for all transition metals with unoccupied d-orbitals, or a near-zero bandgap between the valence band and the conduction band. Both these situations lead to a continuous and partially filled band. Metallic conductors have a very large number of charge carriers n ("free electrons"), but are instead limited by a relatively low mobility μ. Thermal excitation leads to scattering of charges, which makes it less probable for them to move ideally along the current axis, hence lowering the conductivity. This explains why conductivity decreases with increasing temperature in metallic conductors. Still, conductivity in metals is much greater than in semiconductors.

1.8 Doping process

The doping process is an addition of a doping agent into the polymer expecting to enhance the conductivity of the polymer. The modification of electrical conductivity of conducting polymers from insulator to metal can be accomplished either by chemical doping or by electrochemical doping. Both *n-type* (electron donating) and *p-type* (electron accepting) dopants have been used to induce an insulator-to-conductor transition in electronic polymers. Familiar to inorganic semiconductors, these dopants remove or add charges to the polymers. However, unlike substitutional doping that occurs in conventional semiconductors, the dopant atomic or molecular ions are interstitially positioned between π-conjugated polymers chain, and donate charges to or accept charges from the polymer backbone. In this case, the counter ion is not covalently bound to the polymer, but only attracted to it by the Coulombic force. In self-doping cases, these dopants are covalently bound to the polymer backbone [21]. Initially added charges during doping process do not simply start to fill the conduction band to have metallic behavior immediately. The strong

coupling between electrons and phonons near the doped charges causes distortions of the bond lengths. For degenerate ground state polymers such as trans-polyacetylene, doped charges at low doping levels are stored in charged solitons whereas nondegenerate systems they are stored as charged polarons or bipolarons [22-25]. High doping for the non-degenerate polymers results in polarons interacting to form a polaron lattice or electrically conducting partially filled energy band [26, 27]. Bipolarons or the pairs of polarons are formed in less ordered regions of doped polymers [28].

Simultaneous with the doping, the electrochemical potential (the Fermi level) **(Figure 1.4)** is moved either by a redox reaction or an acid-base reaction into a region of energy where there is a high density of electronic states; charge neutrality is maintained by the introduction of counter-ions. The electrical conductivity results from the existence of charge carriers through charge doping and from the ability of those charge carriers to move along the π-bonds; however, disorder restricts the carrier mobility and limits the electrical conductivity in the metallic state. Accordingly, electrical conductivity of doped conjugated polymers is improved due to two reasons:

1. Doping process introduces carriers into the electronic structure. Since every repeating unit is a potential redox site, conjugated polymers can be doped *n*-type (reduced) or *p*-type (oxidized) to a relatively high density of charge carriers.

2. The attraction of an electron in one unit to the nuclei in the neighboring units leads to carrier delocalization along the polymer chain and to charge carrier mobility, which is extended into three dimensions through inter-chain electron transfer.

Charge injection or "doping" onto conjugated conducting polymers leads to the wide variety of interesting and important phenomena which define the field. The doping can be accomplished in a number of ways:

1.8.1 Chemical doping by charge transfer

The first discovery of the ability to dope conjugated polymers involved charge transfer redox chemistry; oxidation (*p*-type doping) or reduction (*n*-type doping), as demonstrated with the following examples:

1. *p*-type

$$(\pi\text{-polymer})_n + \tfrac{3}{2}\, ny\ (I_2) \rightarrow [(\pi\text{-polymer})^{+y}(I_3^-)_y]_n$$

2. *n*-type

$$(\pi\text{-polymer})_n + [Na + (naphthalide)^\bullet]_y \rightarrow [(Na^+)_y(\pi\text{-polymer})^{-y}]_n + (naphthalene)^o$$
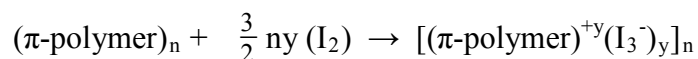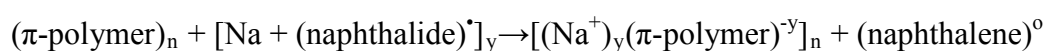
When the doping level is sufficiently high, the electronic structure of conjugated polymers approached to that of a metal.

1.8.2 Electrochemical doping

Although chemical (charge transfer) doping is an efficient and straightforward process, it is normally difficult to control. Complete doping to the highest concentrations yields reasonably high quality materials; however, attempts to obtain intermediate doping levels often result in inhomogeneous doping. Electrochemical doping was originated to solve this problem. In electrochemical doping, the electrode supplies the redox charge to the conducting polymer, while ions diffuse into (or out of) the polymer structure from the nearby electrolyte to compensate the electronic charge. The doping level is determined by the voltage between the conducting polymer and the counter-electrode; at electrochemical equilibrium the doping level can be achieved by setting the electrochemical cell at a fixed applied voltage and simply waiting as long as necessary for the system to come to electrochemical equilibrium as indicated by the current through the cell going to Zero. Electrochemical doping is illustrated by the following examples:

1. *p*-type

$$(\pi\text{-polymer})_n \; + \quad [\text{Li} \; + \; (\text{BF}_4^-)]_{\text{solution}} \qquad \rightarrow \quad [(\pi\text{-polymer})^{+y}(\text{BF}_4^-)_y]_n \; + \; \text{Li}$$

(electrode)

2. *n*-type

$$(\pi\text{-polymer})_n + \text{Li(electrode)} \; \rightarrow \; [(\text{Li}^+)_y(\pi\text{-polymer})^{-y}]_n + [\text{Li} + (\text{BF}_4^-)]_{\text{solution}}$$
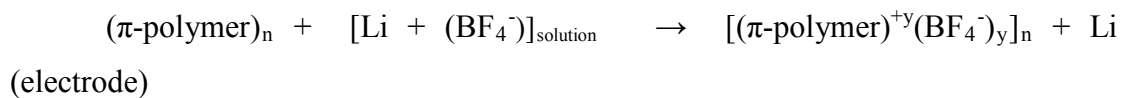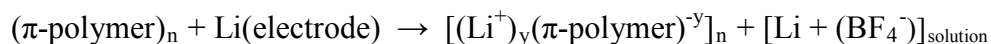
1.9 Conductive Processes

As discussed earlier, in order for a polyheterocycle to exhibit metallic conductivity, it must be highly doped. Intermediate doping results in charge carriers called polarons. Polarons have an unpaired spin, and they are radical cations or radical anions. They exhibit an EPR signal and are delocalized over four to five heterocycle rings. High doping levels result in formation of spinless dication bipolarons.
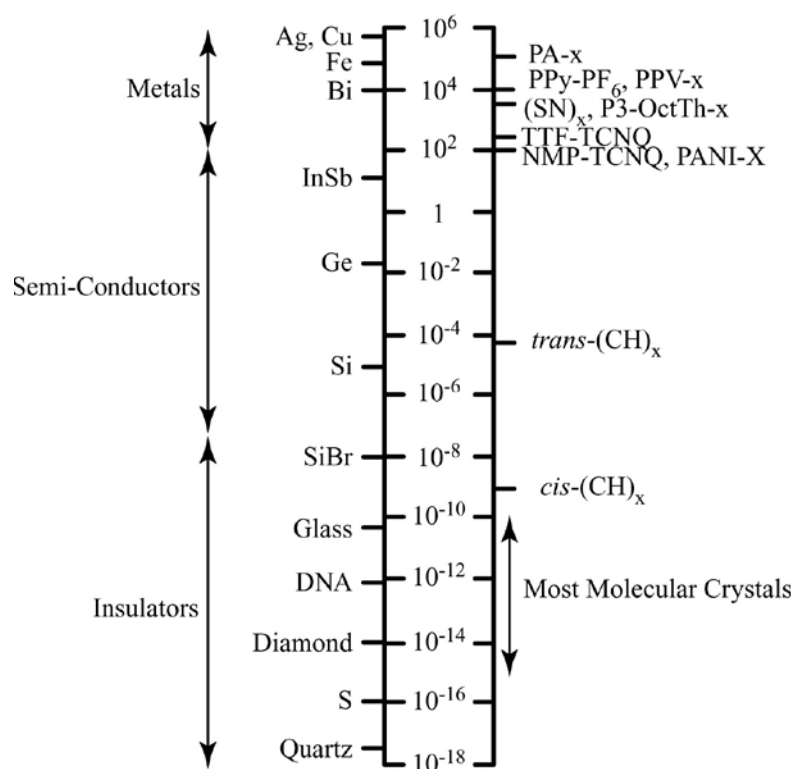
Figure 1.5 Conductivities of various metals and conjugated polymers [16].

1.10 Solitons, Polarons and Bipolarons

Polymer doping leads to the formation of conjugational defects; solitons, polarons and bipolarons in the polymer chain. The presence of localized electronic states of energies less than the band-gap arising from changes in local bond order, including the formation of solitons, polarons and bipolarons, have led to the possibility of new types of charge conduction [29]. Solitons are subdivided into three catogories: neutral soliton, positive soliton and negative soliton. An interesting observation at this point is that charged solitons have no spin; while neutral solitons have spin but no charge. Positively charged soliton occurs when an electron is removed from localized state of a neutral soliton by oxidation. Negatively charged soliton is produced when an electron is inserted by reduction **(Figure 1.6)**.
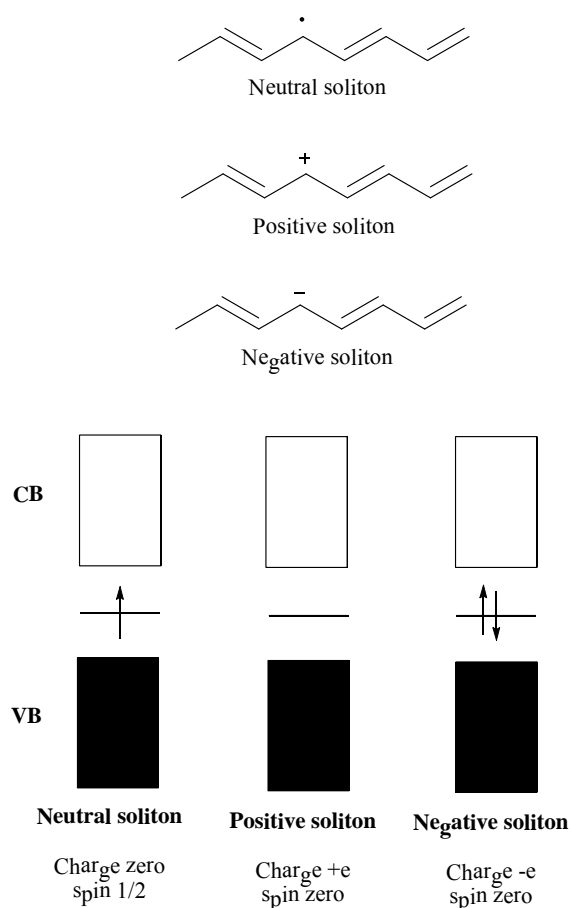
Figure 1.6 Soliton structures of polyacetylene (CB: Conduction ban, VB: Valence band)

Polarons are obtained as a combination of a neutral and a charged soliton on the same polymer chain. Further oxidation causes more and more polarons to form and eventually the unpaired electron of the polaron is removed, or two lose polarons can combine to form dications or bipolarons **(Figure 1.7)** [30].

Neutral polyacetylene

Two polarons by partial oxidation

More polarons by further oxidation

Closeness of polarons provide the interaction of two unpaired electrons to form a new π bond and a mobile bipolaron
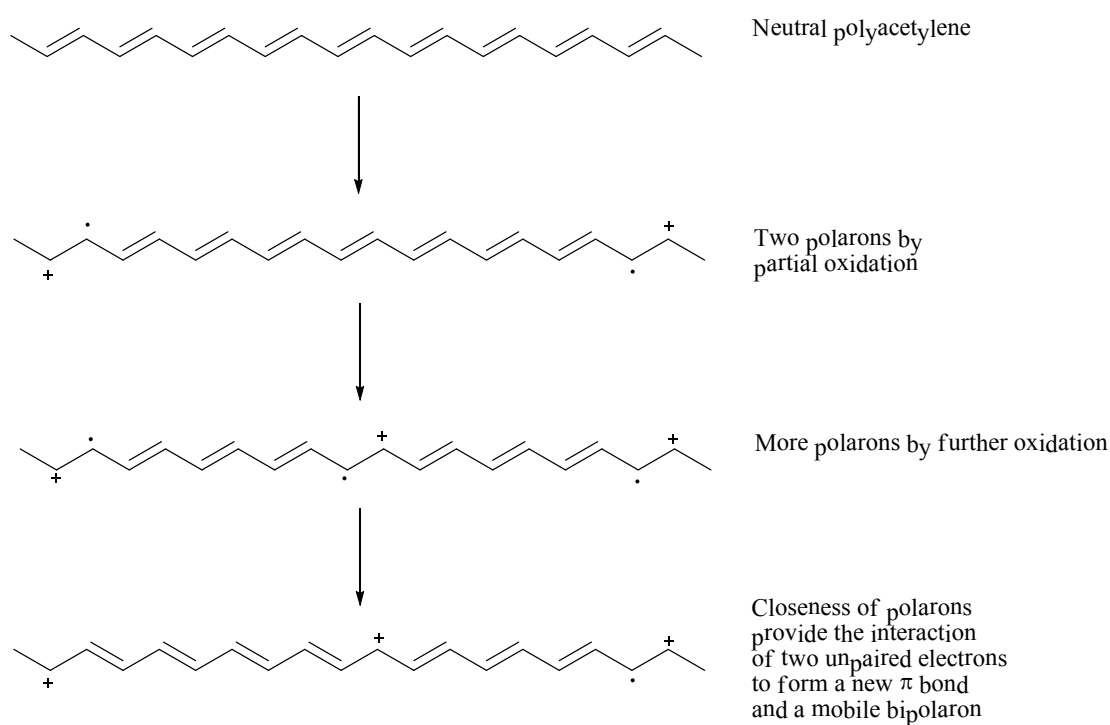
Figure 1.7 Formation of polaron and bipolaron for polyacetylene

The neutral polymer has full valence and empty conduction bands with a separated band gap. Formation of polaron and bipolaron generates new energy levels located at midgap **(Figure 1.8)**.
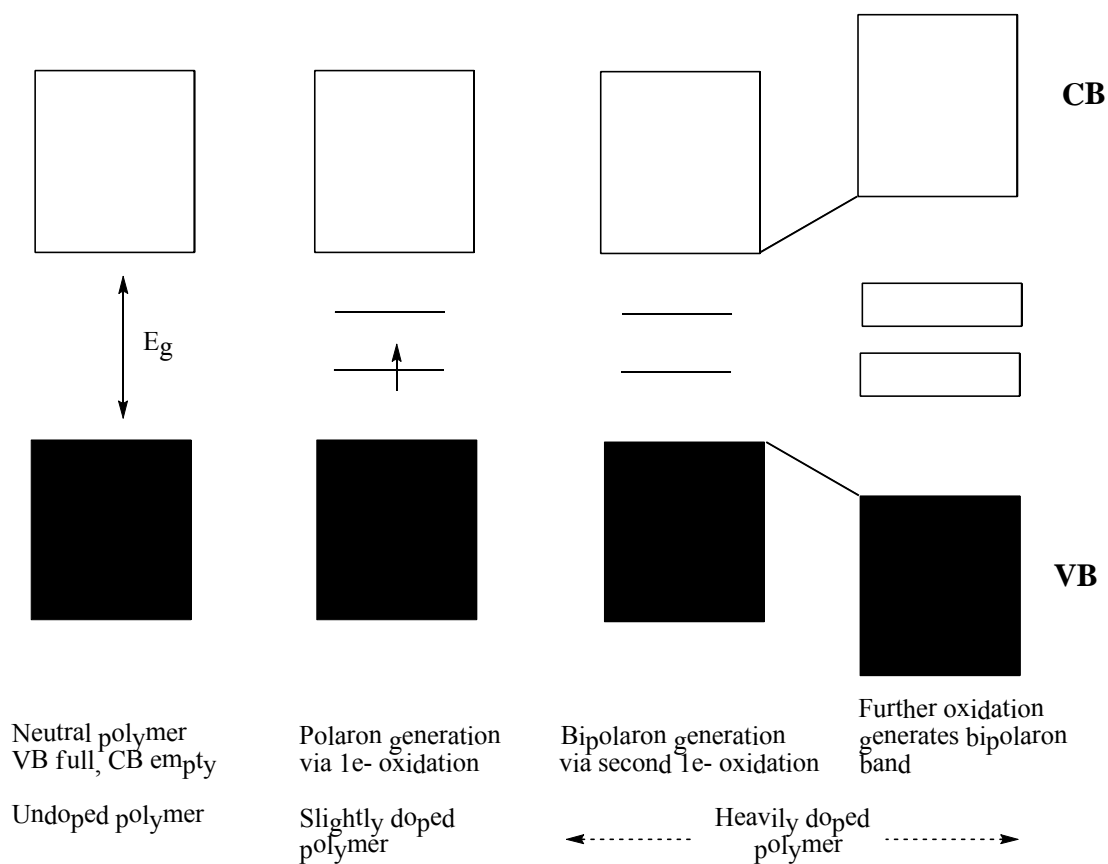
Figure 1.8 Band structure of a conjugated polymer as a function of doping level illustrating polaronic and bipolaronic states in the band gap

1.11 Structural Design and Synthetic Methodologies for Low Band Gap Materials

In order to functionalize a polymer to have the desired electrochemical and optical properties, both the valence and conduction energies can be controlled by the energy gap (the relation of the energy levels to one another) or the position of the energies (oxidation or reduction potentials) and has been thoroughly reviewed [52]. As shown in **Figure 1.9**, evolution of the polymer systems from polyacetylene to poly(BEDOT-Pyridine), shows the effects of heteroatom placement and position of the double bond on band gap and thus color. Low band gap materials will ultimately provide a means for stable n-doped states on the benchtop and highly intrinsically conducting polymer systems.
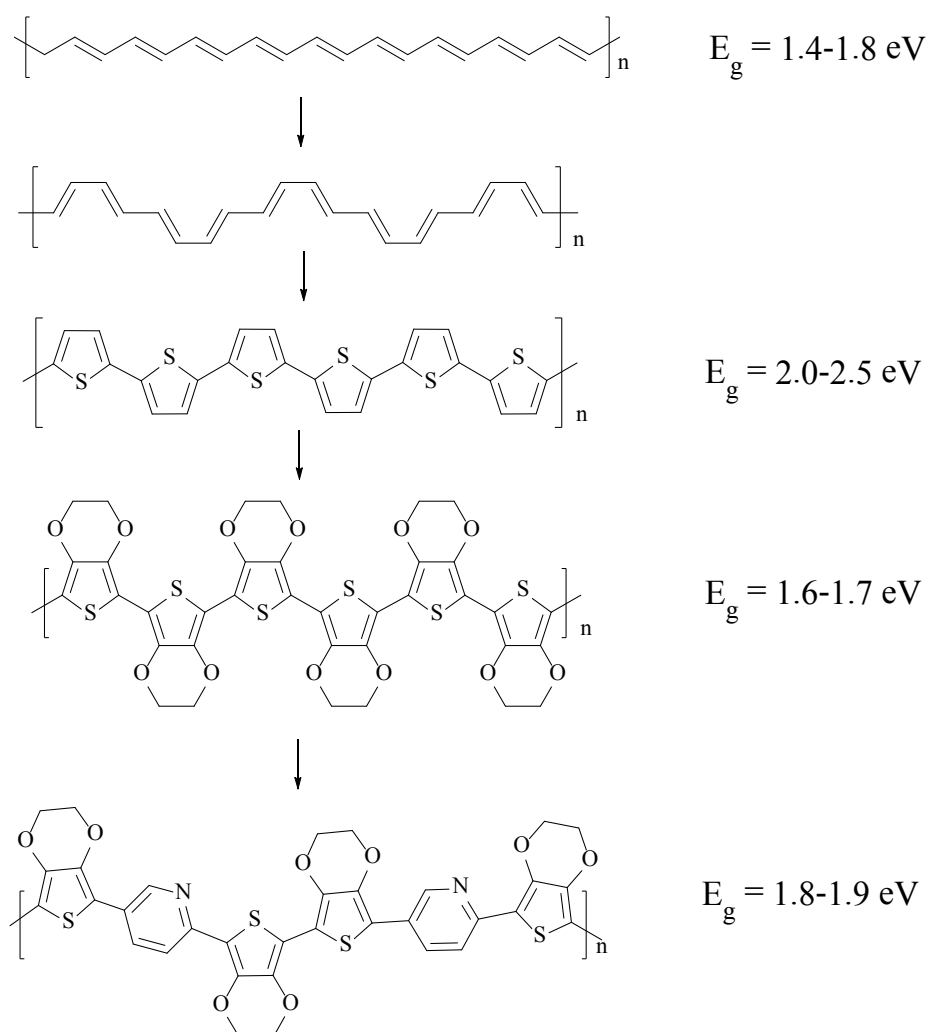
Figure 1.9 Evolution from PA to PEDOT-Pyridine.

In designing low band gap systems, there are a variety of methodologies that can be used to achieve polymers with band gaps less then 2 eV. Five basic approaches have been used to reduce band gap that include controlling bond-length alternation (Peierls distortion), creating highly planar systems, inducing order by interchain effects, resonance effects along the polymer backbone, and using donor-acceptor effects.

Bond-length alternation is the difference in length of the single and double bond along the polyheterocycles backbone. Of these states, the quinoidal form has a much lower band gap than the aromatic state. The classical example of aromaticity

control in conjugated polyheterocylces is polyisothianaphthene (PITN), a polythiophene with a benzene ring fused at the 3- and 4-positions along the polymer backbone. Benzene, with an energy of aromatization of 1.56 eV, is more aromatic than thiophene (1.26 eV). This forces PITN to be more energetically stable in the quinoidal state, which provides for a lowered band gap of 1.1 eV compared to polythiophenes band gap of 2.0 eV.

As shown in **Figure 1.10**, the higher the torsional angle between adjacent rings the larger the band gap of a system. A number of groups have used different methods to achieve highly planar low band gap systems. One successful approach has been ladder-type polymers such as the polyacene family. Another has been synthesis of polyquinoxalines. However, these systems exhibit extreme cases of bond-length alternation and give much higher energy gaps then expected.

The strongest example of the influence between polymer chains is poly (3-hexylthiophene). Regioregular poly(3-alkylthiophene)s have been prepared that show much lower band gaps and better electrochemical properties due to the ordering of the polymer films.

A more recent example of aromaticity effects are the thienyl-S,S-dioxide family of systems. Oxidation of the sulfur on thiophene prevents its lone pair contribution to the rings aromaticity, in effect making it a "pinned" cis-transoid polyacetylene. Copolymers with thiophene give band gaps of 1.5 eV and reduction potentials with $E_{1/2}$ values of -1.1 V vs SCE [53, 54].
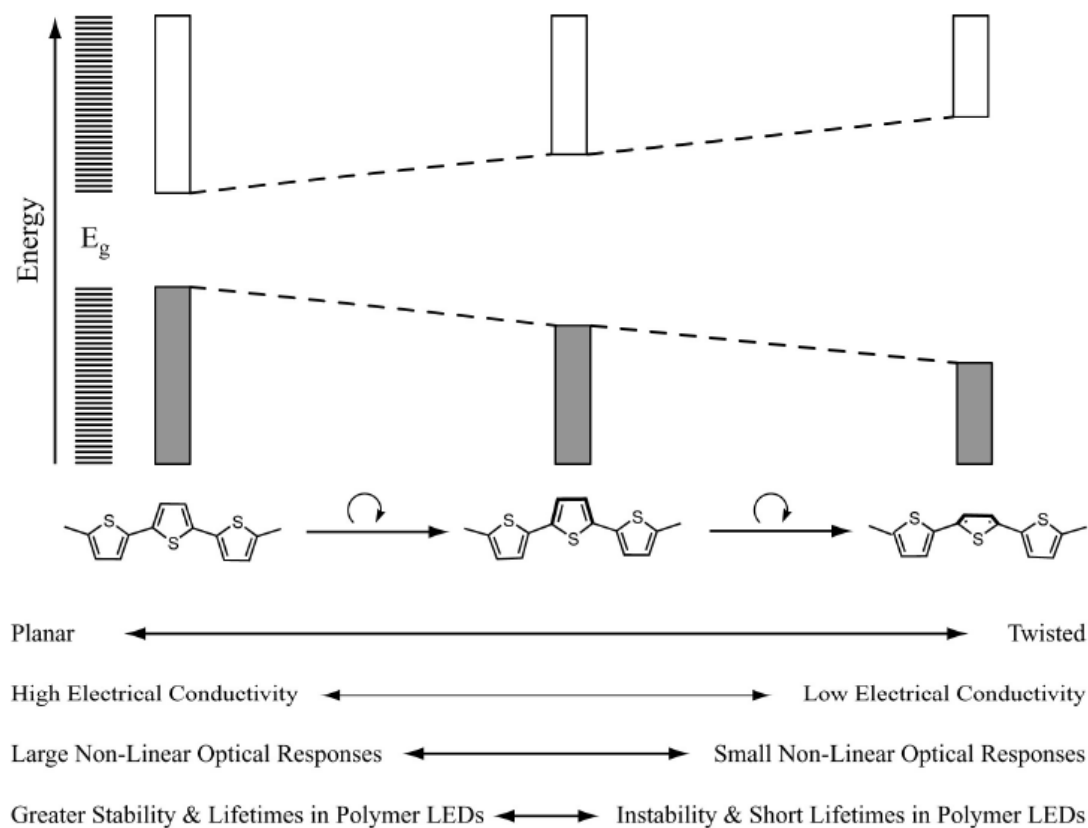
Figure 1.10 Planarity effects on band gap and the electrical and optical properties of conjugated polymers.

1.12 Effective conjugation length (ECL)

Ideal conducting polymers should have its π electrons in the conjugated unsaturated bonds even by distributing throughout the whole chain. This requirement usually does not hold due to the following:

i) Formation of defects in polymer

ii) Twisting of planar structure out of conjugation in the polymer.

Examples of the two reasons above are exemplified in **Figure 1.11**. Formation of a defect in polyacetylene as a saturated sp^3-hybridized methylene caused the disruptive effect in the flow of electrons on polymer chain. In another case, the steric

incumbent between adjacent R groups on HH thienyl units in irregular poly (3-alkylthiophene) brought about the twisting of the thienyl ring planes out of coplanarity, causing an increase in the energy needed to allow the flow of electrons through the polymer chain, hence making the polymer chain less conductive.
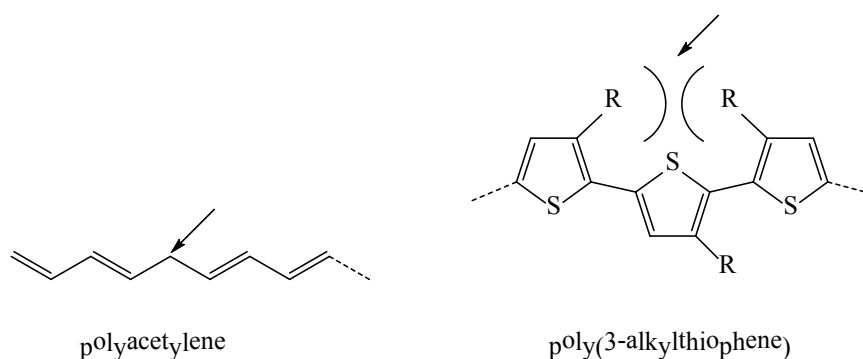
Figure 1.11 A defect in polyacetylene and steric induced structural twisting in poly(3-alkylthiophene).

Another possible reason would be the twisting of polymer chain, which occurs randomly at the single bonds and divided the polymer into separated sections with their own coplanarity (**Figure 1.12**). Twisting of polymer chain would also cause the reduction of conjugation in the polymer.
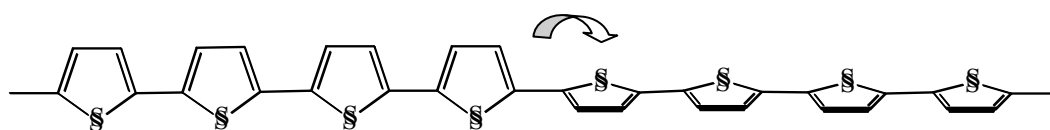
Figure 1.12 Twisting of polythiophene.

1.13 Polythiophene

Polythiophene is composed of repeating five-membered heterocyclic monomeric unit. It is also considered one of the promising classes of conducting polymers for technological used [31]. This is attributed to its good environmental

stability in neutral form, its structural versatility which allows their electronic and electrochemical properties to be modified by chemical means and its characteristics of having non-degenerate ground state for the two limiting structures of polythiophene aromatic ground state and quinoidal ground state [32,33]. For these reasons, polythiophene has been used in many applications such as:

- The electrical properties of the doped conducting sate, for example antitstaic and EMI shielding, gas sensors, radiation detector, and corrosion protective films.

- The electrical properties of the natural semiconducting state such as photovoltaic cell and non-linear optics.

- The electrochemical reversibility of the transition between the doped and the undoped states, for instance, new rechargeable battery, display devices, electrochemical sensor, and modified electrode [33].

Polythiophene with an ideal extended π-conjugation is possible only in polymers with perfectly 2,5-linked repeating units. However, 2,4- and 2,3-couplings as well as hydrogenated thiophene units can also be found in the polymers.

The two main disadvantages of polythiophene are its infusibility and insolubility which results from strong interchain stacking and relative chain rigidity. The standard procedure of attaching long, flexible chains to the conjugated backbone can often have deleterious effects on the electrical conductivity of polymers in their conducting state. A significant discovery demonstrated that polythiophene belongs to one of few cases in which substitution of hydrogen at the 3-position by alkyl chain or electron donating group with flexible chain does not affect polymer conductivity of the polymer, whereas impart solubility and consequently enhance processability. The substituted thienyl was polymerized by a number of chemical and electrochemical methods to yield poly(3-alkylthiophene) [35,36]. The flexible substituents solubilized the polythiophene chains by this disruption of their interchain stacking [36]. This in turn facilitated the processability of these polymers [37].

Diad

(HT)　　　　　　　　　　　　　(HH)

Triad

(HT-HT)　　　　　　　　　　　　(HT-HH)

(TT-HT)　　　　　　　　　　　　(TT-HH)
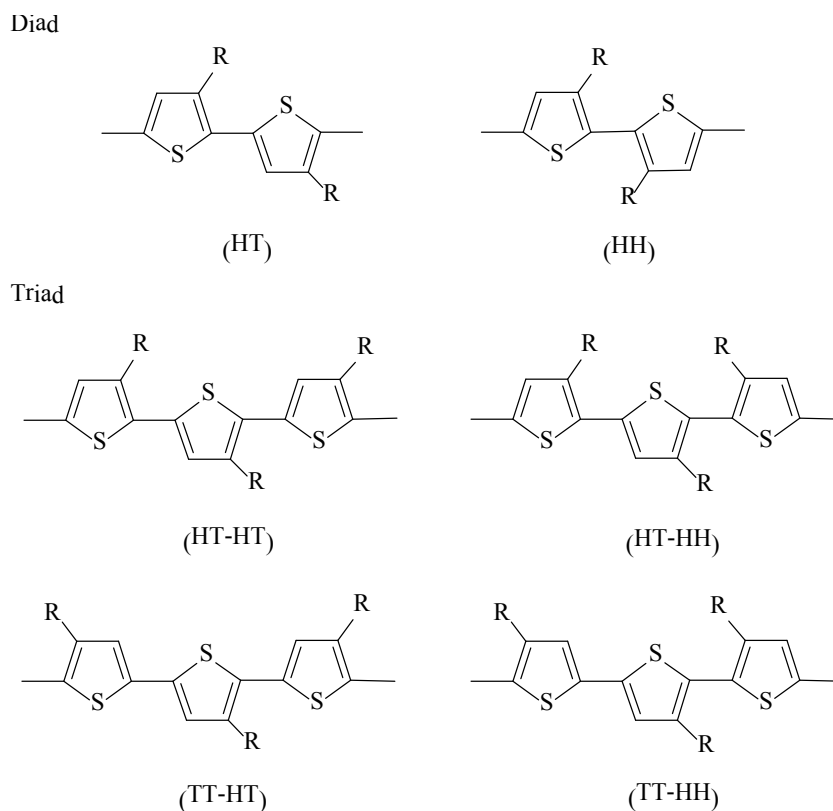
Figure 1.13 Regioisomers of the poly(3-alkylthiophene)s.

The 3-substitutent can be incorporated into the polymer chain with two different regioregularities: head-to-tail (HT) and head-to-head (HH) orientations which can in turn result in four triad regioisomers in the polymer chain, *i.e.* HT-HT, HT-HH, TT-HT, and TT-HH **(Figure 1.13).** Although HT coupling is generally favored, since the less repulsive force of HT coupling is expected about 15-20% of HH coupling is also observed.

1.14 Synthesis of polythiophene

According to many intensive research efforts, polythiophene is generally prepared by means of two main routes which are the electrochemical and the chemical syntheses.

1.14.1 Electrochemical polymerization

Initially, polythiophene was obtained by electrochemical polymerization of thiophene monomers [36]. Even polymer film was produced at the anode surface after electropolymerization, the obtained polymers are not easily processible further. This method is appropriate for the preparation of polymers such as polythiophene and poly(3-methylthiophene). The yield of polymers prepared from electrochemical polymerization is moderate to low, and their structures are not well-defined.

Compared to other chemical and electrochemical syntheses of conducting polymers **(Table 1.2)**, the anodic electropolymerization of the monomer shows several advantages such as absence of catalysts, direct grafting of the doped conducting polymer onto the electrode surface (which is of particular interest for electrochemical applications), easy control of the film thickness by deposition charge, and possibility to carry out in situ characterization of the growing process or of the polymer by electrochemical and/or spectroscopic techniques.

Table 1.2 Comparison between the chemical and electrochemical synthesis

Polymerization Approach	Advantages	Disadvantages
Chemical Polymerization	Large scale production possible	Difficult to make thin film
	Post-covalent modification of bulk conjugated polymer (CP) possible	Synthesis more complicated
	More option to modify CP Backbone covalently	
Electrochemical Polymerization	Thin film synthesis possible	Difficult to remove film from electrode surface
	Ease of synthesis	
	Entrapment of molecules in CP	Post-covalent modification of bulk CP is difficult
	Doping is simultaneous	

The electrochemical formation of conducting polymers is a unique process. Although it displays some similarities with the electrodeposition of metals since it proceeds via a nucleation and phase-growth mechanism, the major difference is that charged species precursors of the deposited material must be initially produced by oxidation of the neutral monomer at the anode surface. The consequence is that various electrochemical and chemical follow-up reactions are possible, making a difficult problem for the elucidation of the electropolymerization mechanism.

As discussed, electrochemical polymerization is very useful method for preparing polymers such as polythiophene, poly(3-methylthiophene), and poly (3-phenylthiophene), which are insoluble and infusible. When these polymers are obtained in the form of powder they cannot be processed into a film or other useful forms [37].

Polythiophene is not stable at the potentials used for the electrochemical polymerization of thiophene, so polythiophene deposited on the anode at the earlier stage of the polymerization is overoxidized and has been damaged, while the process continues to produce new polymer.

1.14.2 Oxidative coupling polymerization with iron (III) chloride

In contrast to electrochemical polymerization, the yield of polythiophene prepared from the oxidative polymerization with iron (III) chloride is relatively high. Moreover, the molecular weight of polymer synthesized by this method is sufficiently high to be cast into a film. Polymers obtained from this method are soluble in common organic solvents and their films can be formed by simply casting its solution on a solid substrate. In addition, many 3-alkylthiophenes are commercially prepared by this method. Sugimoto and coworker [37, 38] elaborated transition metal halides as oxidizing agent for polymerization of 3-hexylthiophene and found that iron (III) chlorides were the effective one **(Figure 1.14)**. The films was fabricated by casting a solution of the resulting poly(3-hexylthiophene) on substrate and the results showed similar characteristics to those prepared by the electrochemical method.

Poly(3-alkylthiophene) was undoped from trace of FeCl$_3$ by extraction with methanol, but this polymer remained in partially doped states. Completely undoped polymer was obtained by reduction with an aqueous solution of hydrazine.
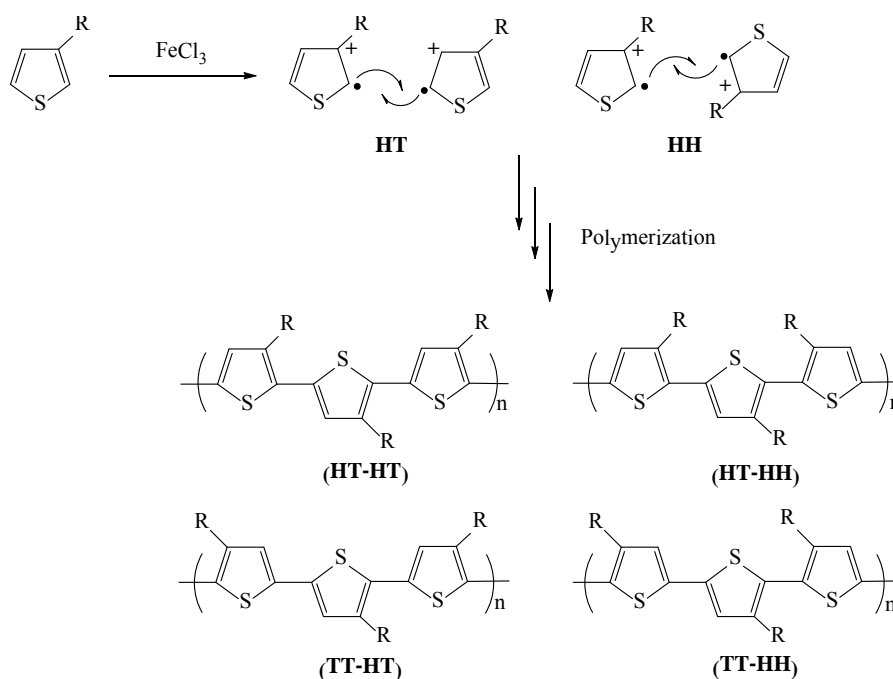
Figure 1.14 The oxidative coupling reaction of 3-alkylthiophene by FeCl$_3$ [38].

Amou [39] studied the polymerization mechanism and polymerization conditions, and found that a lower temperature and concentration were effective for increasing the HT coupling. Niemi [40] performed a detailed study on the polymerization mechanism of 3-alkylthiophene with iron (III) chloride. The results showed that only solid iron (III) chloride was active as an oxidative polymerization agent for 3-alkylthiophene while the soluble part of iron (III) chloride was inert. The solubility of iron (III) chloride in chloroform and the consuming effect of evolved hydrogen chloride gas explained the extra amount of iron (III) chloride that was initially necessary to obtain high conversion in polymerization. A plausible polymerization mechanism of 3-alkylthiophene was proposed to proceed through a radical mechanism, developed on the basis of the crystal structure of iron (III) chloride and quantum chemical computations of thiophene derivatives [38].

1.14.3 Grignard coupling and other chemical polymerizations

Polymerization using a metal-catalyzed cross-coupling technique has been extensively investigated [41, 42]. The reaction is supposed to proceed by an oxidative addition of an organic halide with a metal catalyst and then transmetallation between the catalyst complex and a reactive Grignard or other organometallic reagent (or disproportionation) generates a diorganometallic complex. The last step involves reductive elimination of the coupled product with regeneration of the metal catalyst. Numerous organometallic species (including organomagnesium, organozinc, organoboron, organoaluminum, and organotin) have been demonstrated to be used in cross-coupling reactions with organic halides.

The synthesis of regioregular HT-P3AT was reported by McCullough and coworkers [43] in early 1992 (**Figure 1.16**). This synthetic method [44-48] regiospecifically generated 2-bromo-5-(bromomagnesio)-3-alkylthiophene which was polymerized with catalytic amounts of Ni(dppp)Cl$_2$ using Kumada cross-coupling methods [49] to give P3ATs with 98-100% HT-HT couplings. In this approach, HT-P3ATs were prepared in yields of 44-69% in a one-pot, multistep procedure. Molecular weights of HT-P3ATs are typically in the range of (20-40) $\times$ 10^3 (PDI $\approx$ 1.4). A prepared sample of HT-poly(dodecylthiophene) had M_n = 130,000 (PDI = 2.1).
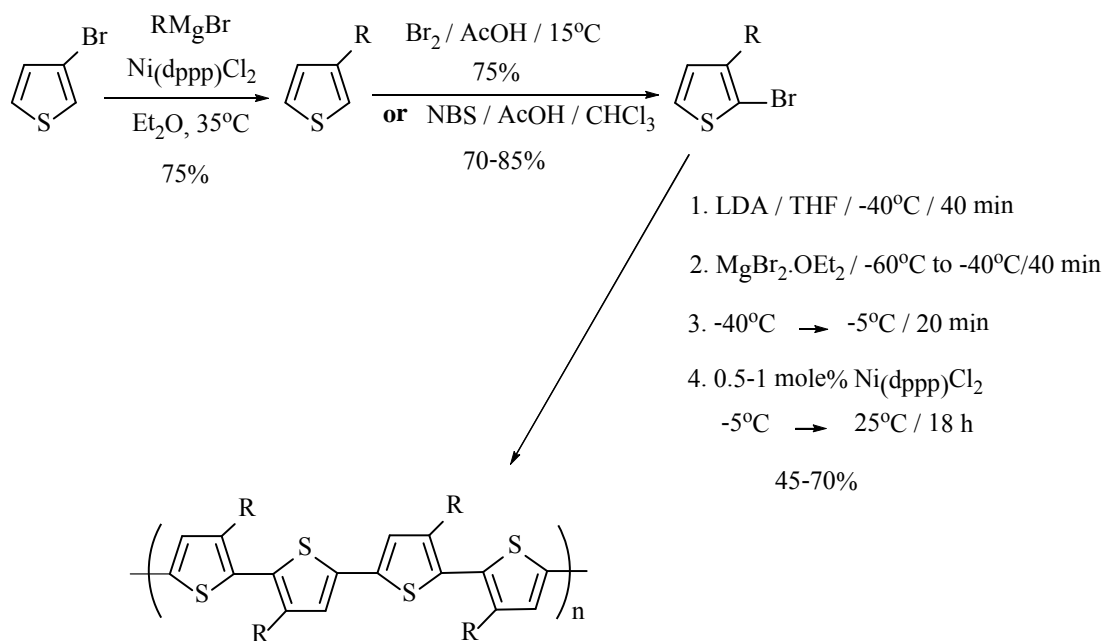
Figure 1.15 The McCullough method for the regiospecific synthesis of poly(3-alkylthiophene)s [43].

1.14.4 Solid state polymerization of PEDOT

Polymerization of PEDOT by traditional oxidative polymerization of 3,4-ethylenedioxythiophene (EDOT) **1** with $FeCl_3$ in organic solvents gives an insoluble blue-black polymer powder. The limitations of traditional polymerization methods can be a serious problem for PEDOT applications as well as for in-depth investigation of molecular order in this conducting polymer. It is generally not possible to obtain a well-defined polymer structure, unless the synthesis of conducting polymers is carried out via pure chemical polymerization routes, without adding any catalysts. A possible

solution for this lies in a solid-state polymerization of a structurally pre-organized crystalline monomer.

The advantages of solid-state polymerization including low operating temperatures, which restrain side reactions and thermal degradation of production, while requiring inexpensive equipment, and uncomplicated and environmentally sound procedures. However, at solid-state polymerization low temperatures, rate of the reactions are slow compared to polymerization in the melt phase because of the reduce mobility of the reacting species, and the slow diffusion of the by-products [47].

Meng and coworkers [50, 51] discovered the solid-state polymerization (SSP) of DBEDOT by chance as a result of prolonged storage (2 years) at room temperature or heated (50-80 °C) of the monomer **(Figure 1.16)**. The colorless crystalline DBEDOT transformed into a black blue material while retaining the morphology. Surprisingly, the conductivity of this decomposition product appeared to be very high (up to 80 S/cm) for an organic solid. Indeed, the most likely explanation for the observed transformation was polymerization with formation of bromine-doped PEDOT.
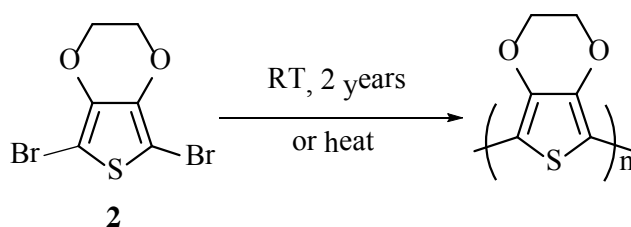
Figure 1.16 Solid-state polymerization of DBEDOT **2**

Meng and coworkers have continued to study solid state polymerization (SSP) of other dihalogen-substituted derivatives of 3,4-ethylenedioxythiophene (EDOT) **1** **(Figure 1.17)**, whose halogen atoms are Cl, Br or I, respectively. The polymerization results indicated that 2,5-dibromo-3,4-ethylenedioxythiophene (DBEDOT) **2** was the most reactive monomer, and polymerization reaction occurred via radical cationic polymerization which electron donating group (3,4-ethylenedioxy group) enhanced the stability of cation intermediate. They also suggested that the distance between bromine atoms of each DBEDOT **2** was less than the summation of van der Waal

radius, confirmed by single-crystal X-ray technique, may be another factor that facilitates the solid state polymerization [50].
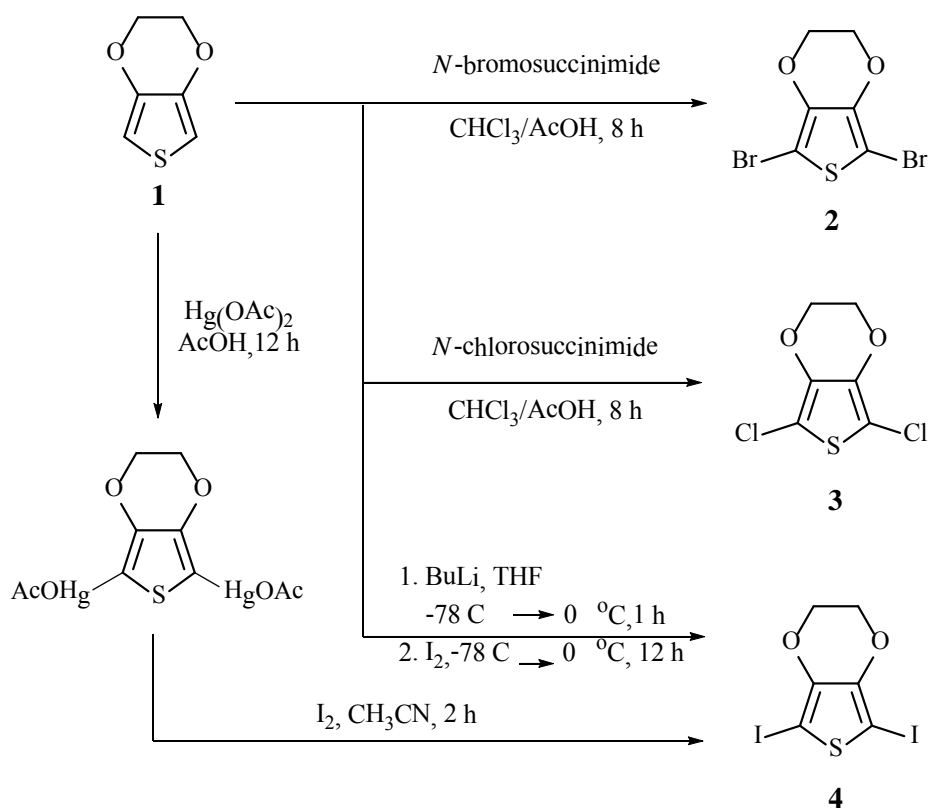
Figure 1.17 Synthesis of dihalo-EDOT monomers [48].

The conductivity of different SSP-PEDOT samples was measured by the four point probe method at room temperature **(Table 1.3)**. The highest conductivity belongs to the polymer prepared at lowest temperature and longest reaction time, which may reflect achievement of a higher degree of order. Indeed, heating above the monomer's melting point results in dramatically reduced conductivity (0.1 S/cm), which rises up to 5.8 S/cm after doping with iodine, approaching the value of an $FeCl_3$-synthesized PEDOT (7.6 S/cm). Not very significant, but certain increase in conductivity of SSP-PEDOT (about 2 times) was found on exposing a sample to iodine vapor.

Table 1.3 Conductivity data of PEDOT polymers [49].

| | Conductivity(σ); S.cm^{-1} | | | | |
	SSP-PEDOT[a]				FeCl$_3$-PEDOT[b]
Reaction temperature(°C)	20	60	80	120	0-5
Reaction time	2 years	24 h	4 h	24 h	24 h
1. Crystal	80	33	20	-[c]	-[c]
2. Pellets as synthesized	30	18	16	0.1	-[d]
3. Pellets after I$_2$ doping	53	30	27	5.8	7.6

[a] Prepared from solid state polymerization

[b] Prepared from oxidative coupling polymerization by FeCl$_3$

[c] cannot be obtained

[d] very small value

From the experiment, they concluded that heating DBEDOT in the solid state resulted in an unprecedented self-coupling reaction and gave highly conductive and relatively well-ordered bromine-doped PEDOT. Furthermore, heating DBEDOT above its melting point led to polymer with a lower conductivity.

As a unique derivative of polythiophene, poly(3,4-ethylenedioxythiophene) (PEDOT), possesses several advantageous properties compared with unsubstituted polythiophene and polythiophene derivatives. PEDOT had received considerable interests attributable to its low band gap, high electrical conductivity, good stability, and excellent optical transparency in the visible region. Even ether groups at β, β' positions of thiophene ring in PEDOT avoided the formation of α-β' linkages defect during polymerization. Thus derivatization of thiophene ring by other substituents such as alkoxy or polyether groups at the β positions could lead to higher solubility and improved physical and chemical properties. Solid state polymerization (SSP) of their new structurally pre-organized crystalline monomers could also result in another well-defined polymer structures with high conductivity. Moreover, this method was uncomplicated, less side reactions and environmentally sound procedures. This research will aim at functionalization of thiophene derivatives carrying alkoxy and

other functional groups, and then the synthesis of new polythiophene derivatives will be attempted from these monomers through solid state polymerization (SSP) or other polymerization methods.

1.15 Literature reviews

At the begining of the 90s, chemists at the Bayer company described a novel conducting polymer poly(3,4-ethylenedioxythiophene) (PEDOT). Owing to several distinct advantages, PEDOT rapidly acquired a prominent position among conducting polymers. A unique combination of moderate band gap and low oxidation potential confers on PEDOT an exceptional stability to the oxidized charged state which furthermore exhibits high conductivity and good optical transparency in the visible spectral region. Based on these properties many applications of PEDOT have been rapidly developed including anti-static coatings, electrode material in supercapacitors or hole injection layer in OLEDs and solar cells.

Although PEDOT was initially viewed as a novel conducting polymer, it became rapidly clear that the EDOT molecule itself presented some specific chemical properties which made it an interesting building block for the synthesis of functional π-conjugated systems. In fact, in addition to their strong electron donor effect, the ether groups at the β,β' positions of thiophene ring prevent the formation of parasitic α–β' linkages during polymerization while conferring a high reactivity to the free α,α' positions [55].

As a result of the multiple utilizations of the EDOT building block in functional π-conjugated systems progressively developed, several groups began to investigate in more detail the chemistry of EDOT or undertook the modification of the chemical structure of the EDOT system itself in order to manipulate its chemo-physical and electronic properties.

Bäuerle et al. (2002) reported the synthesis of EDOT and other 3,4-alkylenedioxy-thiophenes by the double Mitsunobu reaction as shown in **Figure 1.18**[56].
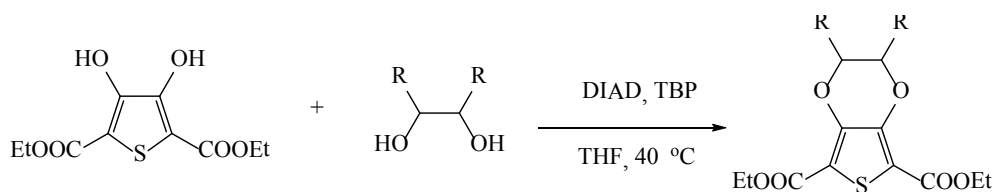
Figure 1.18 Synthesis alkylenedioxythiophenes via Mitsunubu reaction

Hellberg and coworkers (2004) have recently reported a synthesis of EDOT based on a novel one-step synthesis of 3,4-dimethoxythiophene by ring closure of 2,3-dimethoxy-1,3-butadiene. EDOT was then obtained by transetherification of 3,4-dimethoxythiophene using ethylene glycol as shown in **Figure 1.19** [57].
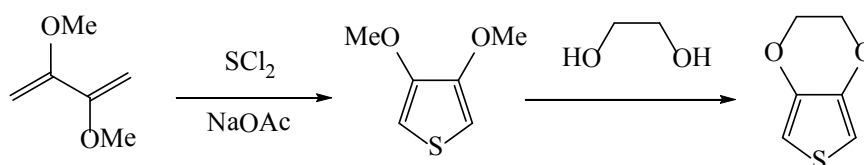
Figure 1.19 Synthesis of 3,4-dimethoxythiophene from 2,3-dimethoxy-1,3-butadiene

Pure chiral disubstituted EDOTs have been prepared by transetherification of 3,4-dimethoxythiophene and electropolymerized into stereo- and regio-regular polymers [58].

A possible solution to this problem consists of the modification of the EDOT structure in order to attach the solubilizing side chain at ethylene bridge. A soluble poly(EDOT-$C_{10}H_{21}$, **5**) was reported by Jonas and coworkers **(Figure 1.19)** [59]. A decyl chain substituted at sp^3 carbon of the ethylene bridge has two undesirable consequences. First, such substitution creates a center of chirality thus giving rise to a considerable number of possible regio- and stereoisomers in the resulting polymer. Second and more importantly, the fact that the alkyl chain can no longer remain coplanar with the π-conjugated system produces an increase of the distance between the conjugated chains and hence an increase of the band gap and a drop of the charge-carrier's mobility.

Replacing the chain attachment to be on an sp^2 carbon, Roncali and coworkers synthesized 3,4-phenylenedioxythiophene (PheDOT) **6 (Figure 1.20)** [60, 61]. In order to obtain soluble polymer compounds, PheDOT-(n-Hexyl) **7** and PheDOT-(n-Hexyl)$_2$ **8** were synthesized by transetherification of 3,4-dimethoxythiophene using the appropriate catechols. The results from cyclic voltammetry indicated that replacement of the ethylenedioxy bridge by a phenylenedioxy moeity leads to a strong stabilization of the cation radical. As shown by *ab* initio computations at the hybrid density functional theory level, the HOMO level of PheDOT **6** is slightly higher than that of EDOT. However whereas the SOMO of the EDOT radical has high coefficients on the 2,5-positions, in agreement with its straightforward electropolymerization, the PheDOT **6** cation radical SOMO coefficients are essentially localized on the dioxin ring and null on the 2,5-positions of the thiophene ring **(Figure 1.21)**. These results are in full agreement with the experiment showing that the high stability of the PheDOT **6** cation radical could not undergo efficient polymerization [60, 61].
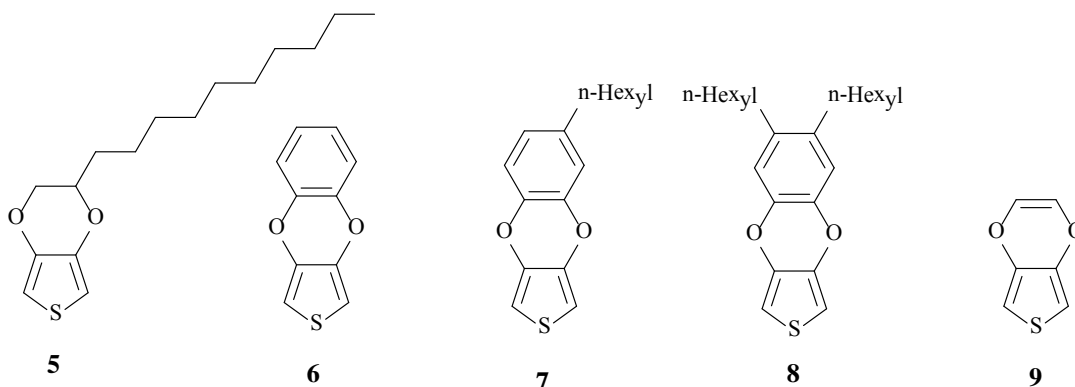
Figure 1.20 The structure of functionalized EDOT derivatives
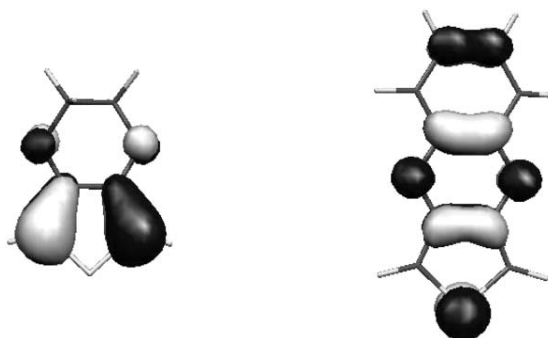
Figure 1.21 SOMO of the cation radicals, Left: EDOT, Right: PheDOT [60, 61]

In 2006, this group has recently reported the synthesis of 3,4 vinylenedioxy-thiophene (VDOT) **9** in which the ethylene bridge of EDOT has been replaced by a vinylene **(Figure 1.20)** [62]. The X-ray data for the dimer reveal a more compact crystal structure than that of EDOT dimer consistent with stronger π-intermolecular interactions. This property associated with the higher oxidation potential of this dimer and its polymer suggests that VDOT-based extended π-conjugated systems should exhibit a better environmental stability than their EDOT analogs.

Wudl and coworkers (2003) reported a surprisingly simple route towards PEDOT, which involves the spontaneous polymerization of 2,5-dibromo-3,4-ethylenedioxythiophene in its crystalline form to obtain high conductivity PEDOT [50, 51]. Very recently, Skabara and coworkers reported the discovery of solid state polymerization in three new dibromothiophene compounds **10-12** as shown in **Figure 1.22**. The X-ray crystallography showed that the molecules are held in close proximity by several short intermolecular contacts [63].

10   **11**   **12**
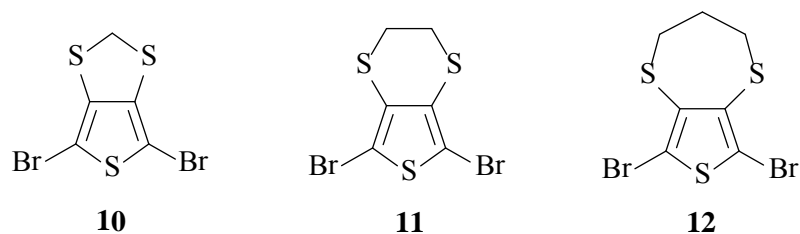
Figure 1.22 The structure of three new dibromothiophene compounds

1.16 Statement of the problem

3,4-Ethylenedioxythiophene (EDOT) represents a class of conducting polymers, which was environmentally stable, easy to synthesize, structurally versatile and high conductivity in doped state. However, unsubstituted EDOTs are insoluble, thereby presenting a significant disadvantage for possible technological applications. An alternate approach to obtain derivatized polymer with high conductivity is the well-ordered polymer synthesis or polymerization of a structurally preorganized crystalline monomer (solid-state polymerization; SSP). This research will be aimed at functionalization of EDOT by substitution at ethylene bridge of this monomer. Furthermore, we will study many properties especially the conductivity of the polymer which was synthesized either from oxidative polymerization with ferric chloride ($FeCl_3$) or solid-state polymerization (SSP) of the newly functionalized monomer.

1.17 Objectives

The goal of the project emphasizes the synthesis of 3,4-ethylenedioxy-thiophene substituted at ethylene bridge and study the processes of polymerizations of thiophene derivative monomers either through the traditional oxidative coupling method and solid-state polymerization (SSP), in order to achieve better compromise between processible and conductive properties of the polymers.

CHAPTER II

EXPERIMENTS

2.1 Chemicals

Thin layer chromatography (TLC) was performed on aluminium sheets precoated with silica gel (Merck Kieselgel 60 F_{254}) (Merck KgaA, Darmstadt, Germany). Column chromatography was performed using silica gel 0.06-0.2 mm or 70-230 mesh ASTM (Merck Kieselgel 60 G, Merck KgaA, Darmstadt, Germany). Solvents used in synthesis were reagent or analytical grades. Solvents used in column chromatography were distilled from commercial grade prior to use. Other reagents were purchased from the following venders:

- Labscan (Bangkok, Thailand): chloroform, concentrated hydrochloric acid, toluene, tetrahydrofuran (THF), dimethylsulfoxide (DMSO), acetonitrile, acetic acid (AcOH),
- Acrös Organic (USA): *N*-bromosuccinimide (NBS), *N*-chlorosuccinimide (NCS), *p*-toluenesulfonic acid (PTSA), calcium hydride (CaH_2), 1,2-dibromoethane, *N*-(2-bromoethyl)phthalimide,
- Carlo Erba Reagent (Milan, Italy): ferric chloride ($FeCl_3$), potassium carbonate (K_2CO_3), sodiumsulfide nonahydrate ($Na_2S.9H_2O$), sodium chloride (NaCl)
- Fluka Chemical Company (Buchs, Switzerland): diethyl oxalate ($CO_2Et)_2$, triethylamine (TEA)
- Merck Co. Ltd. (Darmstadt, Germany): ethanol absolute AR Grade (EtOH), anhydrous sodium hydrogen carbonate ($NaHCO_3$), sodium hydroxide (NaOH), acetone AR Grade, acetonitrile, diethyl ether (Et_2O), sodium iodide (NaI)
- Riedel-de Haën: anhydrous aluminum (III) chloride ($AlCl_3$), *N,N*-dimethylformamide (DMF), sodium (Na)

- Aldrich : 3,4-ethylenedioxythiophene (EDOT), 3,4-dimethoxythiophene (DMT), ethyl chloroacetate, 3,4-dichloro-1-butene, 2,5-dihydroxy-benzoic acid (DHB)

- Wilmad (New Jersey, USA): deuterated chloroform, deuterated dimethylsulfoxide, deuterated acetone

- Fisher : anhydrous sodium sulfate (Na_2SO_4)

- Sigma : α-cyano-4-hydroxycinnamic acid (CCA)

2.2 Instruments and equipments

2.2.1 Melting Point

Melting points were determined with a Stuart Scientific Melting Point SMP1 (Bibby Sterlin Ltd., Staffordshire, UK).

2.2.2 Nuclear Magnetic Resonance Spectrometer (NMR)

The ^{1}H-NMR and ^{13}C-NMR spectra were recorded on a Varian Mercury NMR spectrometer operated at 400.00 MHz for ^{1}H and 100.00 MHz for ^{13}C nuclei (Varian Company, USA) by using deuterated chloroform ($CDCl_3$), deuterated dimethylsulfoxide (DMSO-d_6) or deuterated acetone (Acetone-d_6) as the solvent and tetramethylsilane as the internal standard relative to which the chemical shifts (δ) are given.

2.2.3 Fourier Transform Infrared Spectrometer (FT-IR)

All the monomer and polymer solid samples were mixed with potassium bromide and pressed into pellets and recorded their spectra using a Perkin-Elmer FT-IR, spectrum RXI spectrometer (Perkin Elmer Instruments LLC., Shelton., U.S.A.) Liquid samples were analyzed as neat.

2.2.4 Mass Spectrometer

The mass spectra were recorded on Mass Spectrometer: Waters Micromass Quatto micro API ESCi (Waters, USA). Samples were dissolved in EtOAc, MeOH or acetone.

2.2.5 Matrix-assisted laser desorption/ionisation-time of flight mass spectrometer (MALDI-TOF MS)

Mass spectra were performed on a Matrix Assisted Laser Desorption/ Ionization Time of Fight (MALDI-TOF) : Microflex mass spectrometer (Bruker Daltonik GmbH, Germany). The instrument was equipped with a nitrogen laser to desorbed ionize the samples are deposited. α-Cyano-4-hydroxycinnamic acid (CCA) matrix solution for polymer was prepared in 1:2 acetonitrile/H_2O. The samples were dissolved in 0.1%TFA.

2.2.5 UV-Vis Spectrophotometer

The UV-Vis absorption spectra were recorded on UV-VISIBLE Spectrometer: UV-2550 (Shimadzu Corporation, Kyoto, Japan).

2.2.6 Conductivity Measurements

Four-point probe technique was used for conductivity measurements using (KEITHLEY Semiconductor Characterization System 4200) (**Appendix B**).

2.2.7 X-ray Diffractometer (XRD)

Diffractograms of monomer and polymer by model Rigaku D5000 using a scan range of 5.00-50.00 degree, a scan speed of 5.00 deg min^{-1} and a sample width of 0.020 degree.

2.2.8 Thermogravimetric Analysis (TGA)

The combustion stage and melting point were investigated by a Simultaneous Thermal Analyzer model Netzsch STA 409. Samples were analyzed by heating from 25 °C to 700 °C using 20 °C min^{-1} heating rate under nitrogen atmosphere.

2.2.9 Differential Scanning Calorimeter (DSC)

The thermal behaviours of samples were studied by a Mettler Toledo DSC822^{e}. The specimens of about 7±1 mg were heated under nitrogen atmosphere from 25 to 350 ºC at a scan rate of 20 ºC.min^{-1}. The temperature was then maintained at 350 ºC for 5 min before cooling to 25 ºC at the same rate.

2.2.10 Scanning Electron Microscope (SEM)

The surface morphologies of the polymers were analyzed by using JEM-2100 (JEOL, Tokyo, Japan) scanning electron microscope**.**
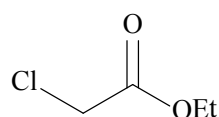
2.2.11 Elemental Analyser (EA)

The elemental analysis of carbon and hydrogen of monomer was investigated by Perkin Elmer PE2400 Series II.

2.3. Monomer synthesis

2.3.1 Williamson synthesis of diethyl 3,4-dihydroythiophene-2,5-dicarboxylate

2.3.1.1 Ethyl chloroacetate 13d

13d

A two-necked round-bottomed flask containing 50 mL (56.5 g, 0.5 mol) of chloroacetyl chloride was equipped with an addition funnel containing 32 mL (25.4 g, 0.55 mol) of EtOH. While the reaction was stirred at 0 ℃, EtOH was added dropwise over a period of 30 min. The reaction mixture was then warmed to room temperature and stirred for another 30 min. The mixture was quenched by 0.5 M NaOH and extracted with diethyl ether. The organic phase was separated and the aqueous phase was extracted twice with ether. The combined organic layer was dried over sodium sulfate. The solvent was removed by a rotary evaporator to give the product as a colorless liquid (55 mL, 99%). ^{1}H-NMR (400 MHz, CDCl$_3$): δ (ppm) 4.21 (q, 2H), 3.99 (s, 2H), 1.23 (t, 3H) (**Figure A.1** , **Appendix A**). ^{13}C-NMR (100 MHz, CDCl$_3$): δ (ppm) 167.5, 62.2, 40.3, 14.1 (**Figure A.2** , **Appendix A**). IR (neat, cm^{-1}): 2968 (-CH st), 1725 (C=O st) (**Figure A.3** , **Appendix A**) [55].

2.3.1.2 Ethyl iodoacetate 13e
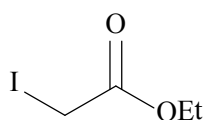
13e

To a stirred solution of sodium iodide (23 g, 0.15 mol) in acetone (100 mL) at room temperature was added dropwise ethyl chloroacetate (11 mL, 0.1 mol) under

nitrogen. The resulting reaction mixture was warmed to 60 ºC and further stirred for 30 min. After cooling back to room temperature, 1 M $NaHCO_3$ (100 mL) was added and extracted three times with dichloromethane. The combined organic layer was dried over sodium sulfate. The solvent was removed by rotary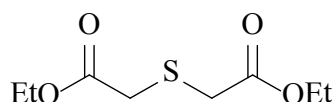 evaporator to obtain the product as a brown liquid (20 g, 91%). ^{1}H-NMR (400 MHz, $CDCl_3$): δ (ppm) 4.18 (q, 2H), 3.62 (s, 2H), 1.22 (t, 3H) (**Figure A.4**, **Appendix A**). ^{13}C-NMR (100 MHz, $CDCl_3$): δ (ppm) 174.1, 71.3, 20.5, 0.2 (**Figure A.5**, **Appendix A**). IR (neat, cm^{-1}): 1745 (C=O) (**Figure A.6**, **Appendix A**).

2.3.1.3 Synthesis of diethyl thiodiglycolate 14

14

A solution of sodium sulfide nonahydrate ($Na_2S.9H_2O$, 12.0 g, 50 mmol) in water (30 mL) was added dropwise to the solution of ethyl chloroacetate (13.2 g, 55 mmol) in acetone (50 mL). The reaction was stirred at 60 ˚C under nitrogen for additional 3 h. After cooling back to room temperature, it was extracted with diethyl ether, washed with 0.5 M NaOH and water. After being dried over anhydrous sodium sulfate, the solution was distilled under reduced pressure to give compound **14** as a yellow liquid. (5.1 g, 50%) ^{1}H-NMR (400 MHz, $CDCl_3$): δ (ppm) 4.13 (q, 4H), 3.32 (s, 4H), 1.23 (t, 6H) (**Figure A.7**, **Appendix A**). ^{13}C-NMR (100 MHz, $CDCl_3$): δ (ppm) 169.5, 61.1, 33.3, 13.9 (**Figure A.8**, **Appendix A**). IR (neat, cm^{-1}): 2980 (-CH st), 2936, 1790 (C=O st), 1289 (-C(O)O st), 1150 (-C-O st) (**Figure A.9**, **Appendix A**).MS: [M+Na]$^+$ m/z = 229.05 (**Figure A.10, Appendix A**).

2.3.1.4 Synthesis of diethyl 3,4-dihydroxythiophene-2,5-dicarboxylate 15

15
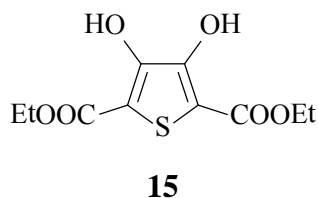
Sodium metal (3.5 g, 0.30 mol) was added into absolute ethanol (75 mL) and then added a mixture of compound **14** (1.02 g, 5 mmol) and diethyl oxalate (0.92 g, 6.3 mmol) dropwise over 30 min in ice bath. The mixture was refluxed for additional 2 h, cooled to room temperature, then poured into water (100 mL) and acidified by concentrate hydrochloric acid to afford a yellow precipitate. The filtered solid was recrystallized from methanol to give compound **15** as white needle crystals. (0.90 g, 70%) mp. 134-135 ˚C. ^{1}H-NMR (400 MHz, CDCl$_3$): δ (ppm) 9.36 (s, 2H), 4.38 (q, 4H), 1.38 (t, 6H) (**Figure A.11**, **Appendix A**). ^{13}C-NMR (100 MHz, CDCl$_3$): δ (ppm) 165.5, 151.6, 107.1, 61.7, 14.0 (**Figure A.12**, **Appendix A**). IR (KBr, cm^{-1}): 3293 (-OH st), 2987 (-CH st), 1661 (C=O st), 1508 (C=C st) (**Figure A.13**, **Appendix A**).MS: [M-H]$^+$ m/z = 259.20 (**Figure A.14, Appendix A**).

2.3.1.5 Synthesis of diethyl 3,4-dialkoxythiophene-2,5-dicarboxylates 16

General procedure: 1 equivalent of compound **15** (520.52 mg, 2 mmol) in dry *N,N*-dimethyl formamide (10 mL) was added the corresponding alkylhalide, followed by 3 equivalents of base (potassium carbonate, K$_2$CO$_3$ or triethylamine, TEA). The mixture was allowed to stir at 90 ˚C under nitrogen and then cooled to room temperature. The mixture was filtered and rinsed with 50 mL diethyl ether. The ethereal mixture was added 4:1 H$_2$O-brine solution which was extracted with ether. The organic extracts were collected and washed twice with the same ratio of H$_2$O-brine solution. After dried by anhydrous Na$_2$SO$_4$, filtered and concentrated in a rotary evaporator, the product **16d** was obtained after column chromatography (1:2 ethyl acetate/hexane) which **16a, 16b** and **16c** were obtained after recrystallization from methanol.

2.3.1.5.1 Synthesis of diethyl 2,3-dihydrothieno[3,4-*b*][1,4]dioxine-5,7-dicarboxylate 16a
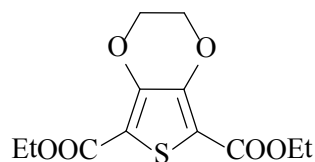
16a

Prepared according to the general procedure from diethyl 3,4-dihydroxy-thiophene-2,5-dicarboxylate **15** (522.2 mg, 2.0 mmol), 1,2-dibromoethane (0.22 mL, 2.6 mmol) and triethylamine (0.9 mL, 6 mmol) in dry DMF (10 mL). The mixture was allowed to stir for 24 hours at 90 ºC. The product was purified by crystallization from methanol to get white needle crystal (240.4 mg, 77%). ^{1}H-NMR (400 MHz, CDCl$_3$): δ (ppm) 4.34 (s, 2H), 4.27 (q, 4H), 1.30 (t, 6H) **(Figure A.15, Appendix A)**. ^{13}C-NMR (100 MHz, CDCl$_3$): δ (ppm) 160.7, 144.9, 111.7, 64.7, 61.2, 14.2 **(Figure A.16, Appendix A)**. IR (KBr, cm^{-1}): 2987 (-CH st), 2941, 1694 (C=O st)**, (Figure A.17, Appendix A)**. MS: [M+H]$^{+}$ m/z = 287.21 **(Figure A.18, Appendix A)**.

2.3.1.5.2 Synthesis of diethyl 2-vinyl-2,3-dihydrothieno[3,4-*b*][1,4] dioxine-5,7-dicarboxylate 16b
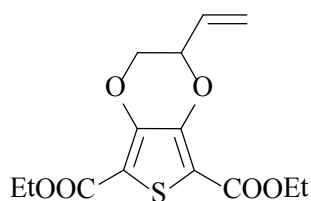

16b

The title compound was synthesized according the general procedure from compound **15** (521.2 mg, 2.0 mmol), 3,4-dichloro-1-butene (0.37 mL, 3.4 mmol) and triethylamine (0.84 mL, 6.0 mmol) in dry DMF (10 mL). The mixture was allowed to stir for 72 hours at 90 ºC. After recover the starting compound, product was purified

by crystallization from MeOH to yield compound **16b** as a   white needle crystal (149.2 mg, 42%). ^{1}H-NMR (400 MHz, CDCl$_3$): δ (ppm) 5.87 (m, 1H), 5.54 (d, 1H), 5.39 (d, 1H), 4.76 (m, 1H), 4.37 (m, 1H), 4.29 (q, 4H), 4.04 (m, 1H), 1.32 (t, 6H) **(Figure A.19, Appendix A)**. ^{13}C-NMR (100 MHz, CDCl$_3$): δ (ppm) 160.7, 144.7, 144.6, 130.5, 120.4, 111.8, 111.6, 74.2, 67.8, 61.3, 61.2, 14.2 **(Figure A.20, Appendix A)**. IR (KBr, cm^{-1}): 2983 (-CH st), 1702 (C=O st), 1502 (C=C st), 1453 (C=C st), 1268 (-C(O)O st). **(Figure A.21, Appendix A)**.   MS: [M+Na] $^{+}$ m/z = 335.27 **(Figure A.22, Appendix A)**.

2.3.1.5.3 Synthesis of diethyl 3,4-bis(2-(1,3-dioxoisoindolin-2-yl)ethoxy) thiophene-2,5-dicarboxylate 16c
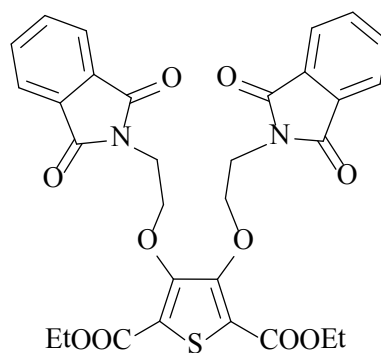
16c

Compound **15**(521.9 mg, 2.0 mmol), *N*-(2-bromoethyl)pthalimide (1529 mg, 6.02 mmol) and triethylamine (0.85 mL, 6.0 mmol) in dry DMF (10 mL). The solution was stirred at 90 ºC overnight. The product was purified by crystallization from MeOH to obtain a white solid (525.1 mg, 43%). ^{1}H-NMR (400 MHz, CDCl$_3$): δ (ppm) 7.78 (s, 4H), 7.65 (s, 4H), 4.33 (s, 4H), 4.07 (q, 4H), 3.99 (s, 4H), 1.16 (t, 6H) **(Figure A.23**, **Appendix A)**. ^{13}C-NMR (400 MHz, CDCl$_3$): δ (ppm) 168.1, 160.0, 152.1, 133.8, 132.1, 123.2, 122.9, 119.8, 71.0, 61.3, 37.7, 14.1 **(Figure A.24**, **Appendix A)**. IR (KBr, cm^{-1}): 3308 (-NH st), 2989 (-CH st), 1688 (C=O st), 1664 (C=O st), 1513 (C=C st) **(Figure A.25**, **Appendix A)**. MS: [M+Na]$^{+}$ m/z = 607.48 **(Figure A.26**, **Appendix A)**.

2.3.1.5.4 Synthesis of diethyl 3,4-bis(2-ethoxy-2-oxoethoxy)thiophene-2,5-Dicarboxylate 16d
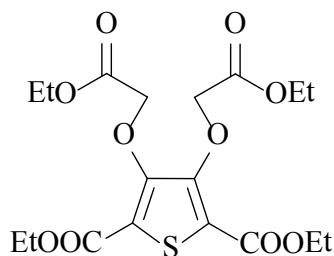
16d

diethyl 3,4-bis(2-ethoxy-2-oxoethoxy)thiophene-2,5-dicarboxylate **16d** was prepared as previous described in the general procedure. Compound **15** (523.5 mg, 1.99 mmol), ethyl chloro acetate (0.65 mL, 6.0 mmol), K_2CO_3 (831.6 mg, 6.03 mmol) in dry DMF (10 mL). The reaction was added KI (1.054 g, 6.35 mmol) and stirred for 48 hours at 90 ºC. Crude was purified by column chromatography using hexane/EtOAc (3:1) as eluent to yield the product as a yellow oil (419.6 mg, 49%). ^{1}H-NMR (400 MHz, CDCl$_3$): δ (ppm) 4.74 (s, 2H), 4.15 (q, 4H), 4.05 (q, 4H), 1.18 (t, 6H), 1.11 (t, 6H) (**Figure A.27**, **Appendix A**). ^{13}C-NMR (100 MHz, CDCl$_3$): δ (ppm) 168.3, 160.1, 150.9, 119.1, 70.1, 61.5, 61.1, 14.0 (**Figure A.28**, **Appendix A**). IR (KBr, cm^{-1}): 2980 (-CH st), 1756 (C=O st), 1720 (C=O st), 1293 (-C(O)O st), 1205 (-C(O)O st) (**Figure A.29, Appendix A**). MS: [M+Na]$^+$ m/z = 455.52 (**Figure A.30**, **Appendix A**).

### 2.3.1.6 Synthesis of diethyl 3,4-alkylenedioxythiophene-2,5-dicarboxylic acid derivatives 17

General procedure: One equivalent of 2,5-dicarbethoxy-3,4-alkylenedioxy-thiophene was stirred at reflux temperature under nitrogen for 10 h with 1 M of NaOH and EtOH. The resulting solution was cooled to room temperature and acidified with 10% HCl to precipitate a white solid product. The product was filtered, washed with water, and dried under vacuum.

2.3.1.6.1 Synthesis of 2,3-dihydrothieno[3,4-*b*][1,4]dioxine-5,7-dicarboxylic acid 17a
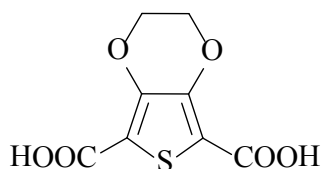
17a

Method I:

As the general procedure, 3,4-ethylenedioxythiophene-2,5-dicarboxylate **16a** (285.4 mg, 1.0 mmol); 10 mL of 1 M NaOH; 1 mL of EtOH. The precipitate was collected by filtration and was washed with water to yield diacid compound as a white solid (220.2 mg, 96 %). ^{1}H-NMR (400 MHz, DMSO): δ (ppm) 4.41 (s, 4H) (**Figure A.35**, **Appendix A**). ^{13}C-NMR δ (100 MHz, DMSO): (ppm) 162.2, 145.1, 112.2, 65.3 (**Figure A.36**, **Appendix A**).

Method II:

To a stirred solution of diethyl 3,4-dihydroxythiophene-2,5-dicarboxylate **15** (261.1 mg, 1 mmol), 1,2-dibromoethane (0.12 mL. 1.3 mmol), triethylamine (0.42 mL, 3 mmol) dissolved in dry DMF (10 mL). The mixture was allowed to stir for 24 h at 90 ℃ under nitrogen. After cooling back to room temperature, the mixture was filtrated and the solvent was added to the solution of 1 M NaOH (10 mL) and EtOH (2 mL). The mixture was refluxed for 10 h. The reaction was allowed to cool to room temperature and poured into water (10 mL). After being acidified by 10% HCl, the white precipitate formed was collected by filtration. The pure product was obtained as white crystals by recrystallization from methanol (78.1 g, 34%).

2.3.1.6.2 Synthesis of 2-vinyl-2,3-dihydrothieno[3,4-*b*][1,4]dioxine-5,7-dicarboxylic acid 17b
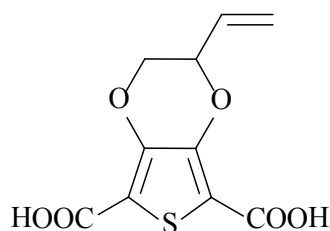
17b

As the general procedure; diethyl 2-vinyl-2,3-dihydrothieno[3,4-*b*][1,4] dioxine-5,7-dicarboxylate **16b** (125.1 mg, 0.4 mmol); 10 mL of 1 M NaOH; 1 mL of EtOH. The precipitate was collect and was washed with water to obtain diacid compound **17b** as a white needle crystals (91.4 mg, 90%). ^{1}H-NMR (400 MHz, Acetone-d6): δ (ppm) 5.91 (m, 1H), 5.48 (d, 1H), 5.31 (d, 1H), 4.80 (m, 1H), 4.38 (m, 1H), 4.04 (m, 1H) (**Figure A.37**, **Appendix A**). ^{13}C-NMR δ (100 MHz, Acetone-d6): (ppm) 161.1, 144.5, 144.0, 132.4, 122.4, 119.4, 112.8, 74.1, 67.3 (**Figure A.38**, **Appendix A**). IR (KBr, cm^{-1}): 3455 (-OH st), 1664 (C=O st) (**Figure A.39**, **Appendix A**).

2.3.1.6.3 Synthesis of 3,4-bis(carboxymethoxy)thiophene-2,5-dicarboxylic acid 17d
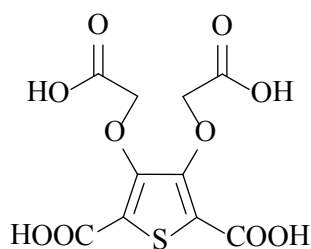
17d

As the general procedure; diethyl 3,4-bis(2-ethoxy-2-oxoethoxy)thiophene-2,5-dicarboxylate **16d** (132.5 mg, 0.3 mmol); 5 mL of 1 M NaOH; 1 mL of EtOH. The precipitate was collect and was washed with water to obtain tetraacid compound

17d as a white solid (93.6 mg, 95%) ^{1}H-NMR (400 MHz, Acetone-d6): δ (ppm) 5.14 (s, 4H) (**Figure A.40**, **Appendix A**). ^{13}C-NMR δ (100 MHz, Acetone-d6): δ (ppm) 170.0, 161.0, 150.8, 118.9, 69.9 (**Figure A.41**, **Appendix A**).

2.3.1.7 Synthesis of 3,4-Alkylenedioxythiophenes

General procedure: One equivalent of 2,5-dicarboxy-3,4-alkylenedioxy-thiophene was heated at 150 °C with 17 mol % of cuprous oxide (Cu$_2$O) in quinoline for 20 h under nitrogen. After cooling, the mixture was filtered and poured into an excess of 10% HCl. The product was extracted with diethyl ether, washed with dilute hydrochroric acid; with dilute sodium hydrogen carbonate; and with water. Ether was removed under reduced pressure after drying the organic layer over anhydrous sodium sulfate. The products were purified by flash column chromatography using dichloromethane as eluent.

2.3.1.7.1 Synthesis of 2,3-dihydrothieno[3,4-b][1,4]dioxine (EDOT) 1

1

As general procedure; 2,3-dihydrothieno[3,4-*b*][1,4]dioxine-5,7-dicarboxylic acid **17a** (230.1 mg, 1.0 mmol); cuprous oxide (25.10 mg, 0.17 mmol); 10 mL of quinoline. Column chromatography using CH$_2$Cl$_2$ as eluent afforded 3,4-ethylene dioxythiophene as a yellow oil (103.48 mg, 73%). ^{1}H-NMR (400 MHz, CDCl$_3$): δ (ppm) 6.36 (s, 1H), 4.22 (s, 2H) (**Figure A.42**, **Appendix A**). ^{13}C⁻NMR δ (CDCl$_3$) (ppm): 141.7, 99.7, 64.7 (**Figure A.43**, **Appendix A**). IR (neat, cm^{-1}): 3107 (CH$_α$- st), 2984 (CH- st), 1486 (C=C), 1371 (C=C), 1060 (CH$_2$O st) (**Figure A.44**, **Appendix A**).
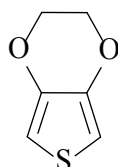
2.3.1.7.2 Synthesis of 2-vinyl-2,3-dihydrothieno[3,4-b][1,4]dioxine
(EDOT-Vinyl) 18b
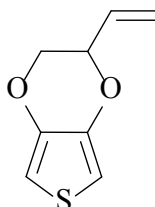
18b

As general procedure; Synthesis of 2-vinyl-2,3-dihydrothieno[3,4-*b*][1,4] dioxine-5,7-dicarboxylic acid **17b** (76.6 mg, 0.3 mmol); Cu_2O (7.2 mg, 0.17 mmol); 10 mL of quinoline. Column chromatography using CH_2Cl_2 as eluent afforded 2-vinylene-3,4-ethylenedioxythiophene as a yellow oil (34.8 mg, 70%). ^{1}H-NMR (400 MHz, $CDCl_3$): δ (ppm) 6.35 (s, 1H), 6.33 (s, 1H), 5.88 (m, 1H), 5.54 (d, 1H), 5.40 (d, 1H), 4.63 (m, 1H), 4.20 (m, 1H), 3.90 (m, 1H) (**Figure A.44**, **Appendix A**). ^{13}C-NMR δ ($CDCl_3$) (ppm): 141.7, 141.4, 119.6, 99.7, 99.6, 70.2, 68.0, 60.4 (**Figure A.45**, **Appendix A**).

2.3.2 Ester of L-tartaric acid

2.3.2.1 L-Tartaric acid dibenzyl ester 21
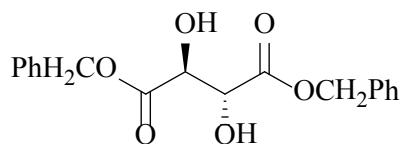
21

A one-necked of round bottomed flask was equipped with a magnetic stirrer and a Dean-Stark trap. The flask containing L-tartaric acid (1.50 g, 10 mmol), benzyl alcohol (3.10 mL, 30 mg) and *p*-toluenesulfonic acid monohydrate (PTSA: 24.5 mg,

0.12 mmol) were dissolved in toluene (30 mL). The mixture was heated under reflux tuluene for 20 h. During this period some amount of water was collected. The mixture was allowed to cool to room temperature, diluted with diethyl ether, and poured into 20 mL of 1 M NaHCO$_3$. The organic phase was separated and the aqueous phase was extracted twice with diethyl ether. The combined organic phases were dried over sodium sulfate. The solvent was removed with a rotary evaporator, and the resulting crude product was triturated with hexane-ether (20:1) to give white crystals of dibenzyl tartrate. The precipitate was collected by filtration and washed with hexane-ether (20:1). The filtrate was further concentrated to give a second crop. The total yield is 6.2 g (94%). mp 49–50 °C; (2.756 g, 93%). mp. 50-51 °C. ^{1}H-NMR (400 MHz, CDCl$_3$): δ (ppm) 7.41 (s, 10H), 5.25 (q, 4H), 4.61 (s, 2H), 2.77 (br, 2H) (**Figure A.46**, **Appendix A**). ^{13}C-NMR (100 MHz, CDCl$_3$): δ (ppm) 172.0, 135.1, 128.4, 128.2, 72.5, 68.1 (**Figure A.47**, **Appendix A**). IR (KBr, cm^{-1}): 3489 (-OH st), 3034 (-CH unsat st), 2946 (-CH st), 1755 (C=O st), 1501-1458 (C=C st), 1283 (-C(O)-O- st), 1086 (-O-CH$_2$- st) (**Figure A.48**, **Appendix A**). [55].

2.3.2.2 L-Tartaric acid dibutyl ester 22

22
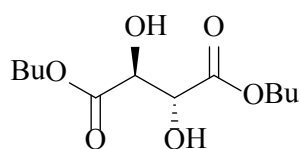
L-Tartaric acid dibutyl ester **22** was obtained in the similar way to that described for dibenzyl tartrate **21**, starting from L-tartaric acid (1.50 g, 10 mmol), n-butanol (2.80 mL, 30 mmol) and PTSA (22.10 mg, 0.12 mmol) were dissolved in toluene (30 mL). The mixture was heated under reflux toluene for 15 h. to yield the product as a colorless oil at room temperature or white needle crystal at 0 °C (2.756 g, 93%). ^{1}H-NMR (400 MHz, CDCl$_3$): δ (ppm) 4.55 (s, 2H), 4.29 (t, 4H), 2.99 (br, 2H), 1.69 (p, 4H), 1.41 (m, 4H), 0.98 (t, 6H) (**Figure A.49**, **Appendix A**). ^{13}C-NMR (100 MHz, CDCl$_3$): δ (ppm) 172.0, 72.1, 66.0, 30.1, 18.2, 13.9 (**Figure A.50**, **Appendix**

A). IR (neat, cm^{-1}): 3470 (-OH st), 2964 (-CH st), 1749 (C=O st), 1281 (-C(O)-O- st), 1088 (-O-CH$_2$- st) (**Figure A.51**, **Appendix A**).

2.3.3 Transetherification of 3,4-dimethoxythiophene

General procedure for transetherification: 1 equivalent of 3,4-dimethoxy thiophene was added to dry toluene; to this 2 equivalent of the corresponding alkyl-substituted ethane-1,2-diol was added, and it was followed by *p*-toluene sulphonic acid (PTSA) as a catalyst. The mixture was allowed to stir at 100 ºC with a continuous flow of nitrogen through the reaction mixture. After cooling, it was extracted with dichloromethane, washed with 0.5 M sodium hydrogen carbonate and water. After being dried over anhydrous sodium sulfate, excess solvent was evaporated and the residue was purified by column chromatography to obtain the product.

2.3.3.1 Synthesis of 3,4-dibutoxythiophene 23
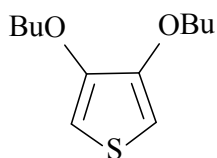
23

A solution of 3,4-dimethoxythiophene (145.1, 1 mmol), with 3 equivalent of n-butanol (0.28 mL, 3 mmol) and a catalytic amount PTSA (20.1 mg) in dry toluene (10 mL) was stirred for 24 h at 100 ºC. The completion of the reaction was monitor by thin layer chromatography (TLC). Toluene was removed under reduced pressure and the residue was diluted with water. The mixture was extracted with diethyl ether. The combined organic layer were watched with dilute NaHCO$_3$ solution and then concentrated. Purification of the crude residue by chromatography on silica gel hexane/CH$_2$Cl$_2$ (3:2) gave product as a yellow oil (230.6 mg, 86%). ^{1}H-NMR (CDCl$_3$) δ (ppm): 6.19 (s, 2H), 3.99 (q, 4H), 1.82 (m, 4H), 1.49 (m, 2H), 0.97 (m, 6H) (**Figure A.52**, **Appendix A**). ^{13}C-NMR δ (CDCl$_3$) (ppm): 147.9, 96.8, 70.2, 31.3,

18.9, 14.1 (**Figure A.53**, **Appendix A**). IR (neat, cm^{-1}): 2954 (CH- st), 1509 (C=O) (**Figure A-54**, **Appendix A**).

2.3.3.2 Synthesis of 3,4-cyclohexylenedioxythiophene (CDOT) 25
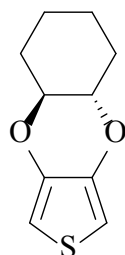
25

To a mixture of 3,4-dimethoxythiophene (431.7 mg, 3.0 mmol); (±) *trans*-1,2-cyclohexanediol (698.6 mg, 6.0 mmol); PTSA (58.1 mg, 0.3 mmol) in 15 mL of dry toluene to stir for 72 h at 100 C. Column chromatography using hexane/CH$_2$Cl$_2$ (3:2) as eluent afforded ±(4a*R*,8a*R*)-4a,5,6,7,8,8a-hexahydrobenzo[*e*]-thieno[3,4-*b*] [1,4] dioxine **25** as a white needle crystals (453.5 mg, 86%). mp. 142-143 ℃; ^{1}H-NMR (CDCl$_3$) δ (ppm): 6.21 (s, 2H), 3.71 (q, 2H), 2.15 (q, 2H), 1.77 (q, 2H), 1.33 (m, 4H) (**Figure A.57, Appendix A**). ^{13}C-NMR δ (CDCl$_3$) (ppm): 141.7, 98.1, 76.2, 39.3, 23.5 (**Figure A.58, Appendix A**). IR (KBr, cm^{-1}): 2947 (CH- st), 1471(C=C), 1402 (C=C), 1026 (CH$_2$O st) (**Figure A.59, Appendix A**). Anal. Calcd for C$_{10}$H$_{12}$O$_2$S: C, 61.20; H, 6.47% Found: C, 61.24; H, 6.43%.

2.3.4 Halogenations of thiophene derivatives (X = Br, Cl)
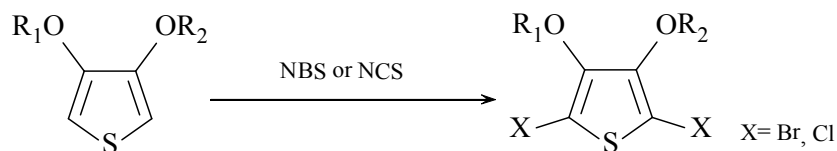
General procedure : In a two-necked 50 mL round bottomed flask was added the thiophene precursor (1 mmol), 2.5 equivalents of *N*-bromosuccinimide (NBS) or *N*-chlorosuccinimide (NCS) and 10 mL of chloroform at room temperature. The

reaction mixture was stirred at ambient temperature. After completion, The reaction mixture was quenched by adding saturated sodium hydrogen carbonate solution. The organic layer was separated, and the aqueous layer was extracted with dichloromethane three times. The combined organic layer was washed with water. After drying over anhydrous sodium sulfate, the solution was evaporated using rotary evaporator. The obtained crude solution was then purified by column chromatography to obtain the corresponding dihalothiophene.

2.3.4.1 2,5-Dibromo-3,4-ethylenedioxythiophene (DBEDOT) 2

2
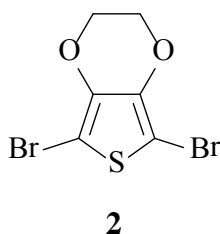
The compound was obtained via bromination of 3,4-ethylenedioxythiophene (EDOT) by adding NBS (0.4450 g, 2.5 mmol) to a stirred solution of EDOT (0.1421 g, 1 mmol) dissolved in chloroform (10 mL) at room temperature under ambient atmosphere for 1 min. The crude mixture was purified by passing through a silica gel column, eluted with 3:2 mixtures of hexane and dichloromethane to get a white solid. It was recrystallized using methanol to produce a white needle crystals (0.4832 g, 85%), mp 96-97 °C; ^{13}H-NMR (400 MHz, CDCl$_3$): δ (ppm) 4.26 (s, 4H) (**Figure A.60**, **Appendix A**) ^{13}C-NMR (100 MHz, CDCl$_3$): δ (ppm) 64.9, 85.5, 139.7 (**Figure A.61**, **Appendix A**). IR (KBr, cm^{-1}): 2949 (-CH st), 1080 (-C-O st) (**Figure A.62**, **Appendix A**). MS: [M-H]$^+$ m/z = 299.1 (**Figure A.63**, **Appendix A**).

### 2.3.4.2 2,5-Dichloro-3,4-ethylenedioxythiophene (DCEDOT) 3
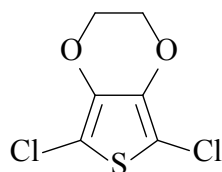
3

The compound was obtained via chlorination of 3,4-ethylenedioxythiophene (EDOT) by adding NCS (0.4450 g, 2.5 mmol) to a stirred solution of EDOT (0.1421 g, 1 mmol) dissolved in chloroform (10 mL) at room temperature under ambient atmosphere for 10 min. The crude mixture was purified by passing through a silica gel column, eluted with 3:2 mixtures of hexane and dichloromethane to get a white solid. It was recrystallized using methanol to produce a white needle crystals (0.4832 g, %). ^{1}H-NMR (400 MHz, CDCl$_3$): δ (ppm) 4.25 (s, 4H) (**Figure A.64**, **Appendix A**). ^{13}C-NMR (100 MHz, CDCl$_3$): δ ☐☐☐(ppm) 137.2, 100.3, 64.8 (**Figure A.65**, **Appendix A**). IR (KBr, cm[-1]): 2949 (-CH st), 1084 (-C-O st) (**Figure A.66, Appendix A**). MS: [M+H]$^+$ m/z = 211.0 (**Figure A.67**, **Appendix A**).

2.3.4.3 2,5-Dibromo-3,4-cyclohexylenedioxythiophene (DBCDOT) 26
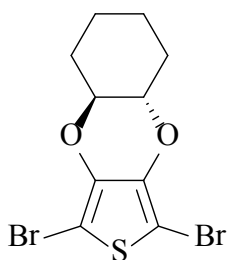
26

Prepared according to the general procedure from 3,4-dimethoxythiophene (491.3 mg, 2.5 mmol) and NBS (1115.4 mg, 6.25 mmol) in chloroform (15 mL). The crude residue was purified by column chromatography using CH$_2$Cl$_2$/hexane (2:3) as eluent to afford the title compound as a white needle crystal (834.6 mg, 94%). ^{1}H-NMR (400 MHz, CDCl$_3$): δ (ppm) 3.78 (m, 1H, 2.34 (m, 1H), 1.83 (m, 1H), 1.52 (m, 1H), 1.41 (m, 1H) (**Figure A.68**, **Appendix A**). ^{13}C-NMR (100 MHz, CDCl$_3$):

δ (ppm) 140.2, 84.8, 77.6 40.1, 23.9 (**Figure A.69**, **Appendix A**). IR (neat, cm⁻¹):
2941(-CH st), 1505-1404 (C=C st), 1065 (-C-O st) (**Figure A.70**, **Appendix A**). Anal.
Calcd for $C_{10}H_{10}O_2Br_2S$: C, 34.92; H, 2.85% Found: C, 34.78; H, 2.83%.

2.3.4.4 2,5-Dibromo-3,4-dimethoxythiophene DBDMT 27
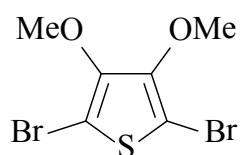
27

The compound was prepared from a reaction of 3,4-dimethoxythiophene
(DMT) (0.1442 g, 1 mmol) and NBS (0.4450 g, 2.5 mmol) in chloroform (10 mL).
The crude mixture was purified by column chromatography, eluted with 4:1 mixtures
of hexane and dichloromethane to get a pale yellow oil of product (0.2583 g,
80%). ^{1}H-NMR (400 MHz, CDCl$_3$): δ (ppm) 3.90 (s, 6H) (**Figure A.71**, **Appendix
A**). ^{13}C-NMR (100 MHz, CDCl$_3$): δ (ppm) 61.2, 95.0, 148.2 (**Figure A.72**, **Appendix
A**). IR (KBr, cm⁻¹): 2945 (-CH st), 1057 (-C-O st) (**Figure A.73**, **Appendix A**). MS:
[M-H]$^+$ m/z = 301.9 (**Figure A.74**, **Appendix A**).

2.4 Polymer synthesis

2.4.1 Oxidative polymerization of 3,4-cyclohexylenedioxythiophene (CDOT)

25
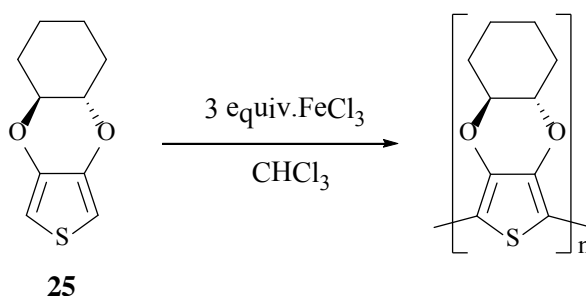
To a well stirred suspension anhydrous FeCl$_3$ (243.6 mg,1.5 mmol) in CHCl$_3$ (20 mL) at room temperature, a solution of 3,4-cyclohexylenedioxythiophene **25** (98.5 mg, 0.5 mmol) in CHCl$_3$ (10 mL) was added dropwise. The reaction mixture was allowed to stirred for 24 h. After cooling, MeOH (20 mL) was added. The resulting dark black suspension was stirred for an additional 2 h at room temperature. The black solid formed was, acetone and hexane, respective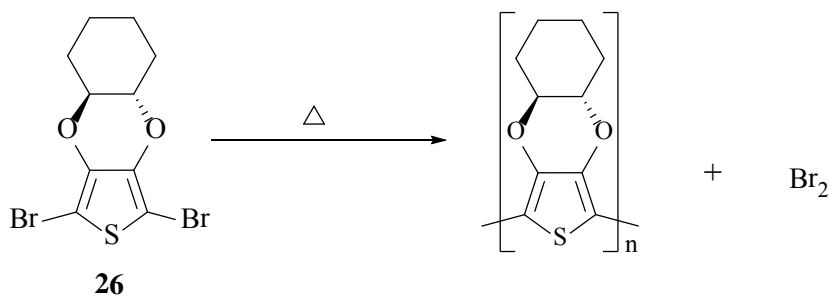ly. The black solid separated by filtration and then washed with MeOH. The black solid was further purified by repeated Soxhlet extraction with MeOH was dried to give the corresponding polythiophene derivatives (62.4 mg, 64%).

2.4.2 Solid state polymerization of of 2,5-dibromo-3,4-cyclohexylene-dioxythiophene (DBCDOT)

In a typical experimental procedure, crystalline 2,5-dibromo-3,4-cyclohexylenedioxythiohene **26** (200 mg) was placed in a round bottle flask that was closed with stopper. The flask was heated at 120 ºC for 24 h, during witch period the original white color of the DBEDOS turned black. The sequence of color changes (from white---grey---dark black) of the material and the appearance of brown bromine vapor in the flask was indicative of the progress of the solid state polymerization. After completion of the reaction, the resulting black PEDOS was collected to afford the bromine-doped polymer in 157 mg.

2.4.3 Dedoping of FeCl$_3$-synthesized and solid-state synthesized PCDOT

To a suspension of well-ground powder of PCDOT (100 mg) in CH_3CN (50 mL) at room temperature was added 50% solution of hydrazonium hydrochloride in water (10 mL). The resulting mixture was stirred overnight at 50 ºC. The black solid was collected by filtration and purified by repeated Soxhlet extraction with acetone and hexane.

2.4.4 Conductivity measurement using Four-point probe conductometer

A polymer from Section 2.3.2.1-2.3.2.3 were pressed for pellet and measured conductivity by Four-point probe conductometer. The measurement was repeated using I_2 doped polymer. Those polymer pellets placed in an iodine chamber. After 24 h, the conductivity of each pellets were measured immediately after being taken out of the container by a Four-point probe conductometer.

CHAPTER III

RESULTS AND DISCUSSION

3.1 Monomer Synthesis

3.1.1 Synthesis of 3,4-dialkoxythiophene derivatives

Alkoxy-thiophenes are the important precursors to generate interesting new materials. They are used as monomers for synthesis of conducting polymer with various applications. The most widely used synthetic route to 3,4-dialkoxythiophenes was the traditional double Williamson synthesis of the intermediate 3,4-dihydroxythiophene [71-75]. This has become our interest to apply such simple procedure to prepare new dialkoxythiophene derivatives that would lead to polymers with improved electronic properties and processability. To achieve the desired product, we started the synthesis by following the five step route illustrated in the previous report [72, 73] as shown in **Scheme 3.1**.
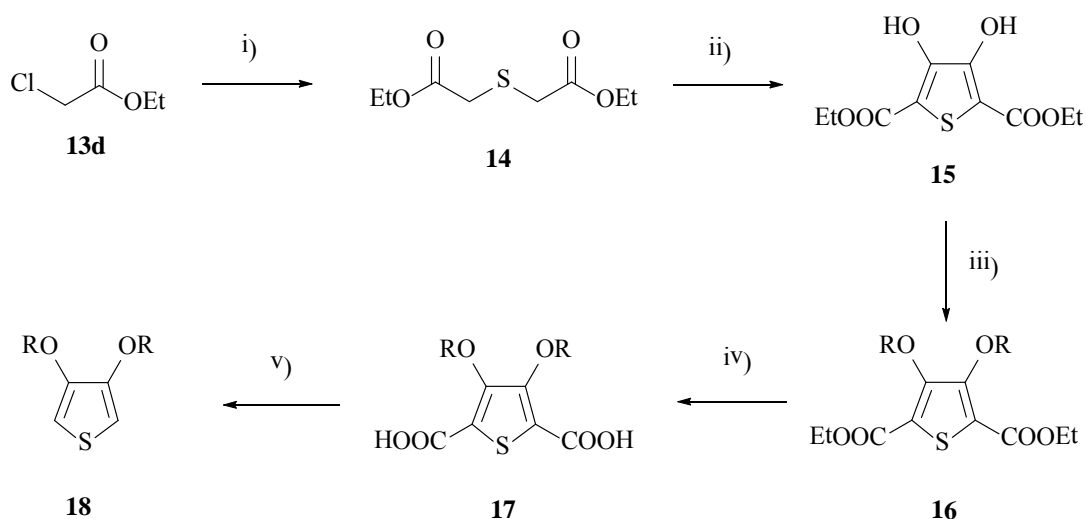
Scheme 3.1 *Reagents and conditions:* i) $Na_2S.9H_2O$, acetone, 60 ºC, 3 h; ii) NaOEt, 0.5 h, $(CO_2Et)_2$, reflux, 1 h, conc.HCl; iii) R-X, base, DMF, 90 ºC; iv) NaOH, EtOH, reflux, 10 h; v) Cu_2O, quinoline, 150 ºC, 20 h.

For these experiments, ethyl chloroacetate **13d** was prepared as a starting material. The reaction of chloroacetyl chloride and ethanol obtained compound **13d** as colorless liquid in excellent yield. This reaction underwent the bimolecular nucleophilic acyl substitution as shown in **Scheme 3.2**. Identification of the product was achieved through FT-IR, ^{1}H-NMR and ^{13}C-NMR spectroscopy. The characteristic quartet and triplet peaks of the newly added ethyl group of compound **13d** clearly operated at δ 4.21, 1.23 ppm in ^{1}H-NMR spectrum (**Figure A.1, Appendix A**) and δ 62.2, 14.1 ppm in ^{13}C-NMR spectrum (**Figure A.2, Appendix A**).
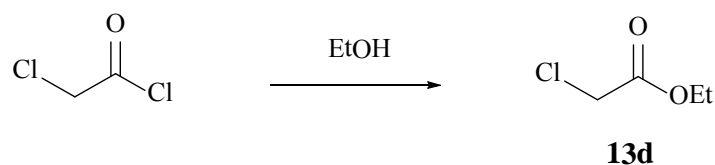
Scheme 3.2 Synthesis of ethyl chloroacetate **13d**

3.1.1.1 Synthesis of diethyl thioglycolate 14

An acetone solution of ethyl chloroacetate **13d** was treated through the S_N2 fashion with sodium sulfide nonahydrate in water. The reaction was stirred for 3 h at 60 °C under nitrogen to give diethyl thioglycolate **14** in 50 %yield (**Entry 2, Table 3.1**), which was much better than ambient atmosphere (**Entry 1, Table 3.1**). Longer reaction time gave only slight increase the product yield (**Entry 3, Table 3.1**).

Table 3.1 Conditions for the synthesis of diester **14**
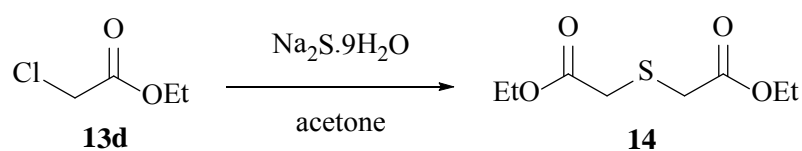
Entry	Conditions	Time (h)	%yield
1	60 °C, air	3	25
2	60 °C, N$_2$	3	50
3	60 °C, N$_2$	24	55

This compound was characterized by ^{1}H-NMR, ^{13}C-NMR, IR and MS. ^{1}H NMR showed the singlet methylene peak at 3.32 ppm and the quartet and triplet ethyl peaks at 4.13 and 1.23 ppm respectively **(Figure A.7, Appendix A)**. In the ^{13}C NMR spectrum, the carbonyl carbon appeared at 169.5 ppm **(Figure A.8, Appendix A)**. In the IR spectrum, the carbonyl group showed a strong absorption band at 1790 cm^{-1} **(Figure A.9, Appendix A)**. Finally, the formation of **14** was supported by the mass value from MS in the positive mode at 229.05 amu [M+Na]$^{+}$ [73] **(Figure A.10, Appendix A)**.

3.1.1.2 Synthesis of diethyl 3,4-dihydroxythiophene-2,5-dicarboxylate 15

The synthesis of diethyl 3,4-dihydroxythiophene-2,5-dicarboxylate **15** began with the Hinsberg reaction [76], which is a condensation of diethyl thioglycolate **14** with diethyl oxalate under basic conditions [77]. The mechanism of this reaction as shown in **Scheme 3.3** is generally understood to consist of subsequent Claisen condensation reactions to produce a diketone intermediate, which readily tautomerizes to the fully conjugated dihydroxythiophene [78, 79].
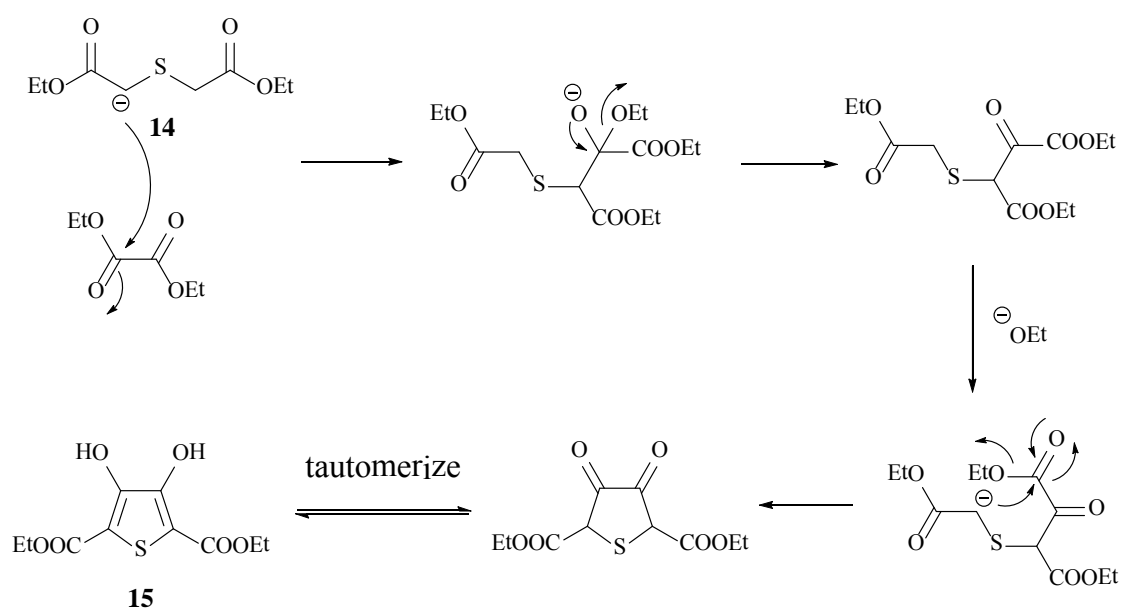

Scheme 3.3 Mechanism of Hinsberg reaction [78, 79].

The preparation of dihydroxythiophene **15** was optimized in various reaction conditions as shown in **Table 3.2**. The diester **14** was condensed with diethyl oxalate to give the dihydroxythiophene product in good yield (70% at lest) **(Entry 2, Table 3.2)**. No erosion of the yield was observed with the scale-up reaction **(Entry 3,Table 3.2)**. Longer reaction time seemed to give poorer results.

This compound was characterized by ^{1}H-NMR, ^{13}C-NMR, IR and MS. ^{1}H-NMR showed a broad singlet OH peak at 9.36 ppm **(Figure A.11, Appendix A)**. In the ^{13}C-NMR the carbonyl carbon appeared at 165.5 ppm and the two carbons of the thiophene ring at 107.1 and 151.6 ppm **(Figure A.12, Appendix A)**. IR spectrum showed very strong board OH stretching appeared at 3293 cm^{-1} and the double bond region at 1661 and 1508 cm^{-1} **(Figure A.13, Appendix A)**. In the mass spectrum, the molecular ion peak appeared in the positive mode at 259.20 amu [M-H]$^+$ **(Figure A.14, Appendix A)**.

Table 3.2 Conditions for the synthesis of dihydroxythiophene **15**
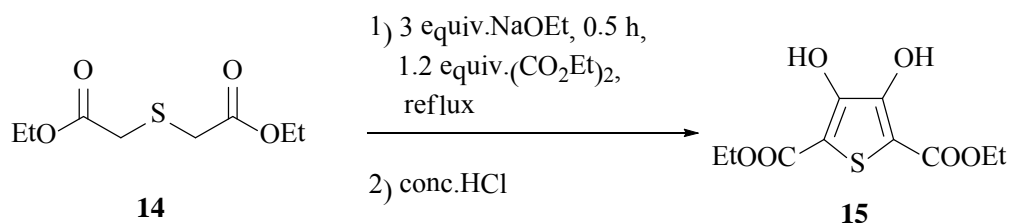
Entry	mmol of starting material	Time (h)	%yield
1	5	1	55
2	10	1	70
3	30	1	68
4	10	2	55
5	30	2	48
6	5	24	41

3.1.1.3 Synthesis of diethyl 3,4-dialkoxythiophene-2,5-dicarboxylates 16

Title compounds were synthesized via the double Williamson etherification under the typical conditions reported in the literature, using diethyl 3,4-dihydroxy thiophene-2,5-dicarboxylate **15**, a base, dry DMF as solvent, and the corresponding alkyl halides **13a-e (Figure 3.1)** [71-75]. The mixture was stirred at 90 °C under nitrogen to obtain the desired product in various range of yield as shown in **Table 3.3**.
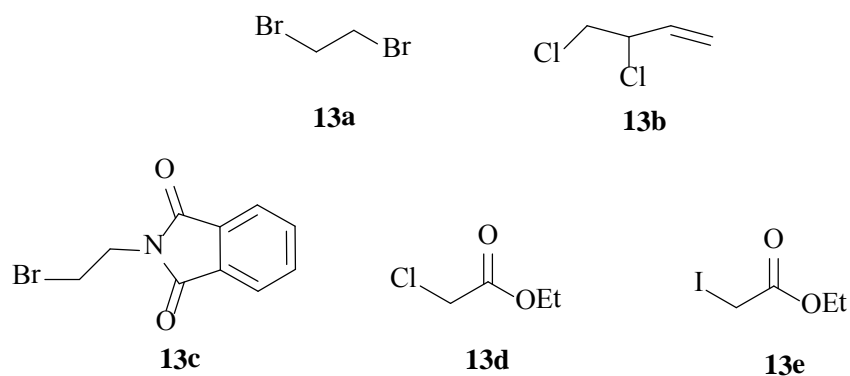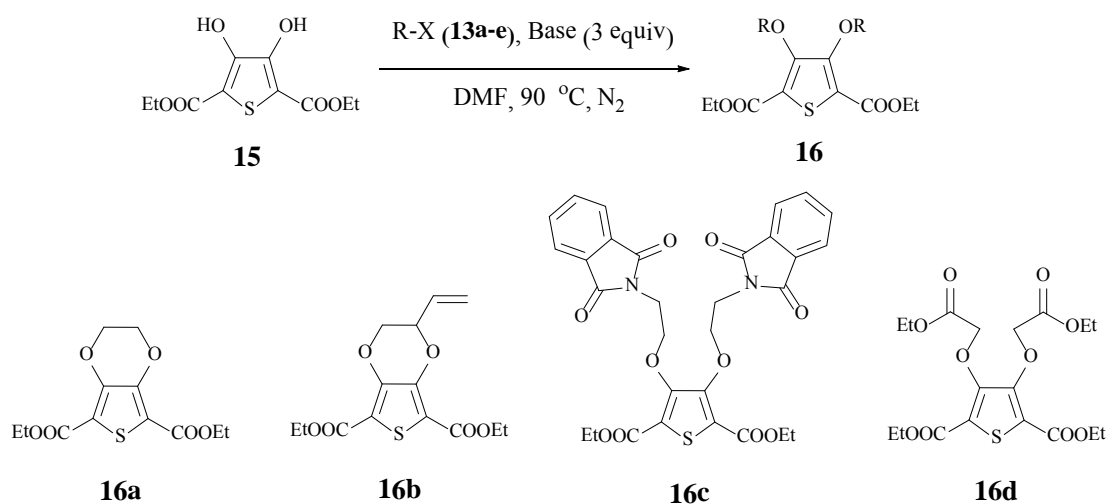

Figure 3.1 Alkyl halides **13a-e** used in the reactions

Table 3.3 Conditions for the synthesis of diethyl 3,4-dialkoxythiophene-2,5-dicarboxylates **16**

Entry	R-X (equiv.)	Base	Time (h)	Product (yield)	Recovery of 15
1	**13a** (1.3)	K_2CO_3	24	**16a** (61%)	-
2	**13a** (1.3)	Et_3N	24	**16a** (77%)	-
3	**13a** (1.3)	Et_3N	18	**16a** (65%)	-
4	**13b** (1.3)	Et_3N	24	**16b** (14%)	-
5[a]	**13b** (1.3)	Et_3N	24	**16b** (14%)	-
6	**13b** (1.7)	Et_3N	48	**16b** (21%)	20%
7	**13b** (2.0)	Et_3N	48	**16b** (9%)	25%
8	**13b** (1.7)	K_2CO_3	48	**16b** (10%)	25%
9	**13b** (1.7)	Et_3N	72	**16b** (42%)	42%
10[b]	**13b** (1.7)	Et_3N	72	**16b** (38%)	54%
11	**13b** (1.7)	Et_3N	84	**16b** (17%)	30%
12	**13c** (3)	K_2CO_3	24	**16c** (18%)	-
13	**13c** (3)	Et_3N	24	**16c** (43%)	-
14	**13c** (3)	Et_3N	48	**16c** (32%)	-
15[c]	**13d** (3)	K_2CO_3	24	**16d** (38%)	-
16[c]	**13d** (3)	K_2CO_3	48	**16d** (49%)	-
17	**13e** (3)	K_2CO_3	24	**16d** (29%)	-
18	**13e** (3)	Et_3N	24	**16d** (11%)	-

[a]The reaction was added 2 equivalents of KI.

[b]The reaction was stirred at 60 ºC.

[c]The reaction was added 3 equivalents of KI.

Following the reported procedure, **16a** could be prepared in good yield, slightly less than that from literature **(Entry 1, Table 3.3)** [56]. Changing the base to Triethylamine (TEA) partly improved the yield **(Entry 2, Table 3.3)**. TEA was cheap, easy to remove, and allowed the reaction to be carried out in a totally homogeneous system. The obtained product **16a** was characterized by MS, IR, ^{1}H-NMR and ^{13}C-NMR spectroscopy. The results matched well with these report in literature [71, 73] **(Figure A.15-A.18, Appendix A)**.

Much more sluggish reactions were observed using the potentially less reactive alkyl dichloride **13b**. Addition of iodide did not help accelerate the reaction. **(Entry 4 and Entry 5, Table 3.3)**. Using 1.7 equivalent of **13b** and longer time obtained **16b** in 21% yield, though the result was not better with even higher equivalents of **13b** **(Entry 6, Table 3.3)**. K_2CO_3 also gave poorer result in this case compound **16b** was produced in only 10%. The best condition was found with a longer reaction time up to 72 h **(Entry 8, Table 3.3)**. Even longer reaction time, however, worsened the result **(Entry 11, Table 3.3)**. Compound **16b** was characterized by MS, IR and NMR spectroscopy, which matched well with the expected structure of the compound **(Figure A.19-A.22, Appendix A)**.

Moderate yields of the highly functionalized **16c** and **16d** could be prepared in similar manners. Using bromo alkyl **13c** and TEA, **16c** was obtained in 43% yield in a reaction of 24 h **(Entry 13, Table 3.3)**. While the longer reaction time was decreased the yield to 32% **(Entry 14, Table 3.3)**. IR spectrum showed stretching absorption bands for C=O ester , C=O amide and C=C aromatic **(Figure A25, Appendix A)**. ^{1}H-NMR spectrum of **16c** was characterized by the appearance of a triplet and a quartet at δ 1.16 and 4.07 ppm assigned for the methyl and methylene protons of the ethyl group respectively. The aromatic region showed signals at 7.78 and 7.65 ppm. The CH_2-O and CH_2-N protons showed triplet at 4.33 and 3.99 ppm respectively **(Figure A-30, Appendix A)**. In the mass spectrum, the molecular ion peak appears in the positive mode at 607.48 $[M+Na]^+$ **(Figure A.26, Appendix A)**.

Some attempts have been made to synthesis compound **16d** using ethyl iodoacetate as a reagent. The yellow liquid ethyl iodoacetate **13e** was synthesized from ethyl chloroacetate **13d** and sodium iodide in acetone in high yield. The iodide ion replaced chloride leaving group via the S_N2 fashion **(Scheme 3.4)**. The precipitation of sodium chloride had drive the reaction to completion. This compound was characterized via FT-IR, ^{1}H-NMR and ^{13}C-NMR. The ^{1}H-NMR spectrum exhibited the singlet methylene peak at 3.62 ppm, shifted upfield from 3.99 ppm of that of the starting material **(Figure A.4, Appendix A)**.
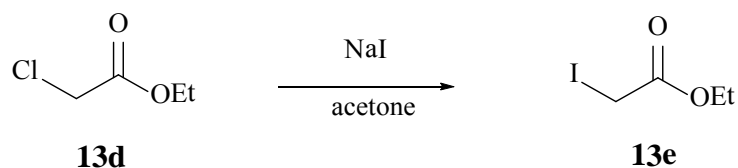
Scheme 3.4 Synthesis of ethyl iodoacetate **13e**

Using iodoacetate **13e**, better yield of **16d** was instead obtained from the reaction using K_2CO_3 as the base **(Entry 17, Table 3.8)**. The slightly acidic α-protons of the esters might have hindered the progress of the reaction. The change to ethyl chloroacetate **13d**, 3 equivalent of KI and longer reaction time, increased the yield of the obtained product to 49% **(Entry 16, Table 3.8)**.

The structure of **16d** was assessed by IR, ^{1}H-NMR, ^{13}C-NMR and MS. IR spectrum of compound **16d** showed strong absorption bands of two type of ester groups at 1726 and 1720 cm^{-1} **(Figure A.29, Appendix A)**. The ^{1}H-NMR spectrum showed singlet peak of the methylene protons at 4.74 ppm along with two sets of signals of the ethyl groups. **(Figure A.27, Appendix A)**. The mass spectrum of this compound show the molecular ion peak $[M+Na]^+$ at m/z 455.53 **(Figure A.30, Appendix A)**.

According to the result above, commercially available alkyl bromide **(13a, 13c)** and alkyl chloride **(13b, 13d)** were chosen as starting materials. Due to the high reactivity of alkyl bromide, this substitution reaction presented in good yield. Using alkyl chloride react slower than alkyl bromide because bromide is a better leaving group than chloride. Compared dibromo **13a** with monobromo **13c**, compound **16a** was produced more than compound **16c**. Monobromo react slower than dibromo because the second alkylation reaction involves a faster intramolecular reaction instead of the two intermolecular. For the reaction with dichloride **13b**, it reacts slowly and requires several days to yield the desired product. Finally, using ethyl iodoacetate obtained **16d** in low yield because the reagent may reversible. When using ethyl chloroacetate and KI to give product in moderate yield.
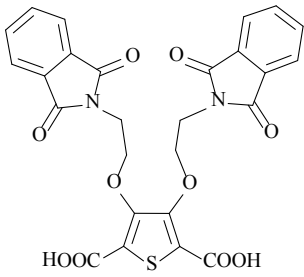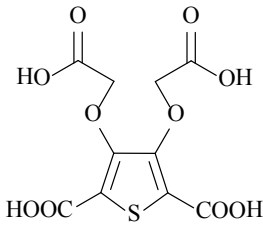
3.1.1.4 Synthesis of 3,4-dialkoxythiophene-2,5-dicarboxylic acid 17

The synthesis of 3,4-dialkoxythiophene-2,5-dicarboxylic acid was outlined in **Scheme 3.1**. Compound **16a, 16b, 16c, 16d** were saponified to yield the desired products in high yields **(Table 3.4)**. All products gave the corresponding structure analyses by IR, NMR and MS techniques. Unfortunately, the hydrolysis of diester **16c** instead obtained phthalimide as the major product. The characteristic signals in ^{1}H-NMR and ^{13}C-NMR spectra that represented the thiophene ring were absent, indicating the unsuccessful hydrolysis and decomposition of the diester **16c** or the expected product **17c** during the reaction **(Figure A.32, Appendix A)**.

**Table 3.4** Hydrolysis of diethylester derivatives **17a-d**
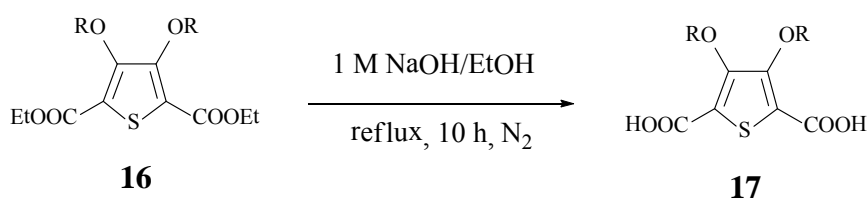
Entry	Starting	Product	Yield (%)
1	**16a**	**17a**	98
2	**16b**	**17b**	90

Entry	Starting	Product	Yield (%)
3	**16c**	\n**17c**	0[a]
4	**16d**	\n**17d**	95

[a]The desired product was not observed

.

The diacid compounds (**17a, 17b, 17d**) were further purified by crystallization from MeOH. The ^{1}H-NMR and ^{13}C-NMR spectra of compound **17a** were similar to the these of starting materials except the absence of the signals of ethyl groups (**Figure A.35, Appendix A**). Similarly, the structures of compounds **17b** and **17d** were confirmed by IR, ^{1}H-NMR and ^{13}C-NMR spectra. All compounds showed the characteristic strong carbonyl stretching peak and strong broad band of carboxyl O-H stretching (**Figure A.37-A.41, Appendix A**).

The one-pot synthesis of the diacid **17a** was attempted by combining the etherification and hydrolysis (**Scheme 3.5**). Double Williamson etherification of diethyl 3,4-dihydroxythiophene-2,5-dicarboxylate **15** with 1,2-dibromoethane in dry DMF, followed by 1M NaOH and EtOH for 10 h gave compound **17a** in 34% yield. Though convenient, the result was inferior to that from two separated reactions which gave 76% of **17a** from two steps.
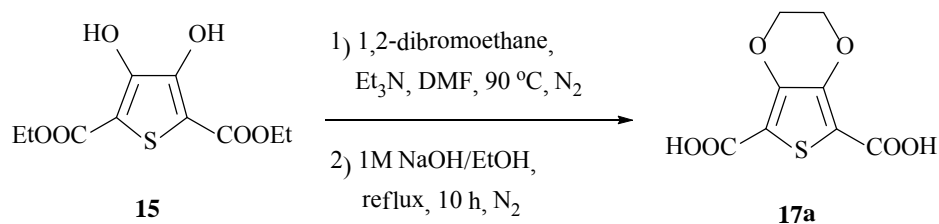
Scheme 3.5 One pot synthesis of diacid **17a**

3.1.1.5 Synthesis of 3,4-dialkoxythiophene derivatives 18

3,4-dialkoxythiophenes were synthesized via decarboxylation of 3,4-dialkoxythiophene-2,5-dicarboxylic acid using copper(I)oxide in quinoline. The desired products were obtained in good yields **(Table 3.5)** except **17d (Entry 3)**, which dark insoluble solid, anticipated to be a polymer or other decomposed products.

**Table 3.5** Decarboxylation of the diacid compounds **17**
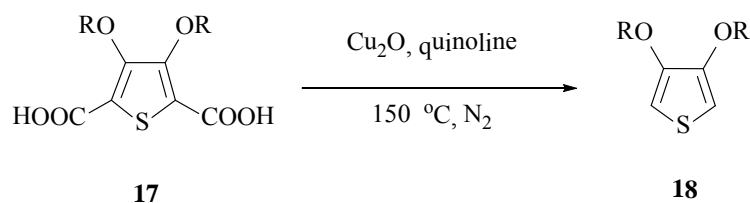
Entry	Starting material	Product	Yield
1	**17a**	**1**	73%
2	**17b**	**18b**	65%
3	**17d**	dark insoluble solid	-

The ^{1}H-NMR and ^{13}C-NMR spectra of EDOT **1** matched with the report in the literature [50] **(Figure A.42, A.43, Appendix A)**. For the new compound **18b**, the ^{1}H-NMR spectrum showed singlet of α-proton of thiophene ring at 6.34 ppm which the disappearance of the carboxyl functional group signals from both ^{1}H-NMR and ^{13}C-NMR spectra **(Figure A.44, A.45, Appendix A)**.

3.1.2 Transetherification of 3,4-dimethoxythiophene

An alternative synthesis of 3,4-dialkoxythiophene was reported via transetherification of 3,4-dimethoxythiophene [60, 61, 80]. This was achieved by treatment with the corresponding alcohol and *p*-toluenesulphonic acid in refluxing toluene. To investigate the use of this procedure, esters of L-tartaric acid were first prepared **(Scheme 3.6)**. Dibenzyl tartrate **21** was synthesized via esterification of L-tartaric acid and benzyl alcohol in reflux toluene using *p*-toluenesulfonic acid (PTSA) as the catalyst [1], giving the product in excellent yield (93%). The product was characterized by FT-IR, ^{1}H-NMR,^{13}C-NMR and MS **(Figure A.46-A.48, Appendix A.)** The ^{1}H-NMR spectrum showed the diastereotopic quartet signals of benzylic protons at 5.25 ppm **(Figure A.46, Appendix A)**.


21 : R = CH$_2$Ph
22 : R = Bu
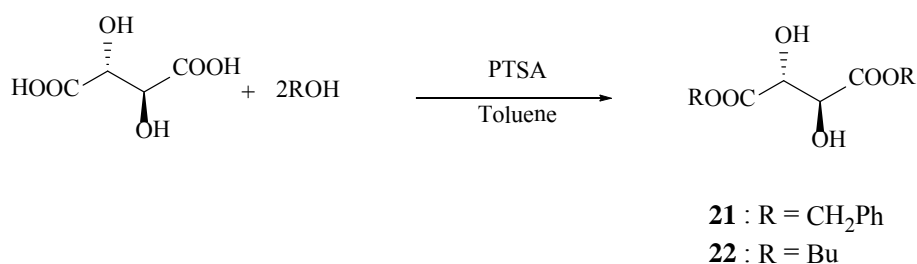
Scheme 3.6 Synthesis of esters of L-tartaric acid
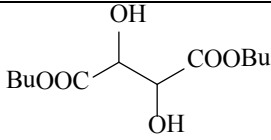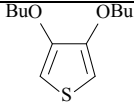
Similar to dibenzyl tartrate **21**, dibutyl tartrate **22** was synthesized by the reaction of L-tartaric acid and n-butyl alcohol in reflux toluene using PTSA as the catalyst, obtained the product in good yield (88%). The structure of dibutyl tartrate **4** was confirmed by FT-IR, ^{1}H-NMR,^{13}C-NMR and MS. **(Figure A.49-A.51, Appendix A)**.

Some attempts were made to find a way to produce 3,4-ethylenedioxy thiophene substituted at ethylene bridge using tartaric acid and their derivatives. Ether exchange of 3,4-dimethoxythiophene and tartaric acid gave only unreacted starting material **(Entry 1, Table 3.6).** Attempted transetherification of dibenzyl tartrate *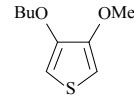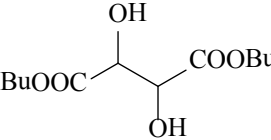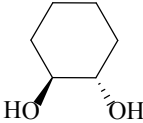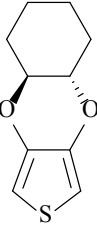*21** gave a mixture of unidentified products that did not contain the desired product **(Entry 2, Table 3.6)**. The change to dibutyl tartrate gave two isolated product **(23, 24)** in 16 and 30 %yield **(Entry 3, Table 3.6)**, identified by ^{1}H-NMR and ^{13}C-NMR **(Figure A.52-A.56, Appendix A)**. This may due to ether exchange between the starting material and the ester. Transetherification with n-butanol obtained the 3,4-dibutoxythiophene **23** in high yield (86%) **(Entry 4, Table 3.6)**. Unfortunately, when this product was replaced as the starting material for the previous transetherification, only unreacted starting material was detected during the reaction **(Entry 5, Table 3.6)**. Surprisingly, ether exchange between 3,4-dimethoxythiophene and (±)*trans*-1,2-cyclohexanediol was carried out obtaining the desired product **25** in high yield (86%) **(Entry 6, Table 3.6)**.

Table 3.6 Transetherification of 3,4-dimethoxythiophene
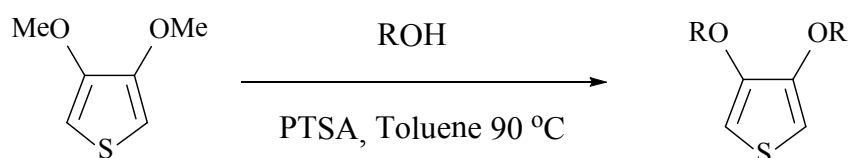
Entry	ROH	Product	Time (h)	%Yield
1		NR	72	-
2	**21**	Many Products	72	-

Entry	ROH	Product	Time (h)	%Yield
3	**22**	**23**	24	16
		24		30
4	BuOH	**23**	24	86
5[a]	**22**	NR	48	-
6	(racemic mixture)	**25**	24	24
			48	74
			72	86
			7 days	42

[a] = using 3,4-dibutoxythiophene (23) as the starting material

The structure of compound **25** was confirmed by ^{1}H-NMR, ^{13}C-NMR and IR. ^{1}H-NMR showed singlet of α-protons of thiophene ring at 6.21 ppm **(Figure A.57, Appendix A)**. The ^{13}C-NMR showed two carbon of thiophene ring and three carbon of cyclohexane ring **(Figure A.58, Appendix A)**. IR spectrum showed absorption band of CH- streching and strong absorption band of C=C thiophene ring at 1471-1420 cm^{-1} **(Figure A.59, Appendix A)** [58].

3.3.1 Halogenation of thiophene derivatives

3.3.3.1 Bromination of 3,4-ethylenedioxythiophene (EDOT)

Since α-position of thiophene ring is generally very reactive towards electrophiles or radicals. Substitution of α-hydrogens by halogenation reaction of 3,4-ethylenedioxythiophene (EDOT) prior to carrying out reactions at the ethylene-bridge may be necessary to prevent side-reactions [48]. Following the bromination procedure by Kellogg and coworkers [49], thiophene was brominated by using N-bromo-succinimide (NBS), and provided moderately pure 2,5-dibromothiophene. The dihalogenated derivatives of EDOT have also been synthesized by direct halogenation of EDOT according to the similar procedure [50, 51] **(Scheme 3.7)**.
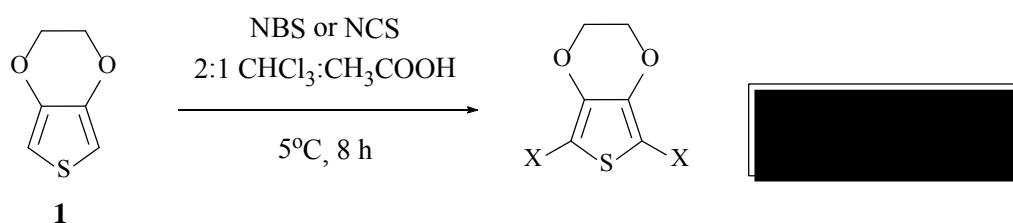
Scheme 3.7 Synthesis of 2,5-dihalo-3,4-ethylenedioxythiophene [48, 49]

The original synthesis of compounds **2** and **3** gave a rather moderate yield and using long reaction times. A better synthetic route has been developed at room temperature and gave a significantly higher yield and a simpler procedure. From table 3.7, Entry 1 showed the original standard procedure using $CHCl_3/CH_3COOH$ mixture with long reaction time. Using light and heat could accelerate the reaction but gave lower yield **(Entry 2, Table 3.7)**. Accidentally, we discovered that a high yield of bromination of EDOT could simply be obtained when treated with NBS in halogenated solvent at room temperature in ambient atmosphere. This condition gives 2,5-dibromo-3,4-ethylenedioxythiophene (DBEDOT) **2** in good purity and yield **(Entry 3 and 4, Table 3.7)**. A crystalline product was obtained after crystallization from methanol.

Table 3.7 Conditions for synthesis of DBEDOT **2**

Entry	equiv. of NBS	Solvent	Conditions	Time	yield
1	2.5	2:1	RT, N_2	6 h	64%
2	2.5	$CHCl_3$:CH_3COOH	hv,reflux, N_2	1 h	55%
3	2.5	2:1	RT	1 min	99%
4	2.1	$CHCl_3$:CH_3COOH	RT	1 min	98%
		$CHCl_3$			
		CH_2Cl_2			

Moreover, *N*-chlorosuccinimide (NCS) has been used as the chlorinating agent for EDOT to give the dichlorothiophene derivative. Treatment of EDOT with 2.5 equivalents of NCS in chloroform under mild condition obtained 2,5-dichloro-3,4-ethylenedioxythiophene (DCEDOT) **3** in good yield comparable to the literature procedure [48] **(Entry 2, Table 3.8)**. When using dichloromethane as the solvent, the reaction was slow and obtained compound **3** in lower yield **(Entry 3, Table 3.8)**. The peak in ^{1}H-NMR spectra at $\delta \sim 6.3$ ppm which corresponds to α-hydrogen signal on the thiophene ring was absent after either bromination or chlorination.

Table 3.8 Conditions for synthesis of DCEDOT **3**.

| Entry	equiv. of NCS	Solvent	Conditions	Time	yield
1	2.5	2:1	RT, N_2	6 h	89%
2	2.5	$CHCl_3$:CH_3COOH	RT	10 min	93%
3	2.5	$CHCl_3$	RT	24 h	69%
		CH_2Cl_2			

3.1.3.2 Bromination of other thiophene derivatives

According to the above described procedure, we chose the optimal condition for bromination other thiophene derivatives (**Table 3.9**). Two plausible pathways of bromination mechanism of thiophene ring had been proposed [50, 52, 64]. In **Scheme 3.8**, the bromination reaction was occurred via acid-catalyzed electrophilic aromatic substitution in polar solvent. Another mechanism was proposed that the reaction was taken place through radical-based single electron transfer followed by aromatic radical substitution as shown in **Scheme 3.9**. The chlorination mechanism is likely to go through the similar mechanism to that of bromination. In our case, it was possible that the EDOT and derivatives were sufficiently active to react with the reagent through the second pathway with no used of acid catalyst. Extension of reaction time could have degraded or polymerized the product obtained and resulted in lower yield.

Table 3.9 Synthesis of 2,5-dibromo-3,4-dialkoxythiophene derivatives
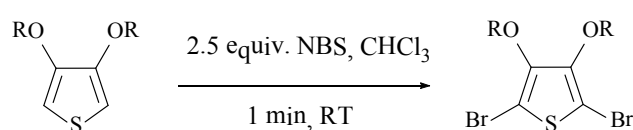
Entry	Substrate	Product	Yield
1	**25**	**26**	94%

2   [thiophene with MeO, OMe]   [dibromothiophene with MeO, OMe, Br, Br]   80%

27
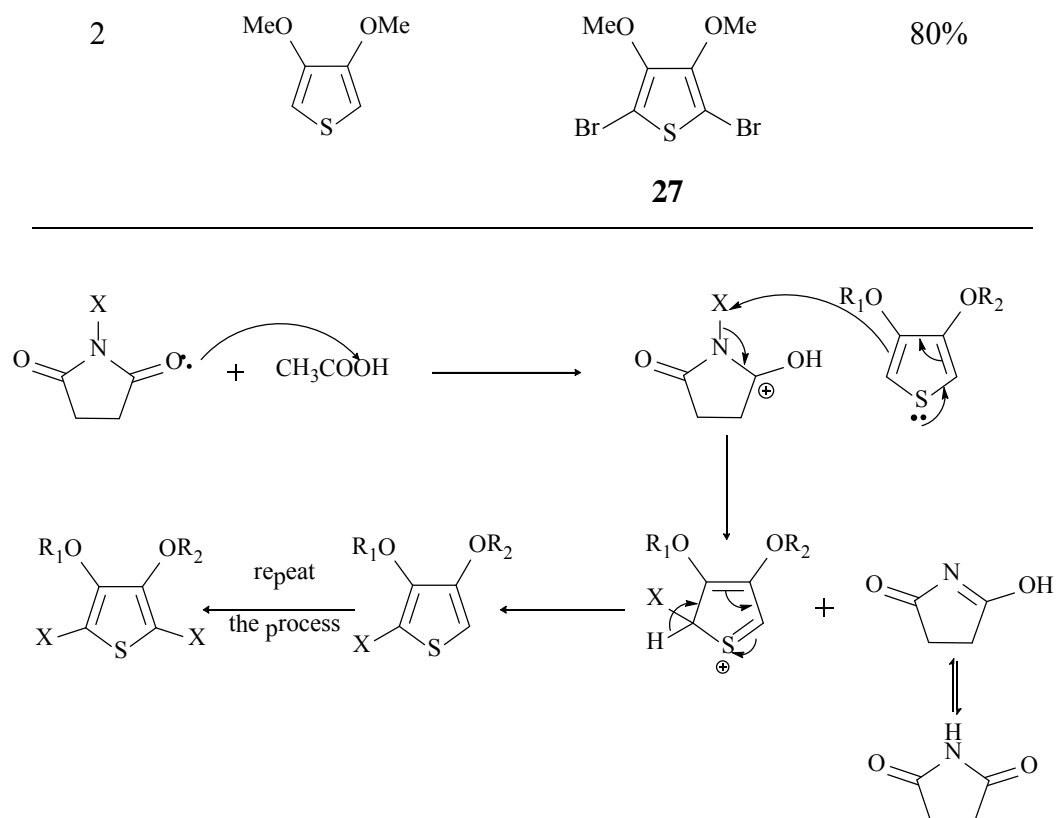
Scheme 3.8 Bromination mechanism through electrophilic aromatic substitution
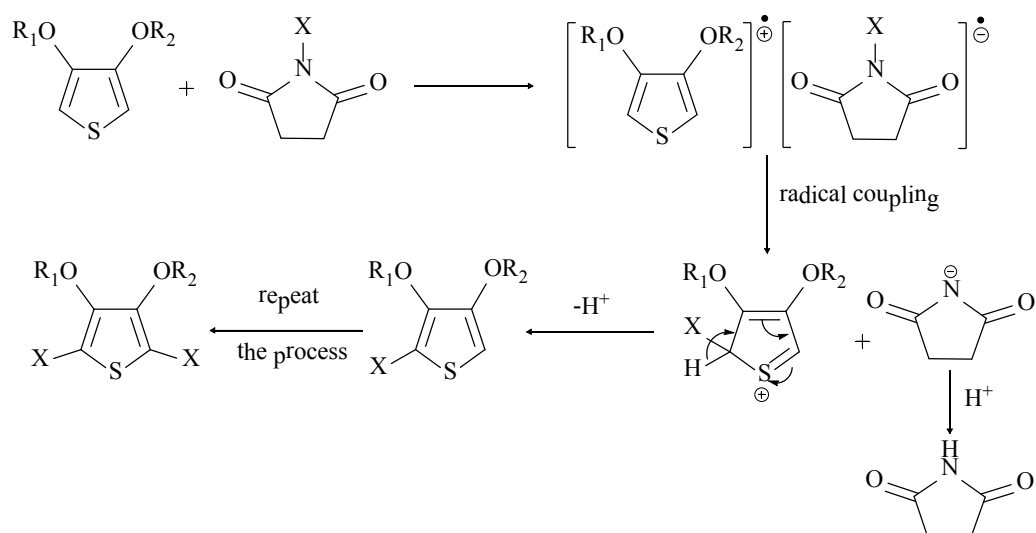
Scheme 3.9 Bromination mechanism through radical-based single electron transfer followed by aromatic substitution

**3.1.4 Attempted synthesis of 3,4-Vinylenedioxythiophene (VDOT)**

3.1.4.1 Investigations of alternative synthesis of VDOT via substitution at
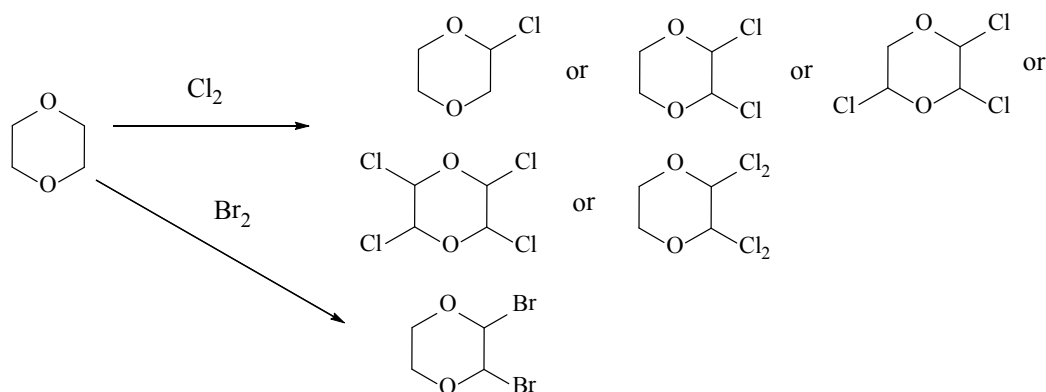**ethylene bridge**

In order to bypass the difficult intramolecular methathesis of the original synthesis [62], some attempts were made to find a simpler way to produce VDOT **9**, the direct substitution at the ethylene bridge of EDOT with halogenating agents followed by elimination were investigated **(Scheme 3.10)**.
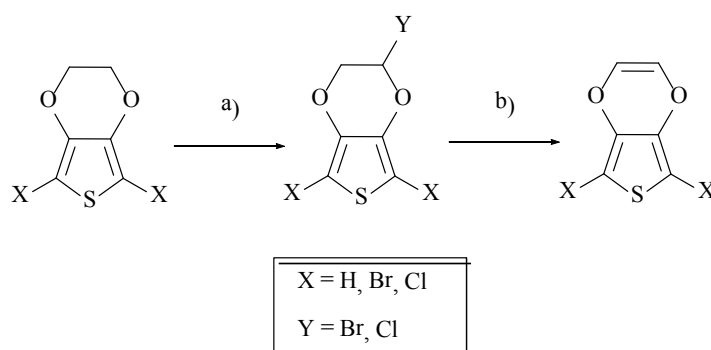

Scheme 3.10 Routes to derivatives of VDOT **9**. a) Halogenation b) Elimination

Several researchers reported the halogenations of 1,4-dioxane to give a number of substituted 1,4-dioxane [65-69] **(Scheme 3.11)**. In our initial studies, attemps to substitute the hydrogen atoms at ethylene bridge of EDOT using NBS in the presence of light gave only unreacted starting material **(Entry 1, Table 3.10)**. The same results were obtained with the bromination of DBEDOT **2 (Entry 2, Table 3.10)** and DCEDOT **3 (Entry 3, Table 3.10)**. A facile substitution at ethylenedioxy bridge of 1,4-dioxane using lead tetraacetate had been described by Kreilein *et al* [70] **(Scheme 3.12)**. This reaction was adopt with DCEDOT **3** using catalytic amount of

Pb(OAc)$_4$. However, the substitution at ethylene bridge was not successful **(Entry 4-5, Table 3.10)**, even with stoichiometric amount of Pb(OAc)$_4$ **(Entry 6, Table 3.10)**.

Scheme 3.11 Halogenations of 1,4-dioxane [65-69].
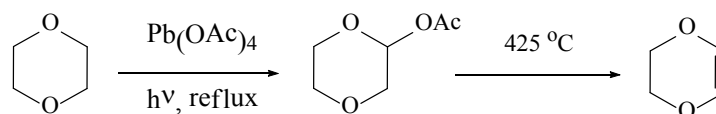
Scheme 3.12 Synthesis of 1,4-dioxene [70].

Table 3.10 Attempted substitution at ethylene bridge of EDOT derivatives.

Entry	Substrate	Reagent	Solvent	Conditions	Results
1	**EDOT 1**	4 equiv.NBS	CHCl$_3$	hv, reflux, N$_2$, 24 h	NR
2	**DBEDOT 2**	5 equiv.NBS	CHCl$_3$	hv, reflux, N$_2$,24 h	debromination
3	**DCEDOT 3**	2.5 equiv.NBS	CHCl$_3$	hv, reflux, N$_2$, 5 days	NR
4	**DCEDOT 3**	0.1equiv. Pb(OAc)$_4$	CH$_3$CN	hv, reflux, N$_2$, 4 days	NR
5	**DCEDOT 3**	0.1equiv.	AcOH	hv, reflux,	NR

		Pb(OAc)$_4$		N$_2$, 3 days	
6	**DCEDOT 3**	1 equiv.	CH$_3$CN	hv, reflux,	NR
		Pb(OAc)$_4$		N$_2$, 2 days	

3.1.4.2 Investigations of alternative synthesis of VDOT via dehydrogenation of ethylene bridge

The initial attempts to substitute at ethylene bridge had proved too difficult. We then decided to attempt the synthesis via direct dehydrogenation of the ethylene bridge. Dehydrogenation of EDOT **1** with 2,3-dichloro-5,6-dicyanobenzoquinone (DDQ) using palladium on carbon (Pd/C) as a catalyst in reflux toluene was, however, unsuccessful **(Entry 1, Table 3.11)**. Using other oxidants in the same reaction or DCEDOT **3** as the starting material were also failed **(Entry 2-5, Table 3.11)**.

Table 3.11 Attempted dehydrogenation of the ethylene bridge of EDOT derivatives
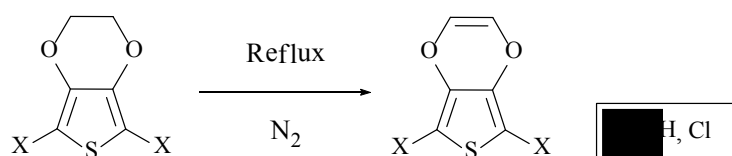
Entry	Substrate	Reagent	Solvent	Results
1	**EDOT 1**	3 equiv.DDQ, Pd/C	toluene	NR
2	**EDOT 1**	1.5 equiv.TEMPO, Pd/C	toluene	NR
3	**DCEDOT 3**	3 equiv.DDQ	1,4-dioxane	NR
4	**DCEDOT 3**	3 equiv.DDQ	toluene	NR

| 5 | **DCEDOT 3** | 3equiv. PCC | CH$_2$Cl$_2$ | NR |

During these failed attempts nevertheless, we learned that long reaction time usually obtained the dark solid precipitate which was anticipated to be poly(3,4-ethylenedioxythiophene) (PEDOT) that could not be dissolved in any organic solvents. This evidence suggested that the reaction performed in extreme conditions could possibly cause the facile debromination or dechlorination from the α-positions of dihalogenated substrates follow immediately by the prematured polymerization reaction to obtain the undesired dark solid insoluble polymer.

## 3.2 Synthesis of polythiophene derivatives

3.2.1 Synthesis of poly(3,4-(cyclohexyliden-1,2-dioxy)thiophene) : PCDOT

Transetherification of 3,4-dimethoxythiophene with 2 equivalents of *trans*-1,2-cyclohexanediol in the presence of a catalytic amount of *p*-toluenesulfonic acid (PTSA) produced white needle crystals **CDOT 25** in good yield (86%). Chemical oxidative polymerization of monomer **25** using 3 equivalents of $FeCl_3$ in chloroform at room temperature for 24 h led to the formation of insoluble PCDOT. After dedoping with hydrazonium dichloride solution, PCDOT was obtained with as dark, mostly insoluble solid in good yield (69%) **(Table 3.12) (Scheme 3.13)**. The small soluble fraction was assumed to be the smaller oligomers.

Unlike poly(3,4-ethylenedioxythiophene) (PEDOT), the recently developed solid-state polymerization (SSP) method with mild conditions was used [48, 49, 82]. White crystals of dibromothiophene derivative **26** was obtained from bromination of **CDOT 25** with 2.5 equivalents of NBS in chloroform at room temperature in excellent yield (94%) **(Scheme 3.13)**. It was easily polymerized within 2-3 h under slight heating (70 ºC) or within several days at room temperature. Increasing the heating temperature significantly decreased the reaction time. During the process, white crystals of **26** slowly transformed to blue-black crystals with a metallic luster **(Figure 3.2).** When comparing the yields of polymerization, all SSP products gave higher than 100% yields when calculated from purely PCDOT with the completely absence of bromine atoms **(Table 3.12)**. Among these products, heating at 120 ºC for 24 h gave the most weight loss of compound **26** from its monomer. This weight loss was due to the loss of bromine gas from the dibromothiophene monomers **26** during the polymerization. It could be implied that the solid state polymerization of this

compound at 120 ºC has the fastest progress approaching complete polymerization than at lower temperature.

The yields exceeding 100% would probably come from some of the bromine molecules that was still left doping on the polymer plus those that still attached on the remaining unreacted monomers and the terminal units of each polymer chain. The solid-state polymerization of PCDOT was insoluble in any organic solvent.
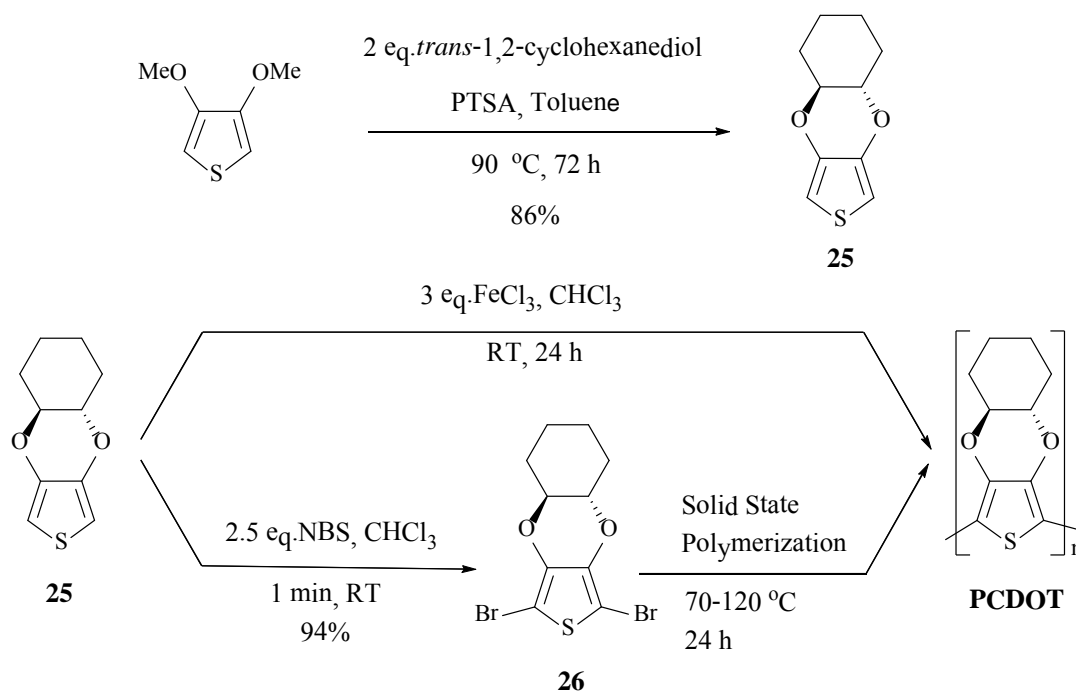
Scheme 3.13 Synthesis of PCDOT

Table 3.12 Yields of the polymerizations towards PCDOT.

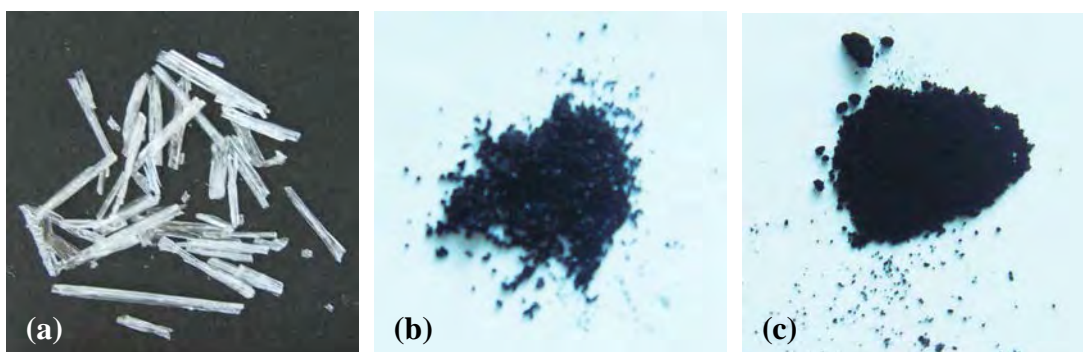| Method of polymerization	T (ºC)	Monomer weight (mg)	Product weight (mg)	% yield
SSP	70	203.5	198.3	>100
SSP	100	200.0	170.5	>100
SSP	120	200.2	156.5	>100
Oxidative	RT	98.1	67.1	69

Figure 3.2 (a) crystals of **26** (b) PCDOT immediately upon heating **26** at 120 ºC for 24 h (c) PCDOT after dedoping with hydrazine hydrochloride

3.2.2 X-Ray crystallography

Single crystal of the **DBCDOT 20** was grown from ethanol solutions and studied by X-ray analysis in order to understand structural features of SSP. The Br…Br contacts might be responsible for solid-state polymerization as observed in 2,5-dibromo-3,4-ethylenedioxythiophene (DBEDOT) [48, 49]. The X-ray crystal analysis of **DBCOT 20** reveals that the Br...Br distance between adjacent molecules to be approximately 4.21 Å. This distance was much larger than the double van der Waals radius of bromine (3.7 Å), and the SSP was indeed observed for DBCDOT. However, Lepeltier et al reported the halogen contacts were not critical for the SSP [84].
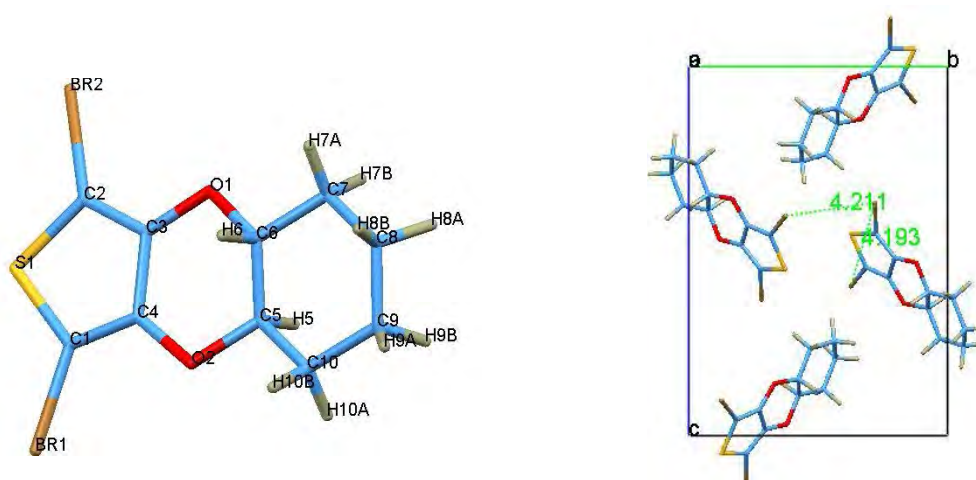

Figure 3.3 X-Ray crystal structure of DBCDOT **26**

3.2.3 FTIR analysis

Figure 3.4 presents the IR spectrum of **CDOT 25** and two PCDOTs in KBr pellets: prepared by oxidative polymerization and solid-state polymerization. The **CDOT 25** shows the αC-H stretching of thiophene ring at 3111 cm^{-1}, which is absent in those of the polymers. FT-IR comparative analysis of PCDOT from SSP and FeCl$_3$ polymerization revealed very similar pattern. All the spectra show aliphatic C-H stretchings at 3000-2850 cm^{-1} and C=C characteristic multiple bands of thiophene between 1504-1359 cm^{-1}. The new broad band around 1630 cm^{-1} appeared only with the polymer, which was suggested to be the alkene-like C=C stretching, due to polyconjugation of the polymer chain [83].
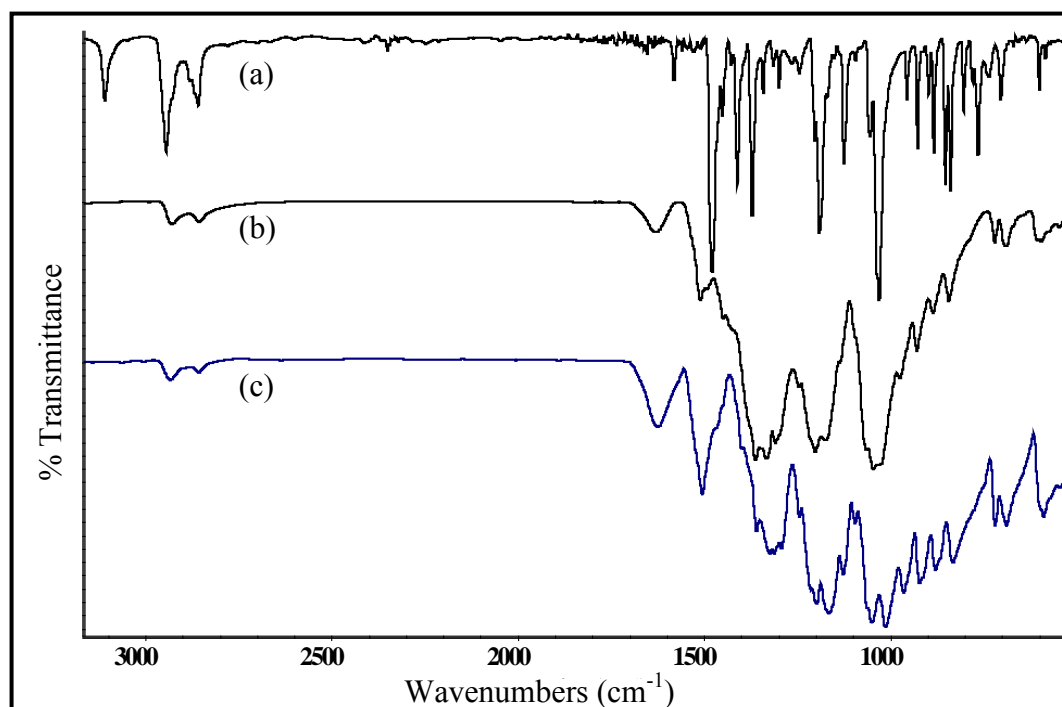

Figure 3.4 FT-IR spectra (KBr pellets) of (a) monomer **25** (b) PCDOT prepared by FeCl$_3$ oxidation polymerization (c) PCDOT prepared by SSP

3.2.4 UV-Vis spectroscopy

The electronic spectrum of $FeCl_3$-polymerized PCDOT shows very broad absorption band that extends beyond the visible region, similar to that was previously reported for fully doped PEDOT [50] **(Figure 3.5)**. Dedoping the polymer with hydrazonium hydrochloride solution limits the range of the absorption band with λ_{max} = 632 nm. The absorption spectra of the doped form of SSP-PCDOT (heated at 120 ℃) shows the similar broad band as that from the $FeCl_3$ polymerization. After dedoping, the spectrum shows two new bands with λ_{max} at 457 and 714 nm **(Figure 3.6)**.
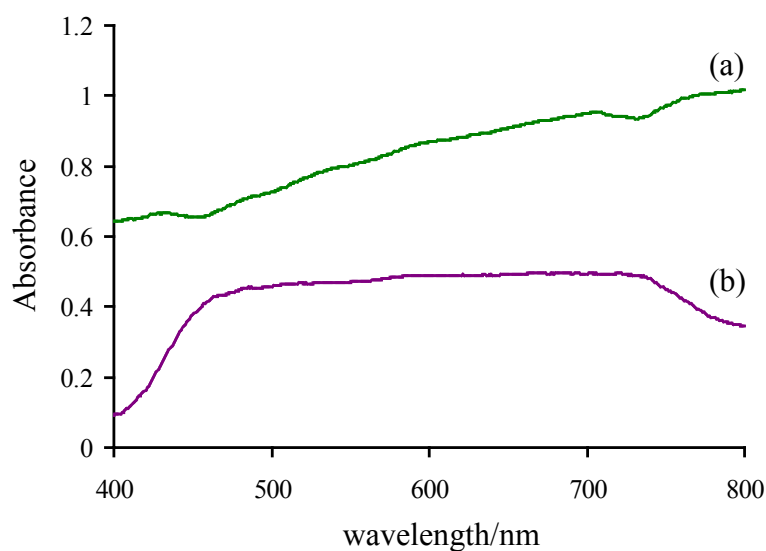

Figure 3.5 Solid UV-visible spectra of (a) $FeCl_3$-polymerized PCDOT (b) PCDOT after dedoping with hydrazonium hydrochloride solution
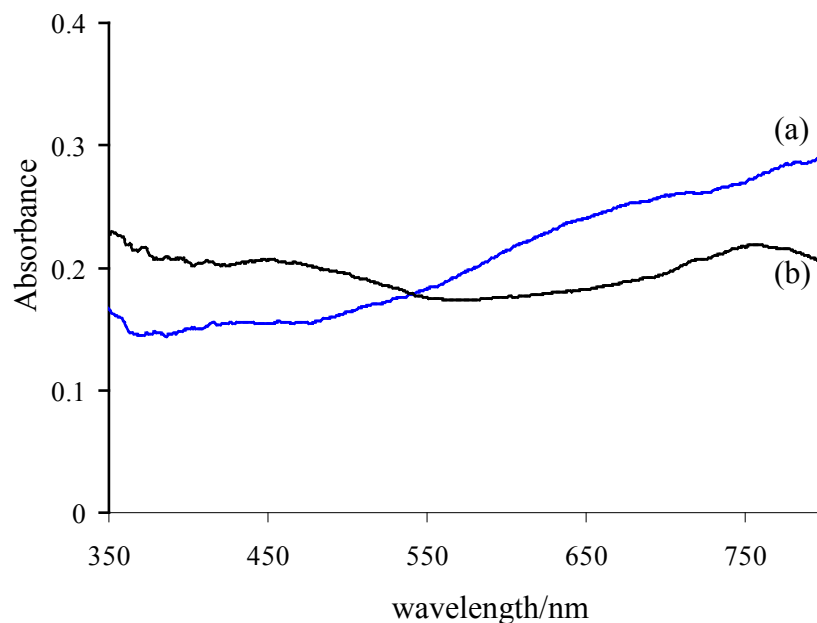
Figure 3.6 Solid UV-visible spectra of (a) SSP-PCDOT (heated at 120 ºC) (b) SSP-PCDOT after dedoping with hydrazonium hydrochloride solution

3.2.5 MALDI-TOF Mass Spectrometry

Routine characterization of the polymers by GPC was hindered by the poor solubility of the doped and neutral polymers. Therefore, MALDI-TOF MS was used to determine the molecular weight of polymers. With 2,5-dihydroxybenzoic acid (DHB) as the matrix, the MS spectrum clearly shows the presence of the polymers containing close to 15 monomer units (theoretical value = 2915.769) (**Figure 3.7**). Using α-cyano-4-hydroxycinnamic acid (CCA) as the matrix revealed the mass differences between each fragmented peak corresponding to the molecular weight of the monomer unit (m/z = 194) (**Figure 3.8**). The actual molecular weights of the PCDOT could be even higher than these measured values because of the insolubility or the difficulty to ionize of the parts with higher molecular weights. Although the results may not give the accurate information on the molecular weights of the polymers, they have confirmed the expected polymeric structure of the obtained products.
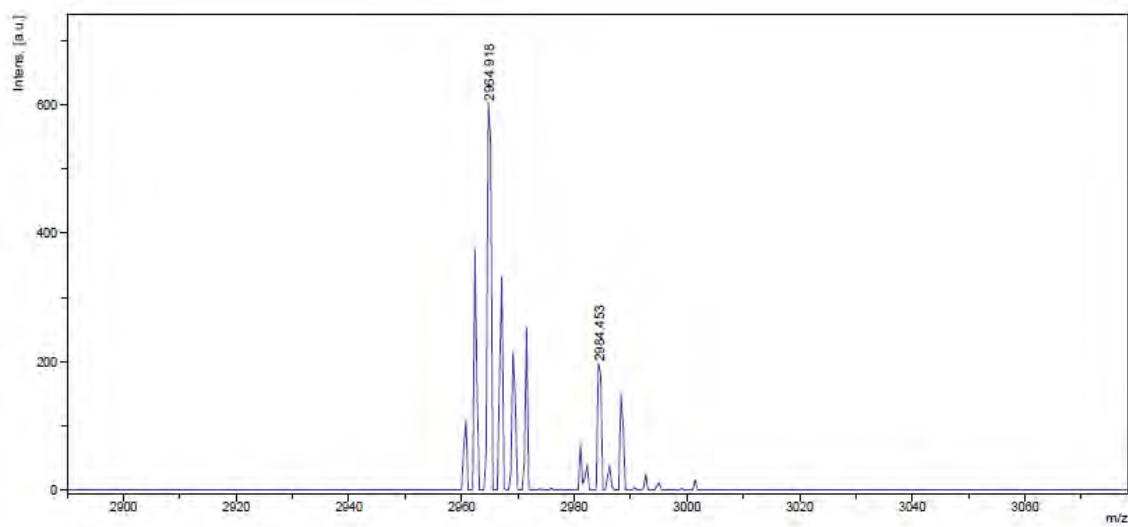
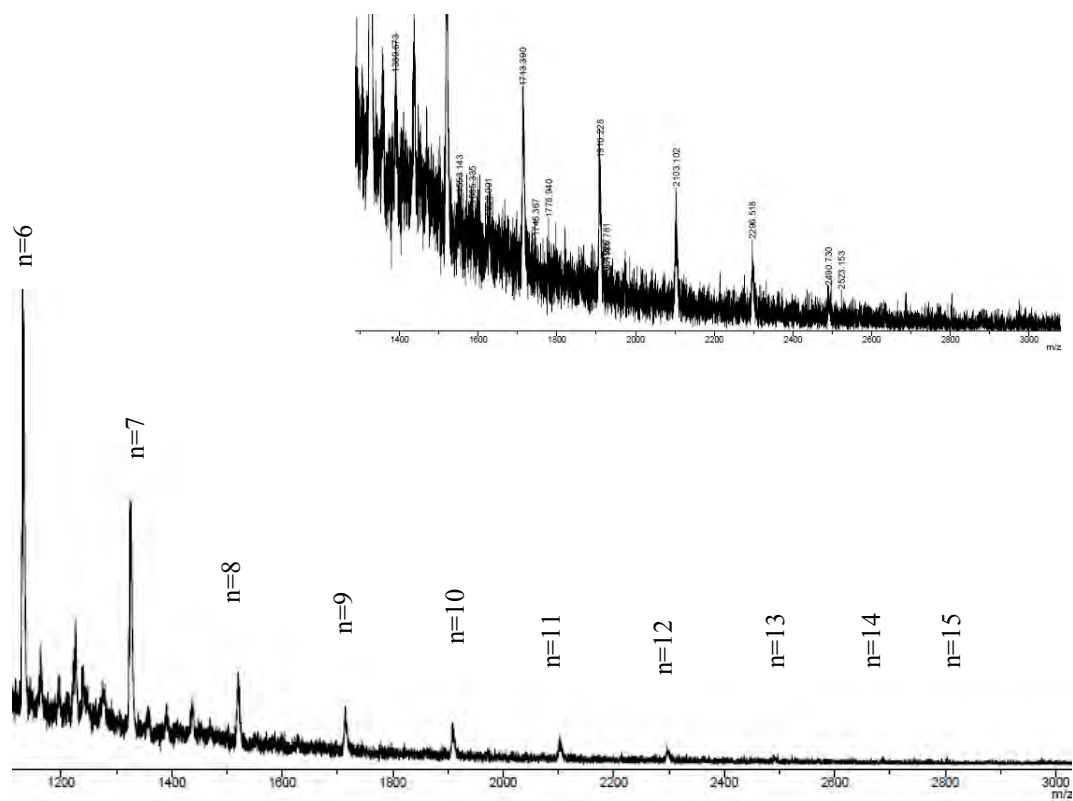**Figure 3.7** MALDI-TOF MS spectrum of SSP-PCDOT (heated at 120 ºC)

Figure 3.8 Expanded Details of MALDI-TOF MS spectrum of SSP-PCDOT showing the fragmented peaks.

3.2.6 Thermogravimetric analysis (TGA)

The Thermal decompositions of monomer **26** and the PCDOT polymer were analysed using a thermogravimetric analyzer (TGA). In this study, the thermal stability and thermal degradation kinetics of various samples were investigated in terms of the onset decomposition temperatures (T_{onset}) and maximum decomposition temperatures (T_d)

The TGA thermograms of all the polymers were carried out under nitrogen atmosphere with the heating rate of 20 ºC/min. **Figure 3.9** displays TGA thermograms of the crystal of monomer **26**, SSP-PCDOT (heated at 120 ºC) and FeCl$_3$-polymerized PCDOT. The T_d values of the samples could be clearly obtained from the derivative thermogravimetric (DTG) curves as shown in **Figure 3.10**. The TGA curve of each sample showed an initial small transition around 100 °C due to moisture evaporation. There are two distinct stages of weight loss in monomer **26** **(Figure 3.9a)**. It can be seen that two onset decomposition temperatures (T_{onset}) were observed with compound **26** at about 217.2 and 346.9 ºC **(Table 3.13)**. The T_d values of this compound were found to be 253.1 and 362.8 ºC. SSP-PCDOT was found to be thermally stable up to ~218 °C **(Figure 3.9b)**, with the decomposition pattern almost resembled that of dibromothiophene **26** whereas the thermal decomposition started above 363 ºC for FeCl$_3$-polymerized PCDOT **(Figure 3.9c)**.

Table 3.13 Decomposition temperature of monomer **26** and PCDOT

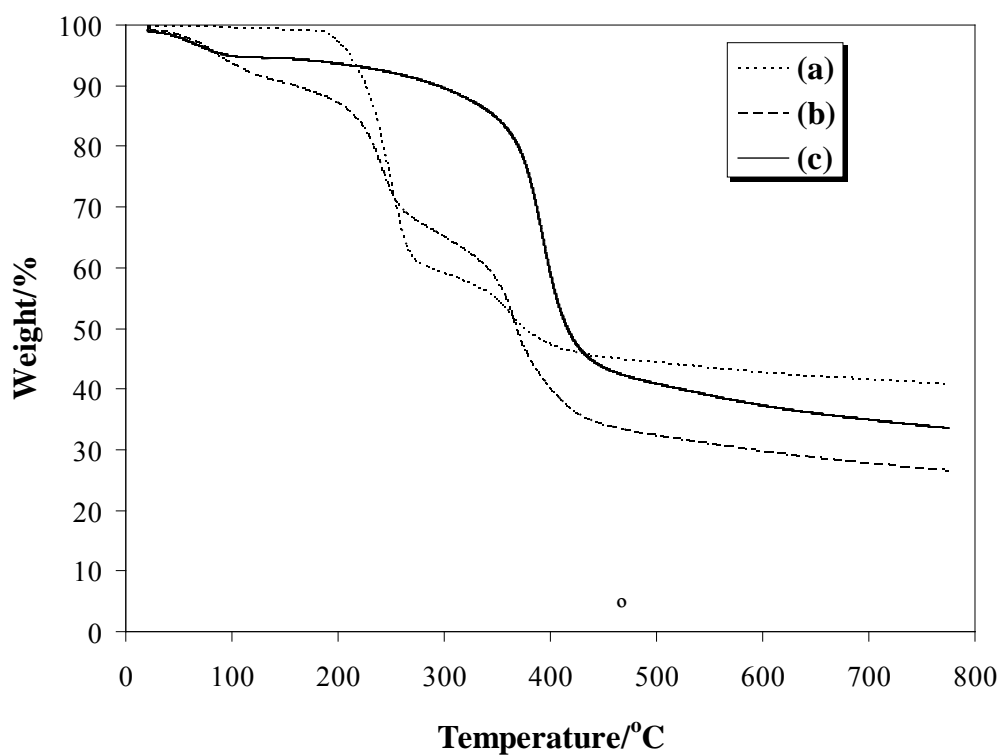| Samples	T_{onset} (ºC)	T_d (ºC)
Monomer **26**	217.2, 346.9	253.1, 362.8
SSP-PCDOT (heated at120 ºC)	218.4, 344.6	240.8, 365.3
FeCl$_3$-polymerized PCDOT	363.2	391.8

Figure 3.9 TGA thermograms of (a) the dibromothiophene **26** (b) the SSP-PCDOT (heated at 120 ºC) (c) FeCl$_3$-polymerized PCDOT
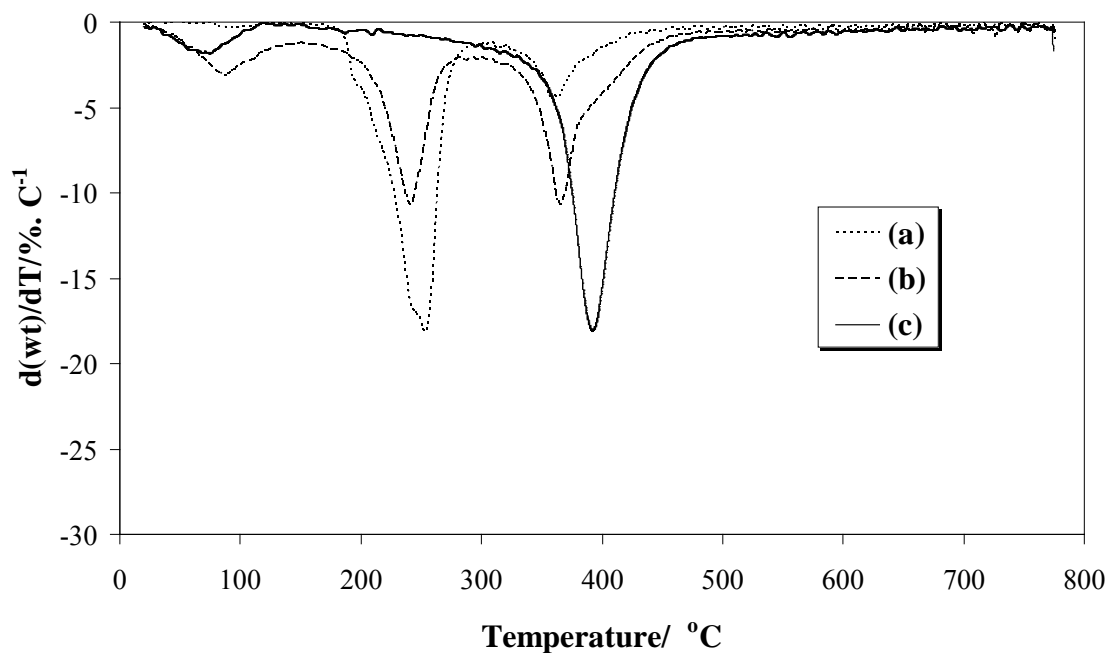

Figure 3.10 DTG thermograms of (a) the dibromothiophene **26** (b) the SSP-PCDOT (heated at 120 ºC) (c) FeCl$_3$-polymerized PCDOT

3.2.3 Differential Scanning Calorimetry (DSC) Studies

DSC method under non-isothermal conditions was used to investigated the melting and crystallization behaviours of dibromothiophene **26**. The data obtained from the DSC heating endotherm was used to determine the melting temperature (T_m) while the DSC cooling exotherm was used to determine the and crystallization temperature (T_c).

The DSC melting of **26** are shown in **Figure 3.11**. The endotherm of this compound shows one melting peak at 130 ºC. The crystallization behaviours of compound **26** was investigated from the cooling thermograms in **Figure 3.11**. This thermogram show two crystallization peaks at around 209 and 248 ºC.
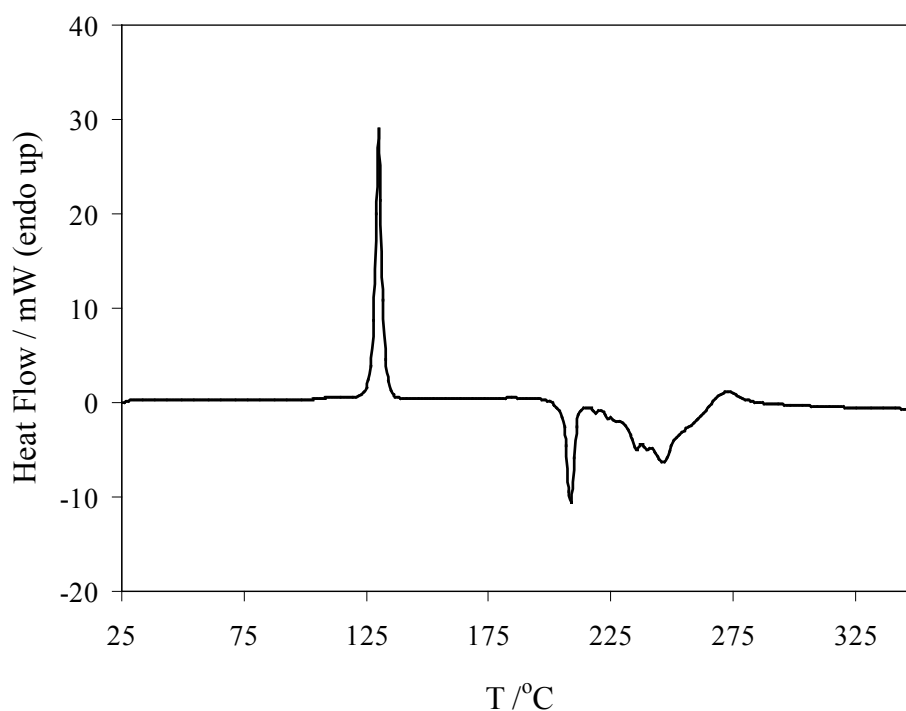

Figure 3.11 DSC curve of dibromothiophene **26**

3.12 Scanning Electron Micrographs (SEM)

For microscopic analysis, it could be seen that the white crystals of the compound **26** had transformed to blue-black crystals that retained the morphology of the starting material **(Figure 3.2)**. **Figure 3.11a,b** showed the smooth surface of crystal monomer **26**. Solid-state polymerization of PCDOT at 70 and 100 ºC for 24 h showed the preservation of the crystalline morphology. However, SEM analysis of SSP-PCDOT heated at 120 ºC showed that the crystalline surface was destroyed during polymerization due perhaps to evaporation of the excess bromine mostly from the surface layer **(Figure 3.11g, h)**. In comparison, FeCl$_3$-polymerized PCDOT, showed no crystallinity on the surface **(Figure 3.11i and j)**.
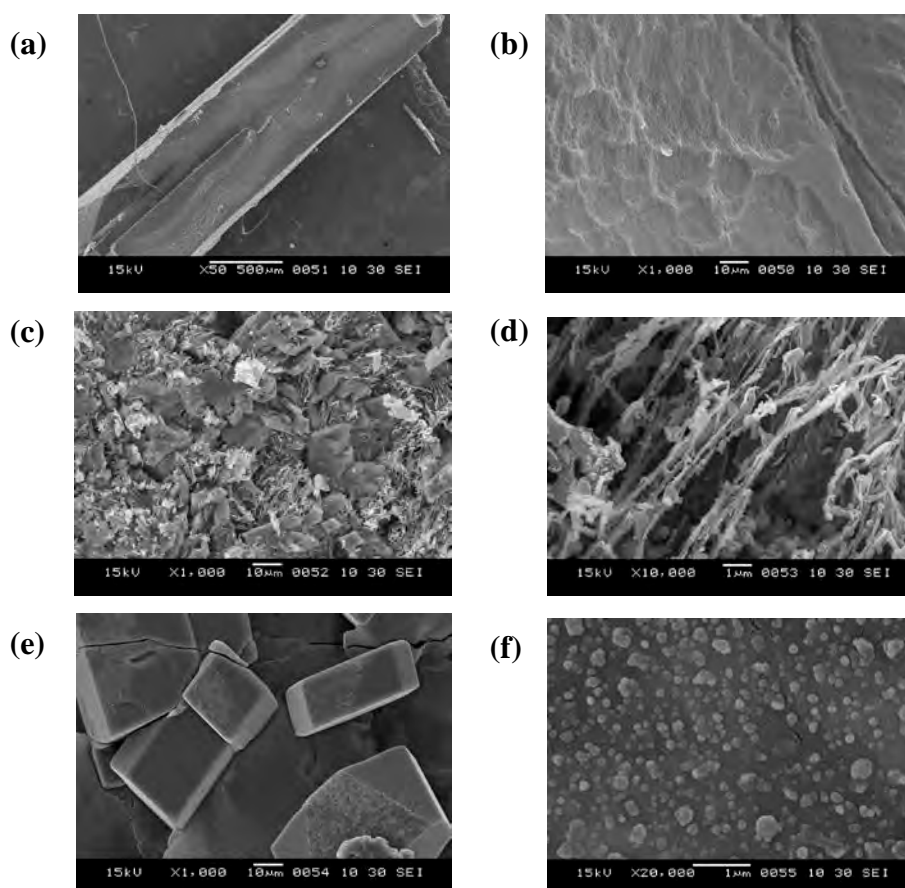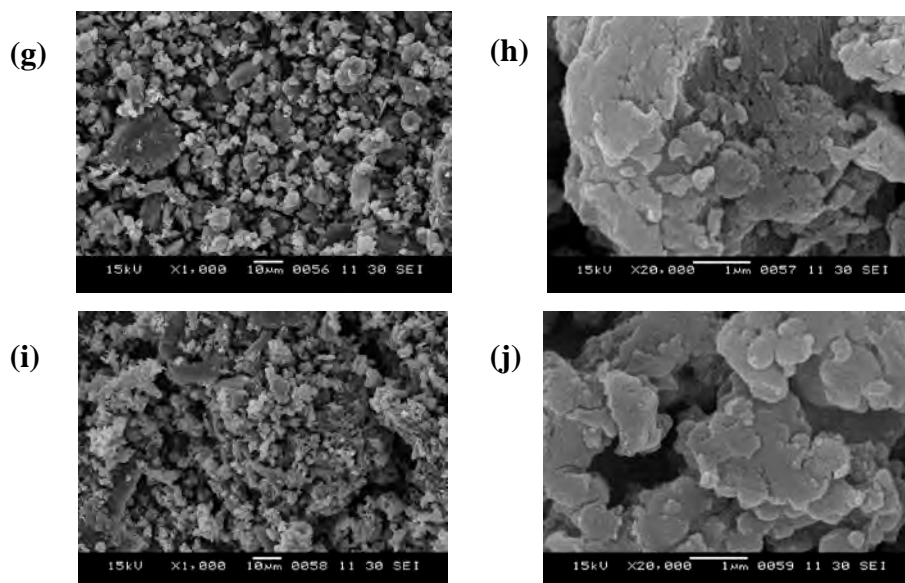
Figure 3.11 SEM surface of (a) the crystal of **DBCDOT 26**; (b) enlargement of the crystal of **DBCDOT 26**; (c) SSP-PCDOT (heated at 70 ºC); (d) enlargement of SSP-PCDOT (heated at 70 ºC); (e) SSP-PCDOT (heated at 100 ºC); (f) enlargement of SSP-PCDOT (heated at 100 ºC); (g) SSP-PCDOT (heated at 120 ºC); (h) enlargement of SSP-PCDOT (heated at 120 ºC); (i) $FeCl_3$-polymerized PCDOT; (j) enlargement of $FeCl_3$-polymerized PCDOT .

3.2.9 Conductivity measurement

Electrical conductivity measurement were carried out using four-point probe technique. Calculation of the conductivity values was shown in **Table B.1, Appendix B**. From **Table 3.14**, the conductivity of $FeCl_3$-polymerized PCDOT rised up to only 0.0197 S/cm after doping with iodine. The highest conductivity belonged to the SSP-polymer prepared at 120 ºC, which probably because of largest extent of polymeric structure within the sample. It conductivity rised up to 40.7 S/cm after doping with iodine, even higher than the reported values of SSP-PEDOT (27-30 S/cm) [48, 49]. Surprisingly, sample storing the polymer at room temperature for 2 weeks gave a sample with the highest conductivity (131 S/cm).

Table 3.14 Conductivity data of the PCDOT.

Samples	σ_{rt} of SSP-PCDOT[a] (S/cm)			σ_{rt} of FeCl$_3$-polymerized PCDOT[a] (S/cm)
Heated Temperature (ºC)	70	100	120	RT
pellets as synthesized	$(9.41\pm1.87)\times10^{-3}$	5.07 ± 0.73	8.04 ± 0.59	$(4.57\pm0.24)\times10^{-3}$
pellets after I$_2$ doping	$(1.80\pm0.26)\times10^{-2}$	11.5 ± 1.1	40.7 ± 4.0	$(1.97\pm0.11)\times10^{-2}$
pellets after storing[b]	0.889 ± 0.191	54.8 ± 12.1	131 ± 30	0.710 ± 0.038

[a] Reported values are the average of three measurements.

[b] The sample were stored in closed vial at room temperature for 3 weeks.

3.2.10 X-ray Powder Diffraction Analysis

We performed X-ray diffraction study on the crystal of monomer **26**, SSP- and FeCl$_3$-polymerized PCDOT. The crystalline **26** revealed a strong and quite sharp diffraction peaks (**Figure 3.12** and **Table B.2, Appendix B**). The strongest peak in the PCDOT diffractogram corresponds to a *d* spacing of 3.55 Å, which is the interplane distance between the dibromothiophene **26** molecules in the stack, relatively close to the value of PEDOT ($d = 3.50$ Å) [48]. These sharp peaks were still retained in all of the SSP-PCDOT powder sample, that indicated the highly crystalline structure of these polymers. In contrast, the XRD measurement of FeCl$_3$-polymerized PCDOT clearly indicated its structure as an amorphous solid.
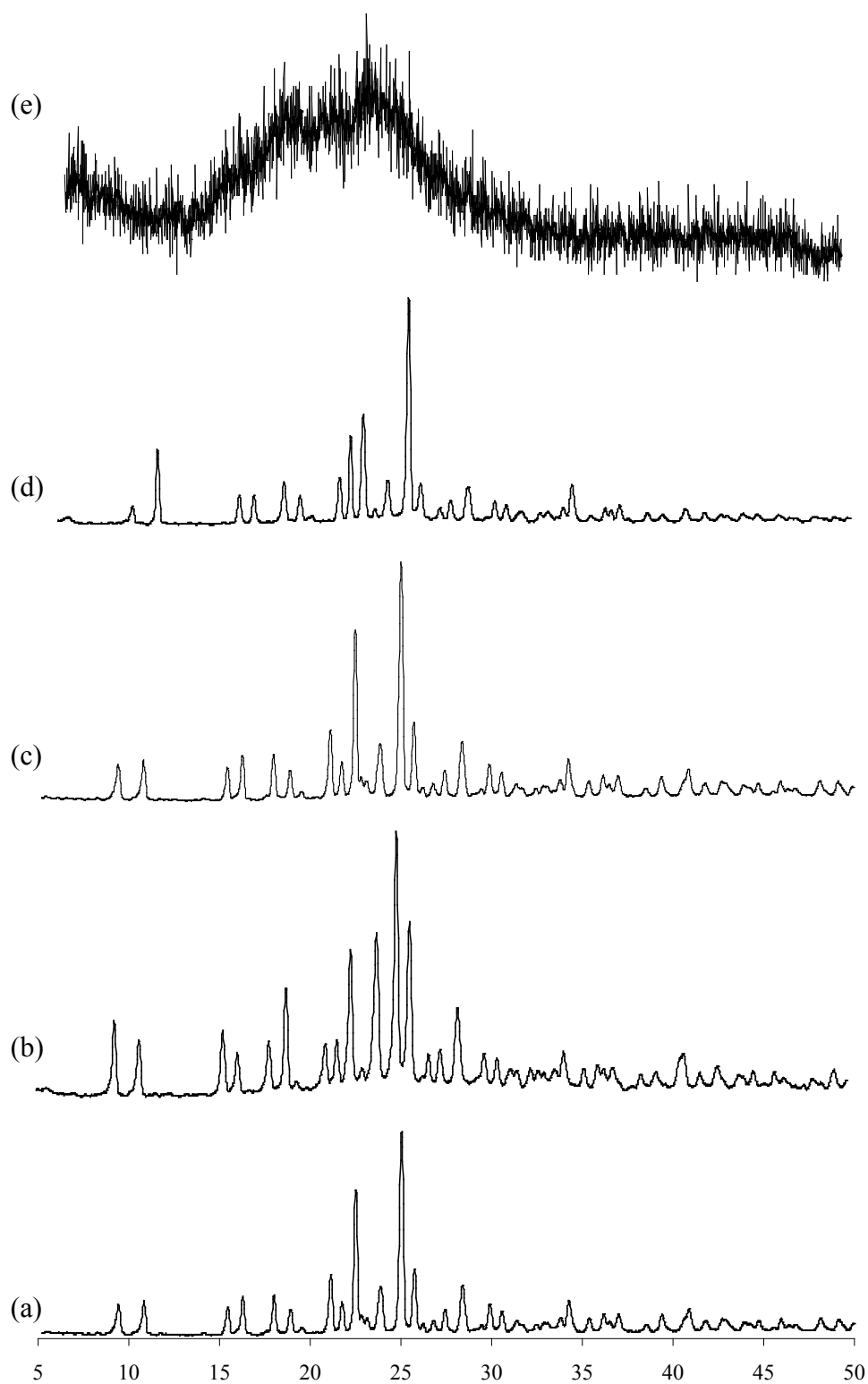
Figure 3.12 XRD spectra of (a) **DBCDOT 26**; (b) SSP-PCDOT heated at 70 °C; (c) SSP-PCDOT heated at 100 °C; (d) SSP-PCDOT heated at 120 °C (e) $FeCl_3$-polymerized PCDOT.

CHAPTER IV

CONCLUSION

Halogenations of various thiophene derivatives with *N*-bromosuccinimide (NBS) and *N*-chlorosuccinimide (NCS) have been carried out giving the products in excellent yields (80-99%). Synthesis of two monomers, 2-vinyl-2,3-dihydrothieno [3,4-*b*][1,4]dioxin (Vinyl-EDOT) **18b** and 3,4-*trans*-cyclohexylenedioxythiophene (CDOT) **25** were successfully achieved. Vinyl-EDOT **18b** was synthesized via the traditional synthesis of thiophene in the five step route. Substitutions of ethyl chloroacetate **13d** with sodium sulfide nonahydrate yielded the diethyl thioglycolate **14** in 50%. Diethyl 3,4-dihydroxy thiophene-2,5-dicarboxylate **15** was synthesized via Hinsberg reaction of diester **14** and diethyl oxalate in 70%. Williamson etherification of **15** and 3,4-dichloro-1-butene **13b** gave the dicarboxylate precursor **16b** in 42%. Hydrolysis of the dicarboxylate **16b** afforded the dicarboxylic acid **17b** in 90%. The diacid **17b** was decarboxylated to yield the new Vinyl-EDOT **18b** in 65%.

In another case, the new 3,4-*trans*-cyclohexylenedioxythiophene (CDOT) **25** was synthesized by transetherification with *trans*-1,2-cyclohexanediol and *p*-toluenesulfonic acid (PTSA) as the catalyst, yielding the product in 86%. Bromination of CDOT **25** with NBS gave 2,5-dibromo-3,4-cyclohexylenedioxythiophene (DBCDOT) **26** in 94% yield.

The synthesis of poly(3,4-cyclohexylenedioxythiophene) (PCDOT) was performed by oxidative coupling polymerization using anhydrous ferric chloride as the oxidative coupling agent, obtaining the product in 69% yield. The solid state polymerization (SSP) of 2,5-dibromo-3,4-cyclohexylenedioxythiophene (DBCDOT) **26** to become PCDOT had been successfully executed. Characterizations of the resulting polymer were performed by NMR, FT-IR and solid UV-Vis techniques. The X-ray structural analysis for DBCDOT revealed the intermolecular Br…Br distances between adjacent molecules to be approximately 4.21 Å. MALDI-TOF spectra of SSP-PCDOT supported the presence of the expected polymers containing up to 15 monomer units with the mass differences between fragmented peaks corresponded to the molecular weight of the monomer **25** (m/z = 194). SEM analysis showed that the

crystal surface of the monomer was partially or totally destroyed during polymerization. The X-ray diffraction study showed no major change in the crystalline structure of the PCDOT even with the sample heated at high temperature. The DSC curve of DBCDOT revealed T_m at 130 ºC and T_c at 209 and 248 ºC. Four-point probe technique was used to measure the conductivities of the samples. The highest conductivity (131 S/cm) was found with the SSP-PCDOT heated at 120 ºC for 24 h and stored at room temperature for another 14 days.

REFERENCES

[1] Chiang, C. K.; Fincher, C. R., Jr.; Park, Y. W.; Heeger, A. J.; Shirakawa, H.; Louis, E. J.; Gau, S. C.; Macdiarmid, A. G. Electrical Conductivity in Doped Polyacetylene. <u>Phys. Rev. Lett.</u> 39 (1997) : 1098-1101.

[2] Shirakawa, H.; Louis, E. J.; MacDiarmid, A. G.; Chiang, C. K.; Heeger, A. H. Synthesis of Electrically Conducting Organic Polymers: Halogen Derivatives of Polyacetylene, $(CH)_x$. <u>J. Chem. Soc., Chem. Commun.</u> (1977) : 578 – 580.

[3] Diaz, A. F.; Kanazawa, K. K.; Gardini, G. P. Electrochemical Polymerization of Pyrrole. <u>J. Chem. Soc. Chem. Commun.</u> (1979) : 635-636.

[4] Forrest, S. R. The Path to Ubiquitous and Low Cost Organic Electronic Appliances on Plastic. <u>Nature</u> 428 (2004) : 911-918.

[5] Saxena, V.; Malhotra, B. D. Prospects of Conducting Polymers in Molecular Electronics. <u>Curr. Appl Phys.</u> 3 (2003) : 293-305.

[6] Bunz, U. H. F. Poly(aryleneethynylene)s: Syntheses, Properties, Structures, and Applications. <u>Chem. Rev.</u> 100 (2000) : 1606-1644.

[7] Skotheim, T. A.; Elesenbaumer, R. L.; Reynolds, J. R. <u>Handbook of Conducting Polymers</u>. 2nd ed. Marcel Dekker: New York, 1998.

[8] Halls, J. J. M.; Walsh, C. A.; Greenham, N. C.; Marseglia, E. A.; Friend, R. H.; Moratti, S. C.; Holmes, A. B. Efficient Photodiodes from Interpenetrating Polymer Networks. <u>Nature</u>. 376 (1995) : 498-500.

[9] Albert, K. J.; Lewis, N. S.; Schauer, C. L.; Sotzing, G. A.; Stitzel, S. E.; Vaid, T. P.; Walt, D. R. Cross-Reactive Chemical Sensor Arrays. <u>Chem. Rev.</u> 100 (2000) : 2595-2626.

[10] McQuade, D. T.; Pullen, A. E.; Swager, T. M. Conjugated Polymer-Based Chemical Sensors Chem. Rev. 100 (2000) : 2537-2574.

[11] Lange, U.; Roznyatoskaya, N. V.; Mirsky, V. M. Conducting Polymers in Chemical Sensors and Arrays. Anal. Chim. Acta. 614 (2008) : 1-26.

[12] Kraft, A.; Grimsdale, A. C.; Holmes, A. B. Electroluminescent Conjugated Polymers-Seeing Polymers in a New Light. Angew. Chem. Int. Ed. 37 (1998) : 402-428.

[13] Paoli, M. A.; Gazotti, W. A. Electrochemistry, Polymers and Opto-Electronic Devices: A Combination with a Future. J. Braz. Chem. Soc. 13 (2002) : 410-424.

[14] Zhou, E.; Tan, Z.; Huo, L.; He, Y.; Yang, C.; Li, Y. Effect of Branched Conjugation Structure on the Optical, Electrochemical, Hole Mobility,and Photovoltaic Properties of Polythiophenes. J. Phys. Chem. B. 110 (2006) : 26062-26067.

[15] Streitwieser, A., Jr. Molecular Orbital Theory for Organic Chemists. Wiley: New York, 1961.

[16] Dubois, C. J. Donor-Acceptor Methods for Band Gab Control in Conjugated Polymers. Ph.D. Dissertation, The Graduate School of the University of Florida, USA, 2003.

[17] Chadwick, J. E.; Kohler, B. E. Optical Spectra of Isolated *S*-cis- and *S*-trans-Bithiophene: Torsional Potential in the Ground and Excited States. J. Phys. Chem. 98 (1994) : 3631-3637.

[18] DiCésare, N.; Belletête, M.; Marrano, C.; Leclerc, M.; Durocher, G.

Intermolecular Interactions in Conjugated Oligothiophenes. 1. Optical Spectra of Terthiophene and Substituted Terthiophenes Recorded in Various Environments. J. Phys. Chem. A. 103 (1999) :795-802.

[19] DiCésare, N.; Belletête, M.; Garcia, E. R.; Leclerc, M. Intermolecular Interactions in Conjugated Oligothiophenes. 3. Optical and Photophysical Properties of Quaterthiophene and Substituted Quaterthiophenes in Various Environments J. Phys. Chem. A. 103 (1999) : 3864-3875.

[20] Heeger, A. J. Semiconducting and Metallic Polymers: The Fourth Generation of Polymeric Materials. Synth. Met. 125 (2002) : 23-42.

[21] Greenham, N. C.; Friend, R. H. Semiconductor Device Physics of Conjugated Polymers, in Solid State Physics, Advances in Research and Application. Academic Press: New York, 1995.

[22] Su, W. P.; Schrieffer, J. R.; Heeger, A. J. Solitons in Polyacetylene. Phys. Rev. Lett. 42 (1979) : 11698-1701.

[23] Brazovskii, S. A. Fröhlich Conductivity at Temperatures Excitations in the Peierls-Fröhlich State. Sov. Phys. JETP Lett. 28 (1978) : 606.

[24] Rice, M. J. Charged π-Phase Kinks in Lightly Doped Polyacetylene. Phys. Lett. A 71 (1979) : 152-154.

[25] Campbell, D. K.; Bishop, A. R. Soliton Excitations in Polyacetylene and Relativistic Field Theory Models. Phys. Rev. B 24 (1981) : 4859-4862.

[26] Epstein, A. J.; Ginder, J. M.; Zuo, F.; Bigelow, R. W.; Woo, H.-S.; Tanner, D. B.; Richter, A. F.; Huang, W.-S.; MacDiarmid, A. G. Very Low Temperature Nuclear Spin Diffusion in trans-Polyacetylene. Synth. Met. 18 (1987) : 303-309.

[27] Strafstrom, S.; Brédas, J. L.; Epstein, A. J.; Woo, H. S.; Tanner, D. B.; Huang, W. S.; MacDiarmid, A. G. Correlation Functions for Hubbard-type Models: The

Exact Results for the Gutzwiller Wave Function in One Dimension. <u>Phys. Rev. Lett.</u> 59 (1987) : 1472-1475.

[28] Pinto, N. J.; Shah, P. D.; Kahol, P. K.; McCormick, B. J. Conducting State of Polyaniline Films: Dependence on Moisture. <u>Phys. Rev. B</u> 53 (1996) : 10690-10694.

[29] Kumar, D.; Sharma, R. C. Advances in Conductive Polymers. <u>Eur. Polym. J.</u> 34 (1998) : 1053-1060.

[30] Li, X.; Jlao, Y.; Li. S. The Syntheses, Properties and Application of New Conducting Polymers. Eur. Polym. J. 27 (1991) : 1345-1351.

[31] Bowden, M. J.; Turner, S. R. <u>Electronic and Photonic Applications of Polymers</u>. ACS Advances in Chemistry Series 210, American Chemical Society: Washington DC, 1998.

[32] Street, G. B. Polarons, Bipolarons, and Solitons in Conducting Polymers. <u>Acc. Chem. Res.</u> 18 (1985) : 309.

[33] Roncali, J. Conjugated Poly(thiophenes): Synthesis, Functionalization, and Applications. <u>Chem. Rev.</u> 92 (1992) : 711-738.

[34] Nalwa, H. S. <u>Handbook of Organic Conductive Molecules and Polymers</u>: Vol. 2 Spectroscopy and Physical Properties. John Wiley & Sons: Chichester, 1997.

[35] Roncali, J.; Garreau, R.; Yassar, A.; Marque, P.; Garnier, F.; Lemaire, M. Effects of Steric Factors on the Electrosynthesis and Properties of Conducting Poly (3-alkylthiophenes). <u>J. Phys. Chem.</u> 91 (1987) : 6706–6714.

[36] Pomerantz, M.; Tseng, J. J.; Zhu, H.; Sproull, S. J.; Reynolds, J. R.; Uitz, R; Amott, H. J.; Haider, M. I. Processable Polymers and Copolymers of 3-Alkylthiophenes and Their Blends. <u>Synth. Met.</u> 41 (1991) : 825-830.

[37] Wang, S.; Takahashi, H.; Yoshino, K. Dependence of Poly(3-alkylthiophene) Film Properties on Electrochemical Polymerization Conditions and Alkyl Chain Length. <u>Jpn. J. Appl. Phys.</u> 29 (1990) : 772-775.

[38] Sugimoto, R.; Takeda, S.; Gu, H. B.; Yoshino, K. Preparation of Soluble Polythiophene Derivative Utilizing Transition Metal Halides as Catalysts and Their Property. <u>Chem. Express</u> 1 (1986) : 635-638.

[39] Amou, S.; Haba, O.; Shirato, K.; Hayakawa, T.; Ueda, M.; Takeuchi, K.; Asai, M. Head-to-Tail Regioregularity of Poly(3-hexylthiophene) in Oxidative Coupling Polymerization with $FeCl_3$. <u>J. Polym. Sci. A: Polym. Chem.</u> 37 (1999) : 1943-1948.

[40] Niemi, V. M.; Knuuttila, P.; Österholm, J. E.; Korvola, J. Polymerization of 3-Alkylthiophenes with $FeCl_3$. <u>Polymer</u> 33 (1992) : 1559-1562.

[41] Allinger, N. L.; Walter T. J. Alkyl Group Isomerization in the Cross-Coupling Reaction of Secondary Alkyl Grignard Reagents with Organic Halides in the Presence of Nickel-Phosphine Complexes as Catalysts. <u>J. Am. Chem. Soc.</u> 94 (1972) : 9268-9269.

[42] Negishi, E. I.; Takahashi T.; Baba, S.; Horn, D. E. V.; Okukado, N. Palladium- or Nickel-Catalyzed Reactions of Alkenylmetals with Unsaturated Organic Halides as a Selective Route to Arylated Alkenes and Conjugated Dienes: Scope, Limitations, and Mechanism. <u>J. Am. Chem. Soc.</u> 109 (1987) : 2393-2401.

[43] McCullough, R. D.; Lowe, R. D. Enhanced Electrical Conductivity in Regioselectively Synthesized Poly(3-alkylthiophenes). <u>J. Chem. Soc., Chem. Commun.</u> (1992) : 70-72.

[44] Robert, S.; Lowe, P. C.; Ewbank, J. L.; Lei, Z.; McCullough, R. D. Regioregular, Head-to-Tail Coupled Poly(3-alkylthiophenes) Made Easy by the GRIM

Method: Investigation of the Reaction and the Origin of Regioselectivity. <u>Macromolecules</u> 34 (2001) : 4324-4333.

[45] McCullough, R. D.; Lowe, R. D.; Jayaraman, M.; Anderson, D. L. Design, Synthesis, and Control of Conducting Polymer Architectures: Structurally Homogeneous Poly(3-alkylthiophenes). <u>J. Org. Chem.</u> 58 (1993) : 904-912.

[46] McCullough, R. D.; Stephanie, T. N.; Williams, S. P.; Lowe, R. D.; Jayaraman, M. Self-Orienting Head-to-Tail Poly(3-alkylthiophenes): New Insights on Structure-Property Relationships in Conducting Polymers. <u>J. Am. Chem. Soc.</u> 115 (1993) : 4910-4911.

[47] McCullough, R. D.; Williams, S. P. Toward Tuning Electrical and Optical Properties in Conjugated Polymers Using Side Chains: Highly Conductive Head-to-Tail Heteroatom-Functionalized Polythiophenes. <u>J. Am. Chem. Soc.</u> 115 (1993) : 11608-11609.

[48] Meng, H.; Perepichka, D. F.; Bendikov, M.; Wudl, F. Solid-State Synthesis of Conducting Polythiophene via an Unprecedented Heterocyclic Coupling Reaction. <u>J. Am. Chem. Soc.</u> 125 (2003) : 15151-15162.

[49] Meng, H.; Perepichka, D. F.; Wudl, F. Facile Solid-State Synthesis of Highly Conducting Poly(ethylenedioxythiophene). <u>Angew. Chem. Int. Ed.</u> 42 (2003) : 658-661.

[50] McCullough, R. D.; Williams, S. P.; Tristram-Nagle, S.; Jayaraman, M.; Ewbank, P. C.; Miller, L. The First Synthesis and New Properties of Regioregular, Head-To-Tail Coupled Polythiophenes. <u>Synth. Met.</u> 69 (1995) : 279-282.

[51] Chen, T. A.; Rieke, R. D. The First Regioregular Head-to-Tail Poly(3-hexylthiophene-2,5-diyl) and a Regiorandom Isopolymer: Ni vs Pd Catalysis of 2(5)-Bromo-5(2)-(bromozincio)-3-hexylthiophene Polymerization. <u>J. Am. Chem. Soc.</u> 114 (1992) : 10087-10088.

[52] Roncali, J. Synthetic Principles for Bandgap Control in Linear π-Conjugated Systems. Chem. Rev. 97 (1997) : 173-206.

[53] Barbarella, G.; Favaretto, L.; Sotgiu, G.; Zambianchi, M.; Arbizzani, C.; Bongini, A.; Mastragostino, M. Controlling the Electronic Properties of Polythiophene through the Insertion of Nonaromatic Thienyl S,S-dioxide Units. Chem. Mater. 11 (1999) : 2533-2541.

[54] Bongini, A.; Barbarella, G.; Favaretto, L.; Zambianchi, M.; Mastragostino, M.; Arbizzani, C.; Soaví, F. Synth. Met. 101 (1999) : 13-14.

[55] Roncali, J.; Blanchard, P.; Frère, P. 3,4-Ethylenedioxythiophene (EDOT) as a Versatile Building Block for Advanced Functional π-Conjugated Systems. J. Mater. Chem. 15 (2005) : 1589–1610.

[56] Caras-Quintero, D.; Bäuerle, P. Efficient Synthesis of 3,4-Ethylenedioxy-thiophenes (EDOT) by Mitsunobu Reaction. Chem. Commun. (2002) : 2690-2691.

[57] Kieseritzky, F. V.; Allared, F.; Dahstedt, E.; Hellberg, J. Simple One-Step Synthesis of 3,4-Dimethoxythiophene and Its Conversion into 3,4-Ethylenedioxythiophene (EDOT). Tetrahedron Lett. 45 (2004) : 6049-6050.

[58] Caras-Quintero, D.; Bäuerle, P. Synthesis of the First Enantiomerically Pure and Chiral, Disubstituted 3,4-Ethylenedioxythiophenes (EDOTs) and Corresponding Stereo- and Regioregular PEDOTs. Chem. Commun. (2004) : 926-927.

[59] Groenendaal, L.; Zotti, G.; Jonas, F. Optical, Conductivity and Magnetic Properties of Electrochemically Prepared Alkylated Poly(3,4-Ethylenedioxy-thiophene)s. Synth. Met. 118 (2001) : 105-109.

[60] Roquet, S.; Leriche, P; Perepichka, I.; Jousselme, B.; Levillian, E.; Frère, P.; Roncali, J. 3,4-Phenylenedioxythiophene (PheDOT): a Novel Platform for the

Synthesis of Planar Substituted π–Donor Conjugated Systems. J. Mater. Chem. 14 (2004) : 1396-1400.

[61] Perepichka, I. F.; Roquet, S.; Leriche, P.; Raimundo, J.-M.; Frère, P.; Roncali, J. Electronic Properties and Reactivity of Short-Chain Oligomers of 3,4-Phenylenedioxythiophene (PheDOT). Chem. Eur. J. 12 (2006) : 2960-2966.

[62] Leriche, P.; Blanchard, P.; Frère, P.; Levillian, E.; Mabon, G.; Roncali, J. 3,4-Vinylenedioxythiophene (VDOT): a New Building Block for Thiophene-Based π-Conjugated Systems. Chem. Commun. (2006) : 275-277.

[63] Spencer, H. J.; Berridge, R.; Crouch, D. J.; Wright, S. P.; Giles, M.; McColloch, I.; Coles, S. J.; Hursthouse, M. B.; Skabara, P. J. Further Evidence for Spontaneous Solid-State Polymerization Reactions in 2,5-Dibromothiophene Derivatives. J. Mater. Chem. 13 (2003) : 2075-2077.

[64] Chanphen, A. Synthesis and Polymerization of 3,4-Dialkoxythiophene. Master's Thesis, Program of Petrochemistry and Polymer Science, Faculty of Science, Chulalongkorn University, 2008.

[65] Summerbell, R. K.; Lunk, H. E. Monochloro-*p*-dioxane and Trichloro-*p*-dioxanes. J. Org. Chem. (1958) : 499-500.

[66] Christ, R.; Summerbell, R. K. A Synthesis of Homologs of Dioxane. J. Am. Chem. Soc. 55 (1933) : 4547-4548.

[67] Summerbell, R. K.; Umhoeffer, R. R., Lappin, G. R. 2,2,3,3,-Tetrachloro-1,4-dioxane. J. Am. Chem. Soc. 69 (1947) : 1352-1354.

[68] Kucera, J. J., Carpenter, D. C. The Catalytic Chlorination of Dioxane. J. Am. Chem. Soc. 57 (1935) : 2346-2347.

[69] Dehm, H. C. 2,3-dibromo-*p*-dioxane. J. Org. Chem. 23 (1958) : 147-148.

[70] Kreilein, M. M.; Eppich, J. C.; Paquette, L. A. 1,4-Dioxene. Org. Synth. 82 (2005) : 99-104.

[71] Kumar, A.; Welsh, D. M.; Morvant, M. C.; Piroux, F.; Abboud, K. A.; Reynold, J. R. Conducting Poly(3,4-alkylenedioxythiophene) Derivatives as Fast Electrochromics with High-Contrast Ratios. Chem. Mater. 10 (1998) : 896-902.

[72] Spencer, H. J.; Skabara, P. J.; Giles, M.; McCulloch, I.; Coles, S. J.; Hursthouse, M. B. The First Direct Experimental Comparison between the Hugely Contrasting Properties of PEDOT and the All-Sulfur Analogue PEDTT by Analogy with Well-Defined EDTT–EDOT Copolymers J. Mater. Chem. 15 (2005) : 4783-4792.

[73] Guo. K.; Hao. J.; Zhang, T.; Zu, F.; Zhai, J.; Qiu, L.; Zhen, Z.; Lui, X.; Shen, Y. The Synthesis and Properties of Novel Diazo Chromophores Based on Thiophene Conjugating Spacers and Tricyanofuran Acceptors Dyes Pigm. 77 (2005) : 657-664.

[74] Frontana-Uribe, B. A., Heinae, J. Efficient Route for the Synthesis of 3,4-Cycloalkoxy-2,5-diethoxycarbonylthiophenes Obtained with Bulky Alkyl Dibromides using Trialkylamines as Base–Solvent. Tetrahedron Lett., 47 (2006) : 4635-4640.

[75] Lima, A.; Schottland, P.; Sadki, S.; Chevrot, C. Electropolymerization of 3,4-Ethylenedioxythiophene and 3,4-Ethylenedioxythiophene Methanol in the Presence of Dodecylbenzenesulfonate. Synth. Met. 93 (1998) 33-41.

[76] Pei, Q.; Zuccarello, G.; Ahlskog, M.; Inganas, O. Electrochromic and Highly Stable Poly(3,4-ethylenedioxythiophene) Switches between Opaque Blue-Black and Transparent Sky Blue. Polymer Papers. 35 (1994) : 1347-1351.

[77] Pope, J.; Buttry, D.; White, S.; Corcoran, R. Single Component Sulfur-Based Cathodes for Lithium-Ion Batteries. US 6,859,726 B1: 2005.

[78] Wynberg, H.; Kooreman, H. J. The Mechanism of the Hinsberg Thiophene Ring Synthesis. J. Am. Chem. Soc. 87 (1965) : 1739-1742.

[79] Li, J. J. Name Reactions in Heterocyclic Chemistry. Wiley: New York, 2004.

[80] Gaupp, C. L.; Welsh, D. M.; Reynolds, J. R. Poly(ProDOT-Et2): A High-Contrast, High-Coloration Efficiency Electrochromic Polymer. Macromol. Rapid Commun. 23 (2002) 885–889.

[81] Furuta, K.; Gao, Q.-Z.; Yamamoto, H. Chiral(Acyloxy)Borane Complex-Catalyzed Asymmetric Diels-Alder Reaction: (1R)-1,3,4-Trimethyl-3-Cyclohexane-1-Carboxaldehyde. Org. Synth. 9 (1998) : 722-727.

[82] Patra, A.; Wijsboom, Y. H.; Zade, S. S.; Li, M.; Sheynin, Y.; Leitus, G.; Bendikov, M. Poly(3,4-ethylenedioxyselenophene). J. Am. Chem. Soc. 130 (2008) : 6734-6736.

[83] Szkurlat, A.; Palys, B.; Mieczkowski, J.; Skompska, M. Electrosynthesis and Spectroelectrochemical Characterization of Poly(3,4-dimethoxythiophene), Poly(3,4-dipropyloxythiophene) and Poly(3,4-dioctyloxythiophene) Films. Electrochim. Acta 48 (2003) : 3665-3676.

[84] Lepeltier,M.; Hiltz, J.; Lockwood, T.; Bélanger-Gariépy, F.; Perepichka, D, F. Towards Crystal Engineering of Solid-State Polymerization in Dibromothiophenes. J. Mater. Chem. (19) 2009 : 5167–5174.

APPENDIX A

δ ppm

Figure A.1 ^{1}H-NMR (CDCl$_3$) spectrum of ethyl chloroacetate **13d**

δ ppm

Figure A.2 ^{13}C-NMR (CDCl$_3$) spectrum of ethyl chloroacetate **13d**
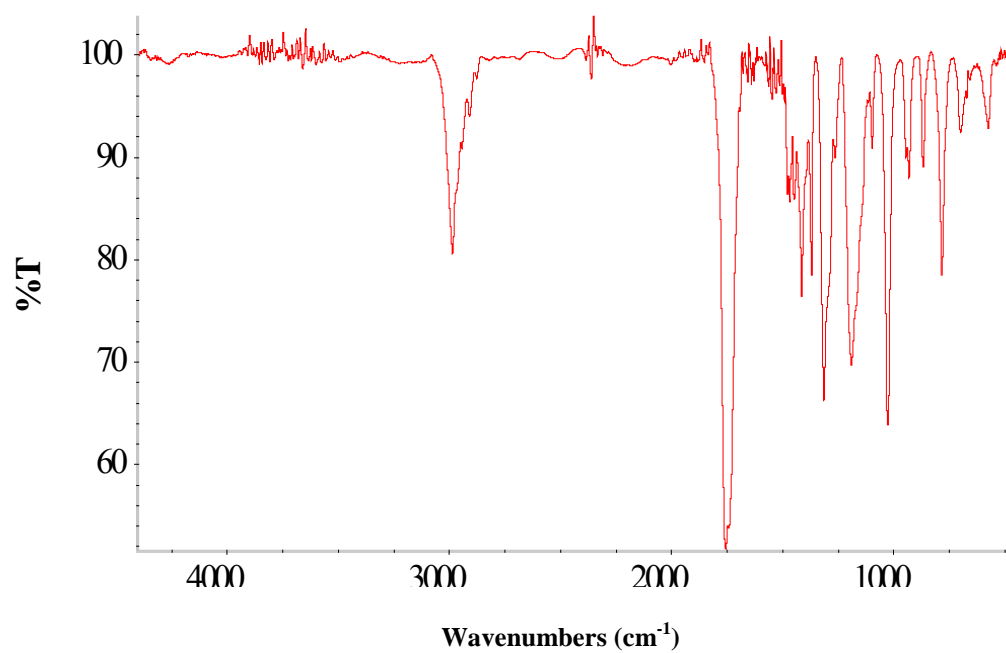
Figure A.3 IR spectrum of ethyl chloroacetate **13d**

δ ppm

Figure A.4 ^{1}H-NMR (CDCl$_3$) spectrum of ethyl iodoacetate **13e**

δ ppm
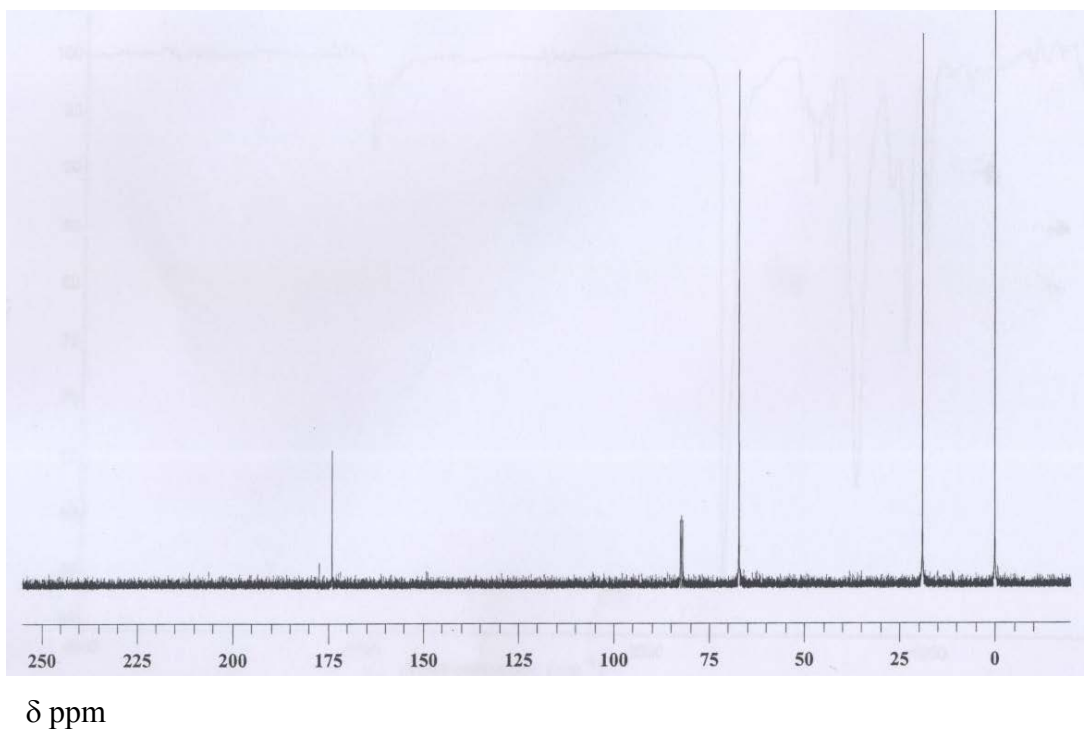
Figure A.5 ^{13}C-NMR (CDCl$_3$) spectrum of ethyl iodoacetate **13e**
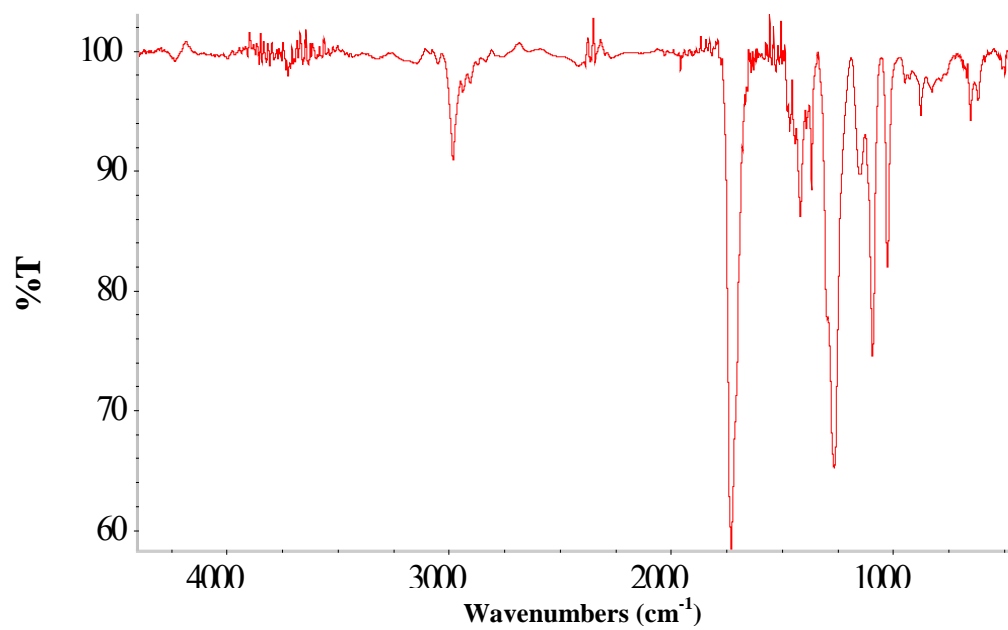
Figure A.6 IR spectrum of ethyl iodoacetate **13e**

δ ppm

Figure A.7 ^{1}H-NMR (CDCl$_3$) spectrum of diethyl thiodiglycolate **14**

δ ppm

Figure A.8 ^{13}C-NMR (CDCl$_3$) spectrum of diethyl thiodiglycolate **14**
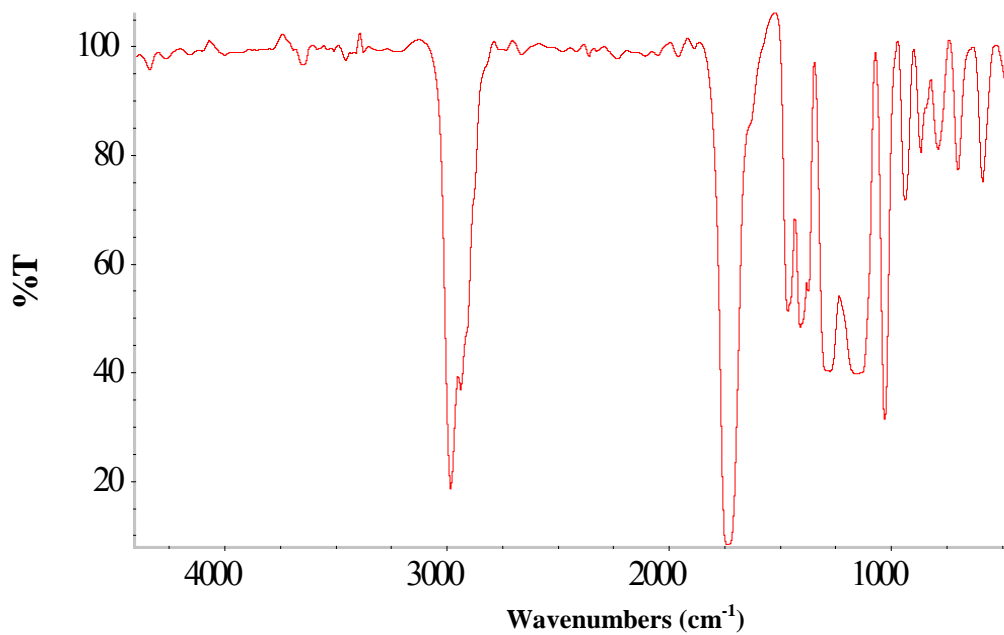
Figure A.9 IR spectrum of diethyl thiodiglycolate **14**
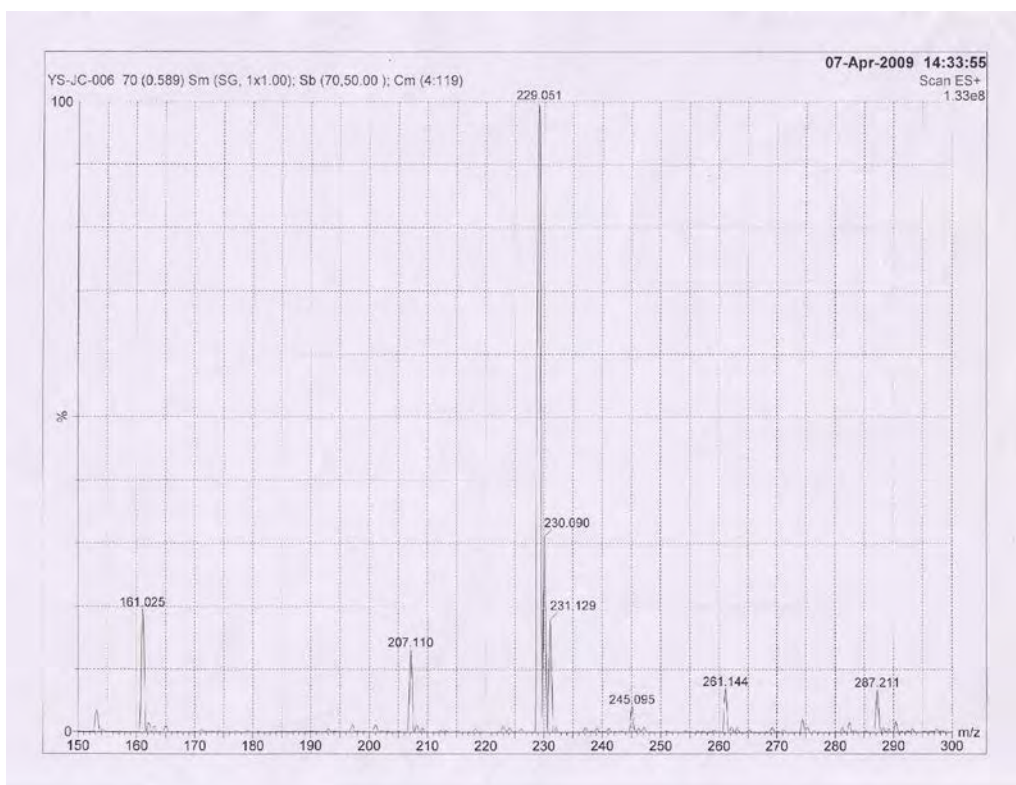
Figure A.10 Mass spectrum of diethyl thiodiglycolate **14**

δ ppm

Figure A.11 [superscript:1]H-NMR (CDCl₃) spectrum of compound **15**

δ ppm

Figure A.12 [superscript:13]C-NMR (CDCl₃) spectrum of compound **15**
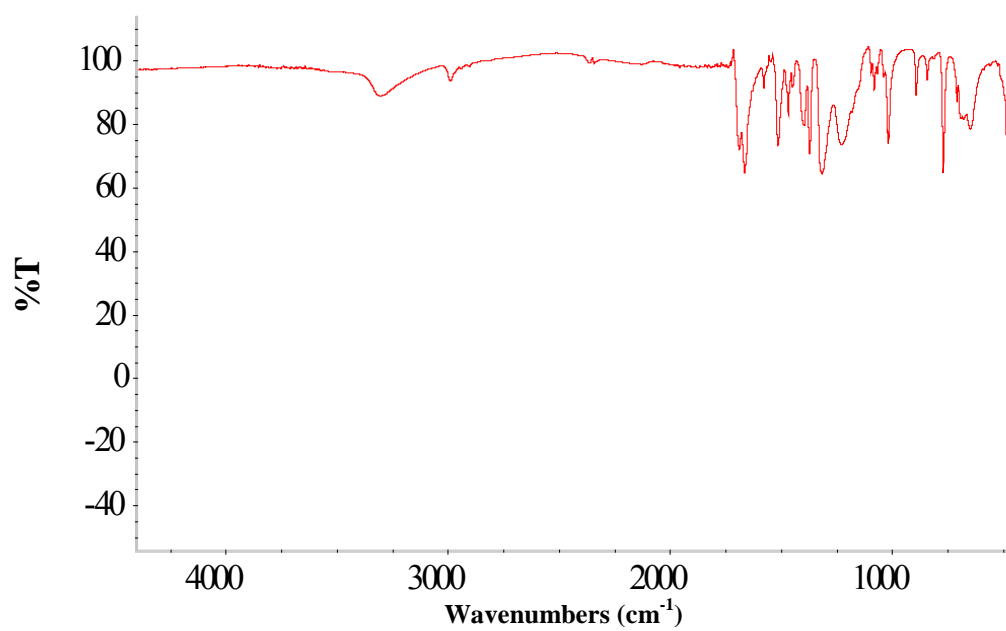
Figure A.13 IR spectrum of compound **15**
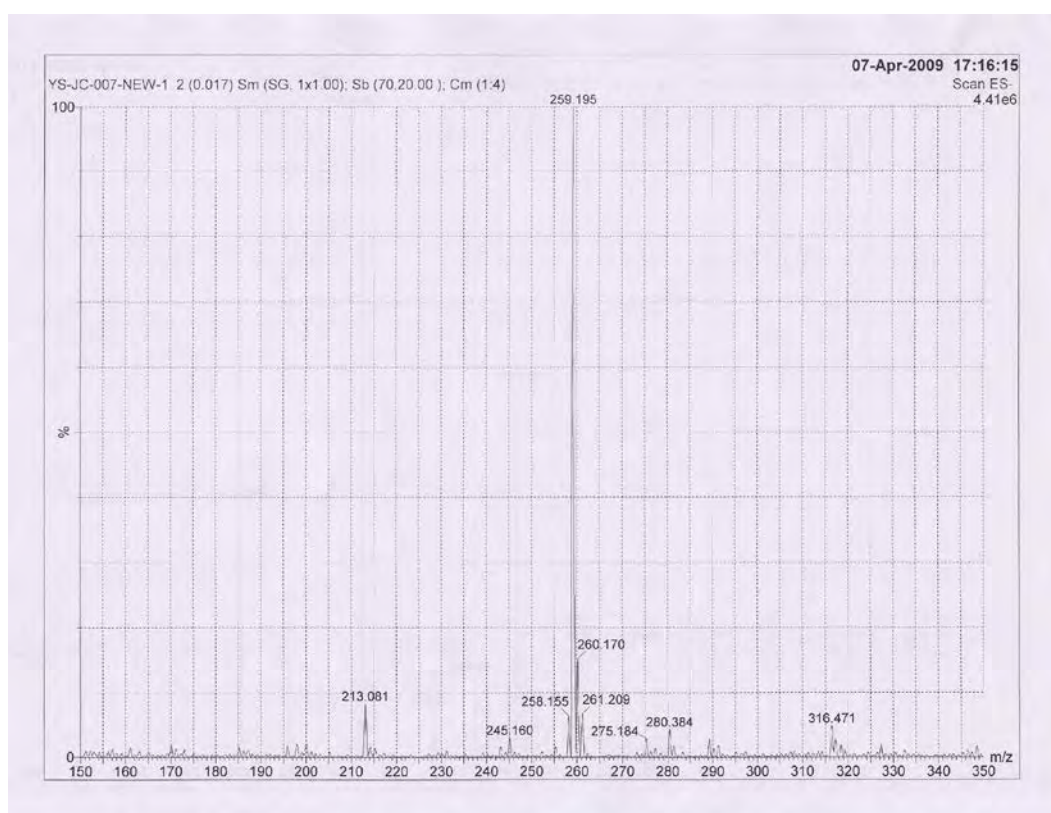
Figure A.14 Mass spectrum of compound **15**

δ ppm

Figure A.15 ^{1}H-NMR (CDCl$_3$) spectrum of compound **16a**

δ ppm

Figure A.16 ^{13}C-NMR (CDCl$_3$) spectrum of compound **16a**
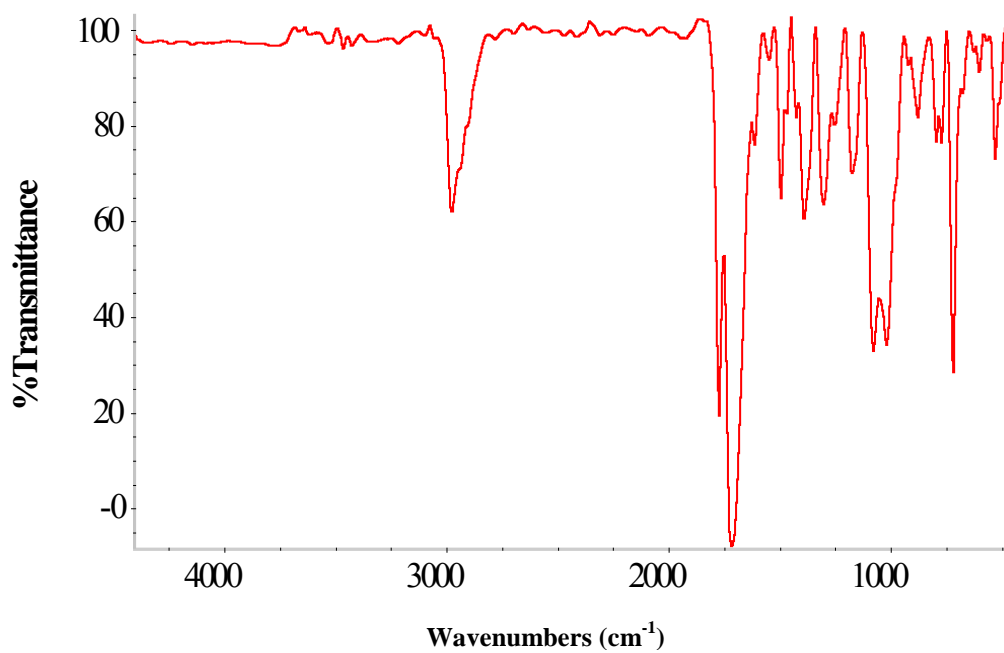
Figure A.17 IR spectrum of compound **16a**
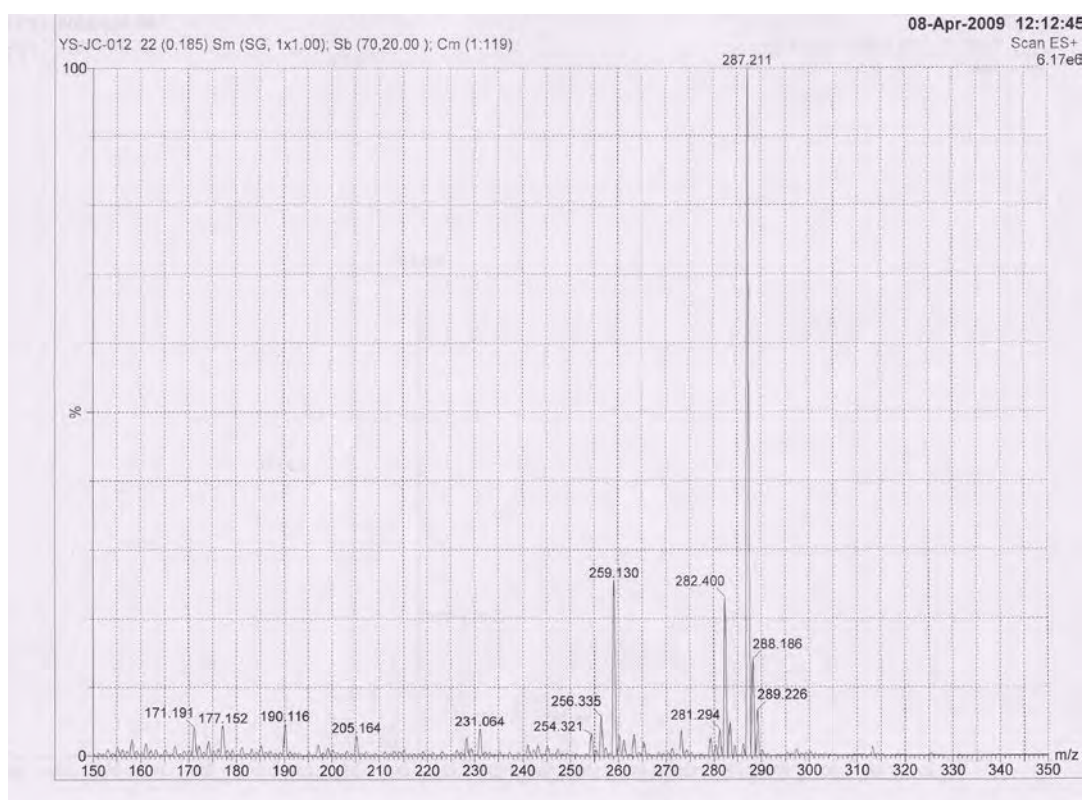
Figure A.18 Mass spectrum of compound **16a**

δ ppm

Figure A.19 ^{1}H-NMR (CDCl$_3$) spectrum of compound **16b**

δ ppm
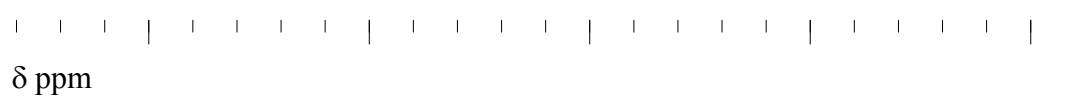
Figure A.20 ^{13}C-NMR (CDCl$_3$) spectrum of compound **16b**
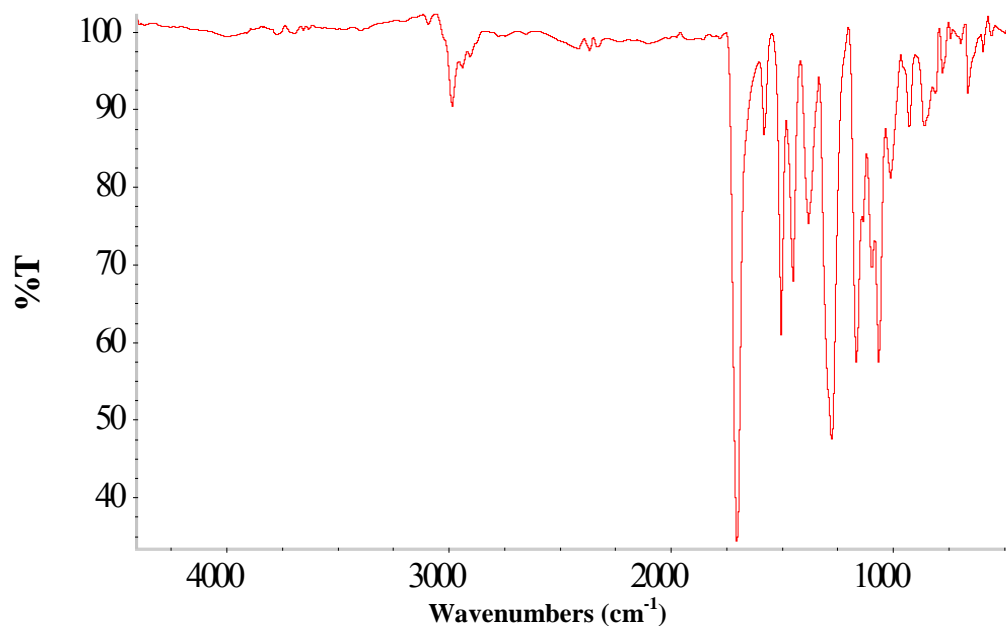
Figure A.21 IR spectrum of compound **16b**
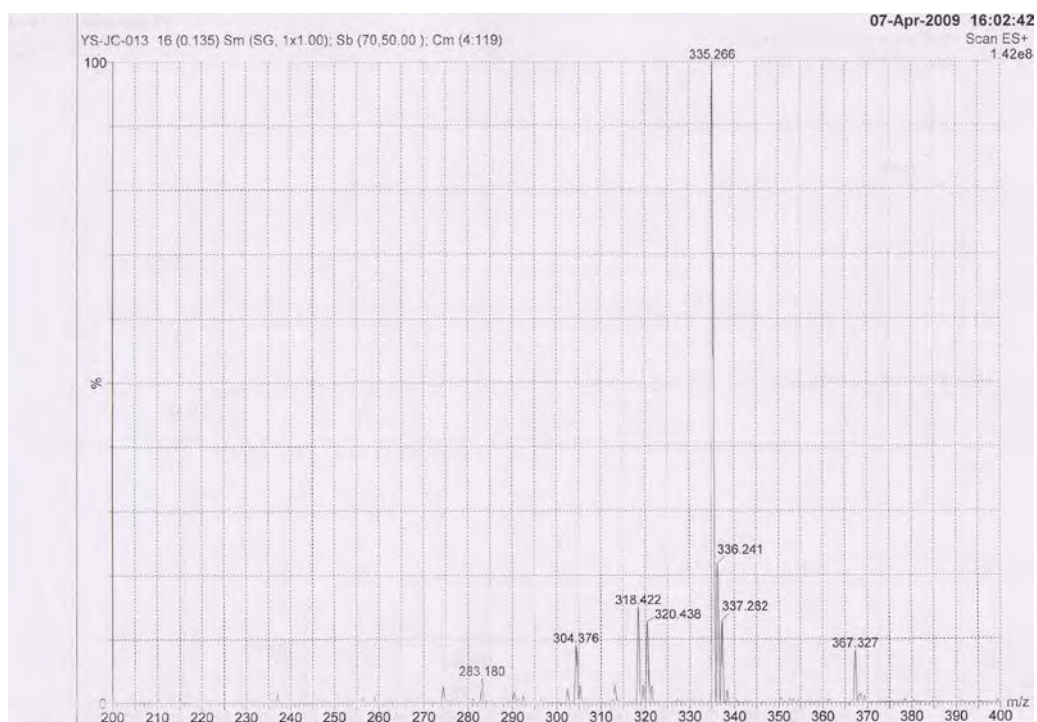
Figure A.22 Mass spectrum of compound **16b**

| ' ' ' ' | ' ' ' ' | ' ' ' ' | ' ' ' ' | ' ' ' ' | ' ' ' ' | ' ' ' ' | ' ' ' ' | ' ' ' ' |

δ ppm

Figure A.23 ^{1}H-NMR (CDCl$_3$) spectrum of compound **16c**

| ' ' ' | ' ' ' ' | ' ' ' ' | ' ' ' ' | ' ' ' ' | ' |

δ ppm

Figure A.24 ^{13}C-NMR (CDCl$_3$) spectrum of compound **16c**
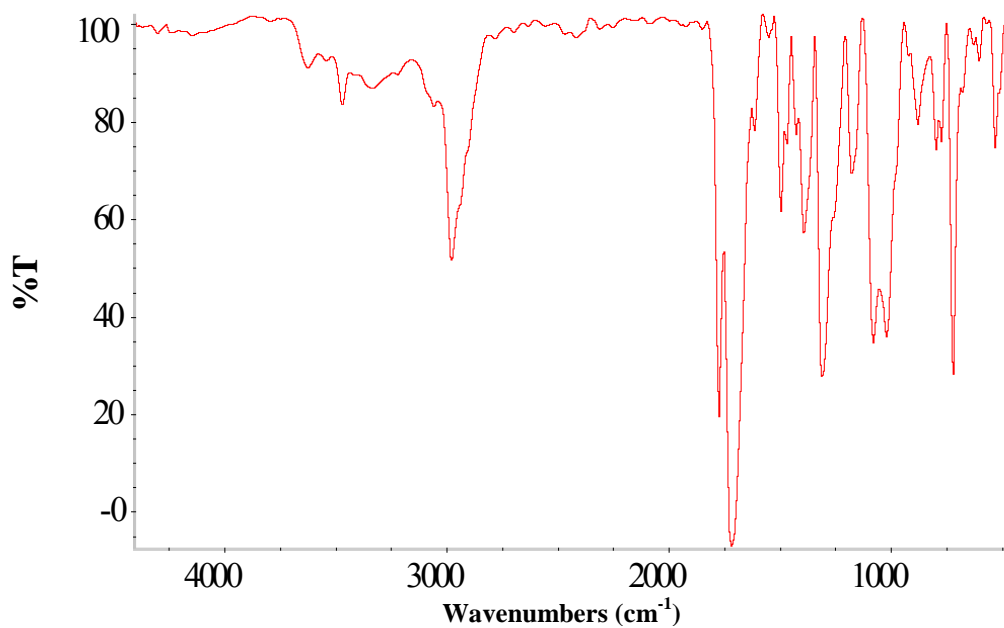
Figure A.25 IR spectrum of compound **16c**
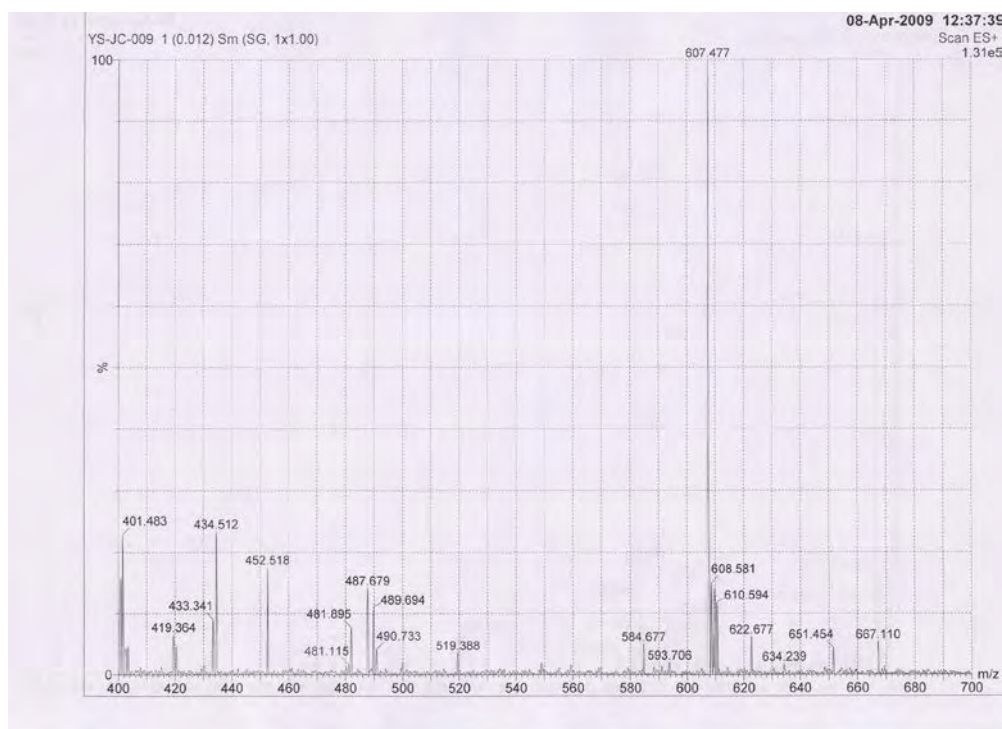
Figure A.26 Mass spectrum of compound **16c**

δ ppm

Figure A.27 ^{1}H-NMR (CDCl$_3$) spectrum of compound **16d**

δ ppm

Figure A.28 ^{13}C-NMR (CDCl$_3$) spectrum of compound **16d**
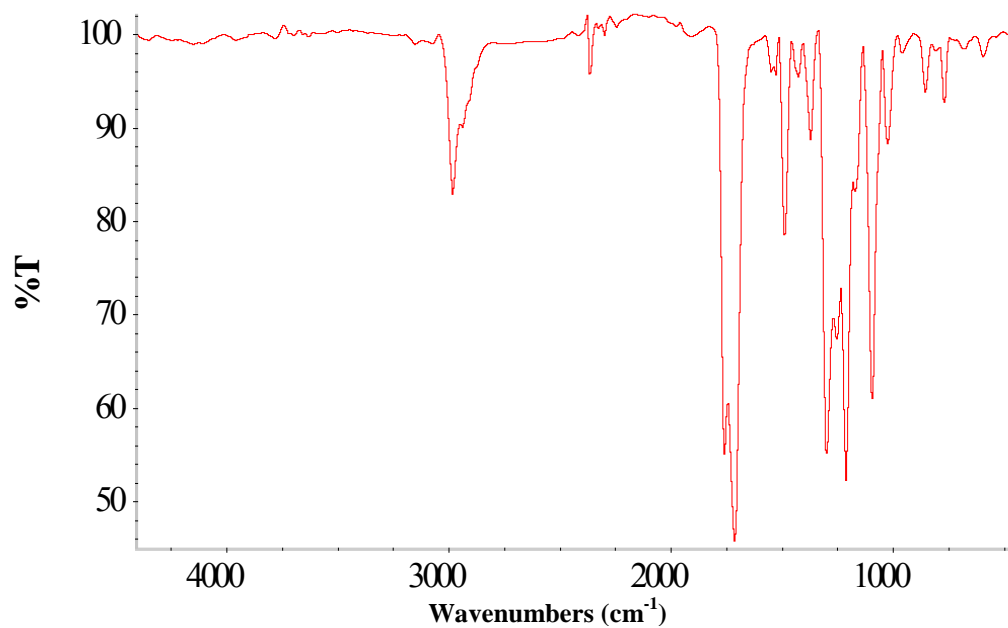
Figure A.29 IR spectrum of compound **16d**
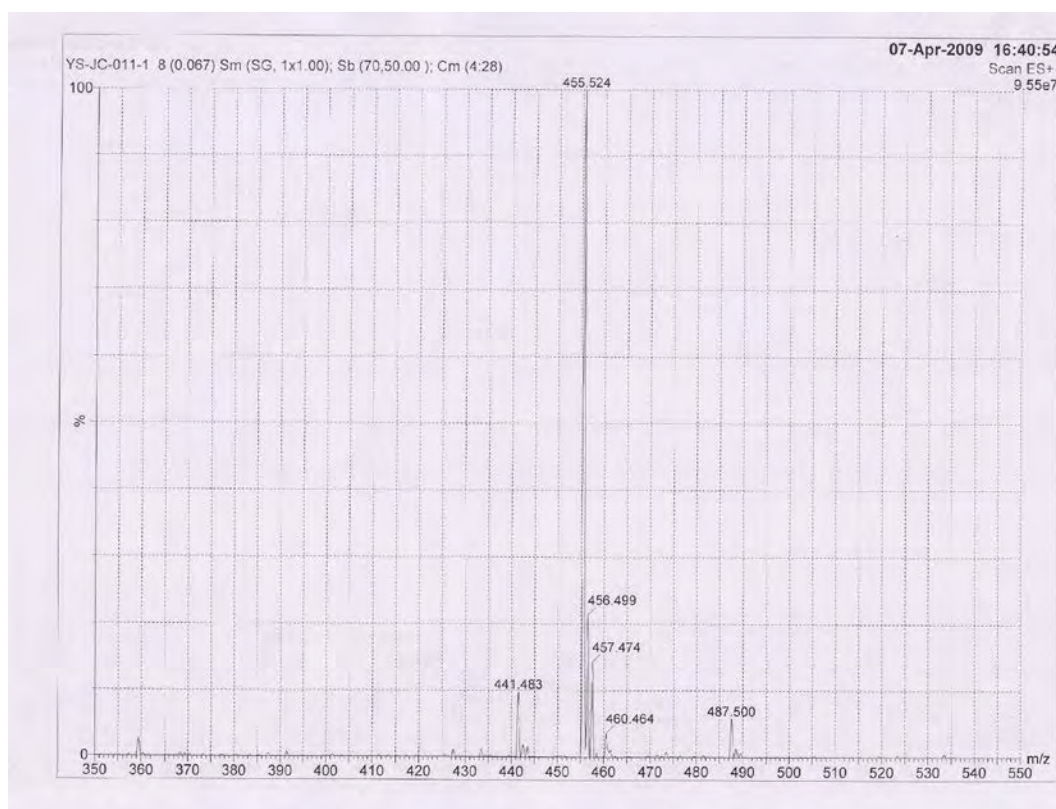
Figure A.30 Mass spectrum of compound **16d**

δ ppm

Figure A.31 ^{1}H-NMR (DMSO) spectrum of compound **19**

δ ppm

Figure A.32 ^{13}C-NMR (DMSO) spectrum of compound **19**

δ ppm

Figure A.33 ^{1}H-NMR (DMSO) spectrum of compound **20**

δ ppm

Figure A.34 ^{13}C-NMR (DMSO) spectrum of compound **20**

δ ppm

Figure A.35 ^{1}H-NMR (DMSO) spectrum of compound **17a**

δ ppm

Figure A.36 ^{13}C-NMR (DMSO) spectrum of compound **17a**

δ ppm

Figure A.37 ^{1}H-NMR (Acetone-d$_6$) spectrum of compound **17b**

δ ppm

Figure A.38 ^{13}C-NMR (Acetone-d$_6$) spectrum of compound **17b**
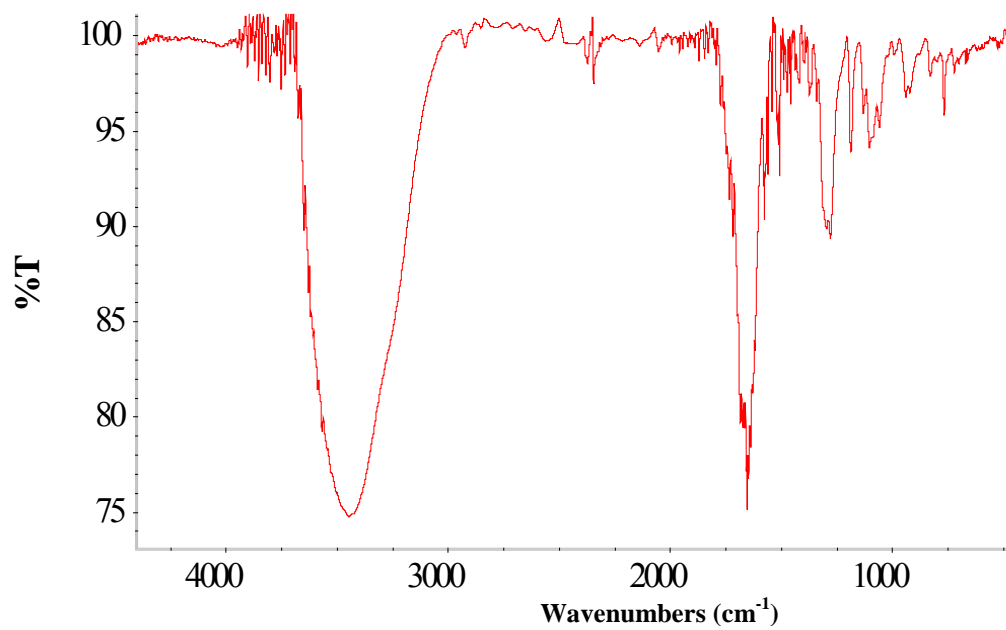
Figure A.39 IR spectrum of compound **17b**

δ ppm

Figure A.40 ^{1}H-NMR (Acetone-d$_6$) spectrum of compound **17d**

δ ppm
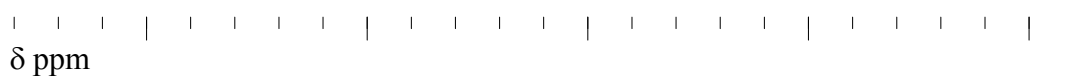
Figure A.41 ^{13}C-NMR (Acetone-d$_6$) spectrum of compound **17d**

δ ppm

Figure A.42 ^{1}H-NMR (CDCl$_3$) spectrum of EDOT **1**

δ ppm

Figure A.43 ^{13}C-NMR (CDCl$_3$) spectrum of EDOT **1**

δ ppm

Figure A.44 ^{1}H-NMR (CDCl$_3$) spectrum of compound **18b**

δ ppm

Figure A.45 ^{13}C-NMR (CDCl$_3$) spectrum of compound **18b**

δ ppm

Figure A.46 ^{1}H-NMR (CDCl$_3$) spectrum of dibenzyl tartrate **21**

δ ppm

Figure A.47 ^{13}C-NMR (CDCl[3]) spectrum of dibenzyl tartrate **21**
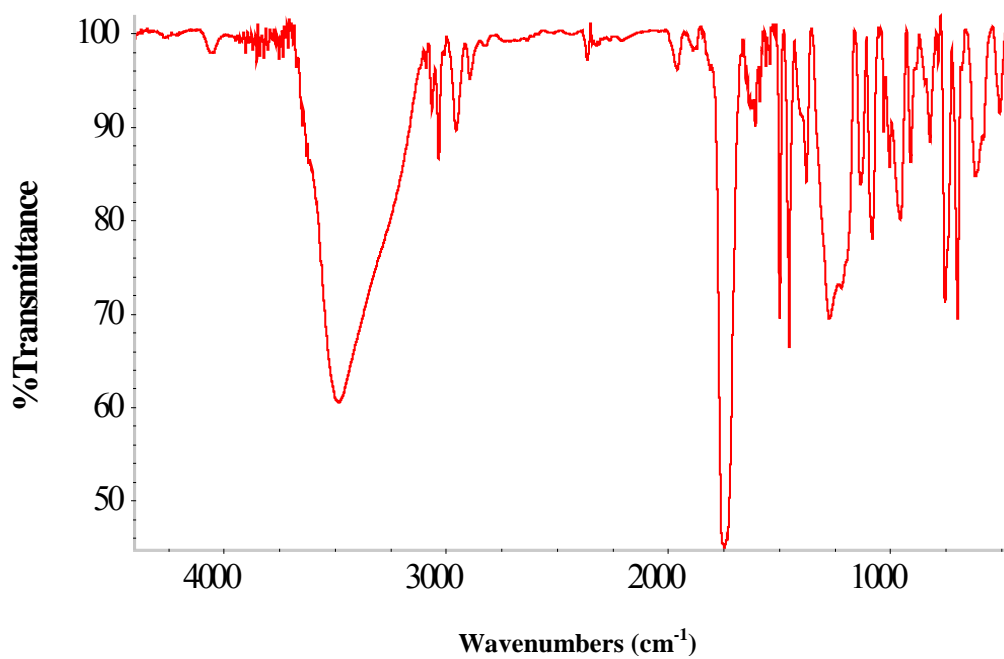
Figure A.48 IR spectrum of dibenzyl tartrate **21**

δ ppm

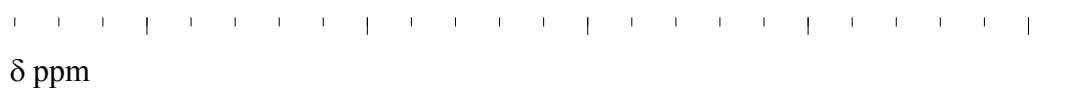**Figure A.49** ^{1}H-NMR (CDCl$_3$) spectrum of dibutyl tartrate **22**

δ ppm

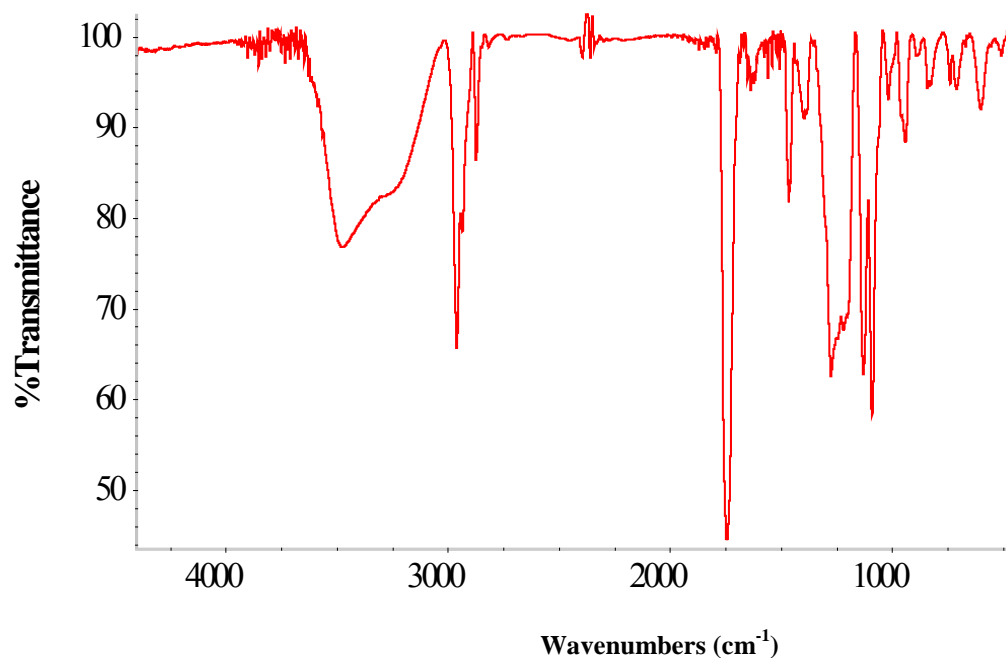**Figure A.50** ^{13}C-NMR (CDCl$_3$) spectrum of dibutyl tartrate **22**

Figure A.51 IR spectrum of dibutyl tartrate **22**

δ ppm

Figure A.52 ^{1}H-NMR (CDCl$_3$) spectrum of 3,4-dibutoxythiophene **23**

δ ppm

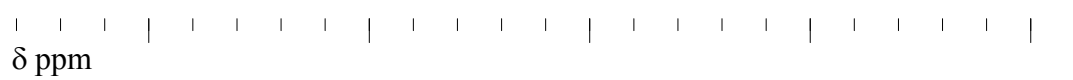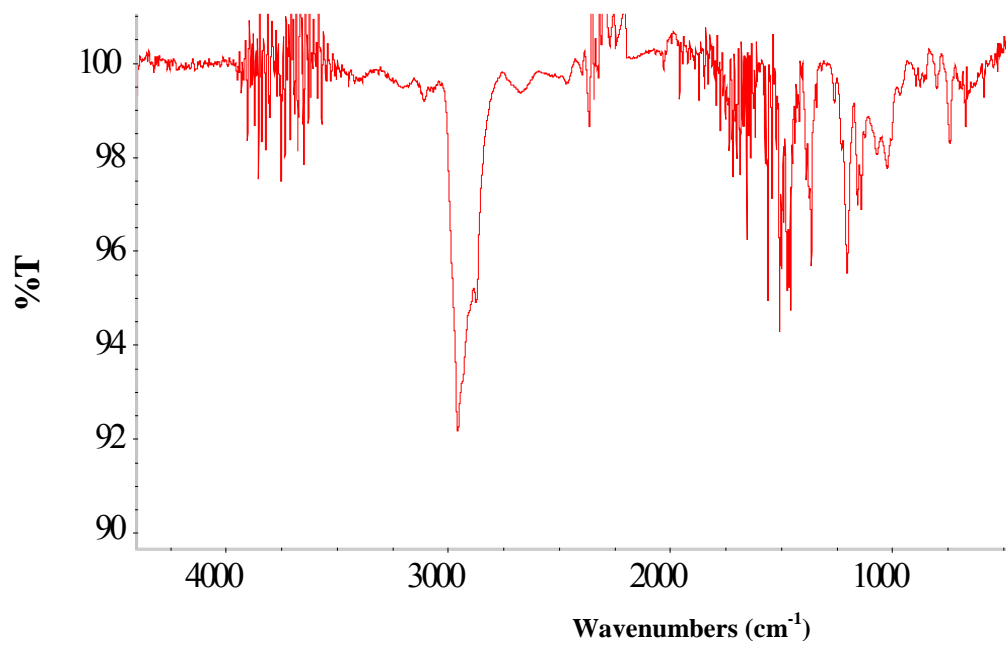**Figure A.53** ^{13}C-NMR (CDCl$_3$) spectrum of 3,4-dibutoxythiophene **23**

Figure A.54 IR spectrum of 3,4-dibutoxythiophene **23**

δ ppm

Figure A.55 ^{1}H-NMR (CDCl$_3$) spectrum of 3,4-dibutoxythiophene **24**

δ ppm

Figure A.56 ^{13}C-NMR (CDCl$_3$) spectrum of 3,4-dibutoxythiophene **24**

δ ppm

Figure A.57 ^{1}H-NMR (CDCl$_3$) spectrum of CDOT **25**

δ ppm

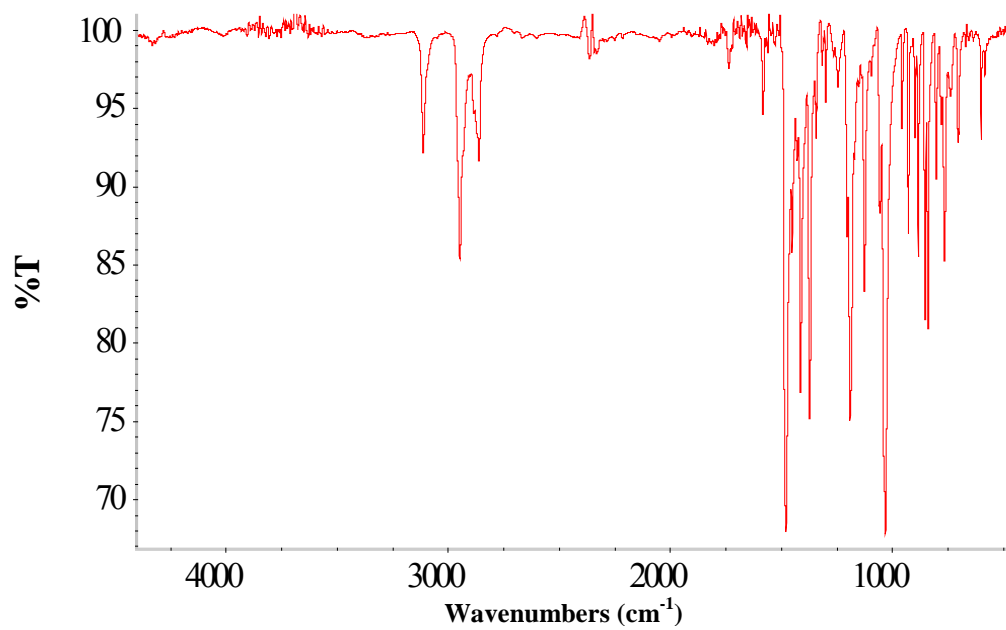**Figure A.58** ^{13}C-NMR (CDCl$_3$) spectrum of CDOT **25**

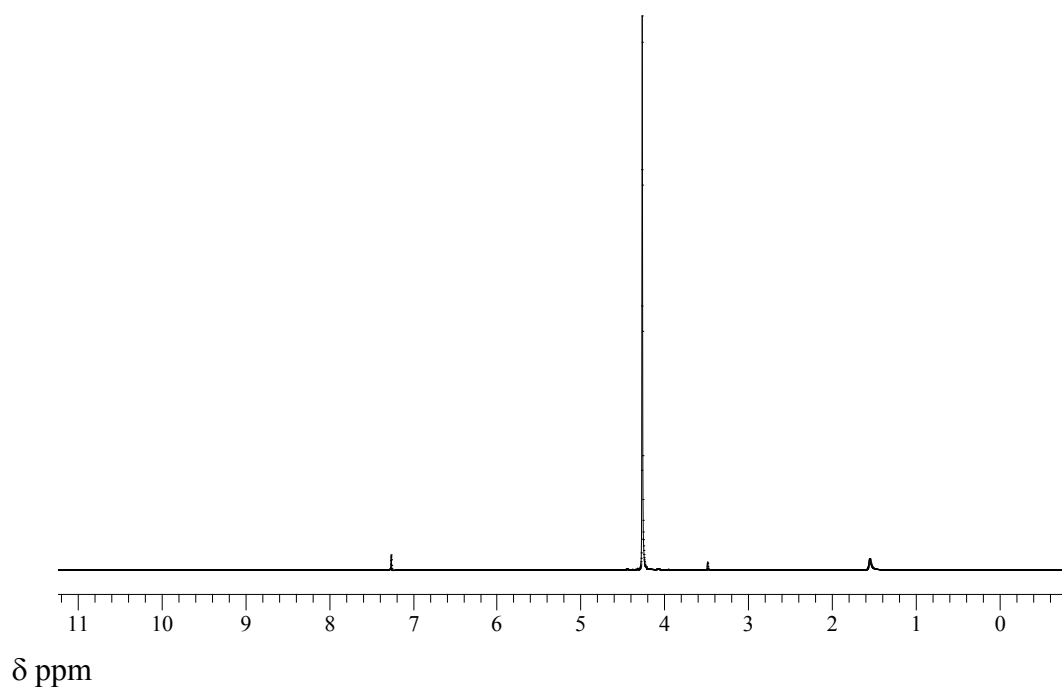**Figure A.59** IR spectrum of DBCOT **25**

δ ppm

Figure A.60 ^{1}H-NMR (CDCl$_3$) spectrum of DBEDOT **2**

δ ppm

Figure A.61 ^{13}C-NMR (CDCl$_3$) spectrum of DBEDOT **2**
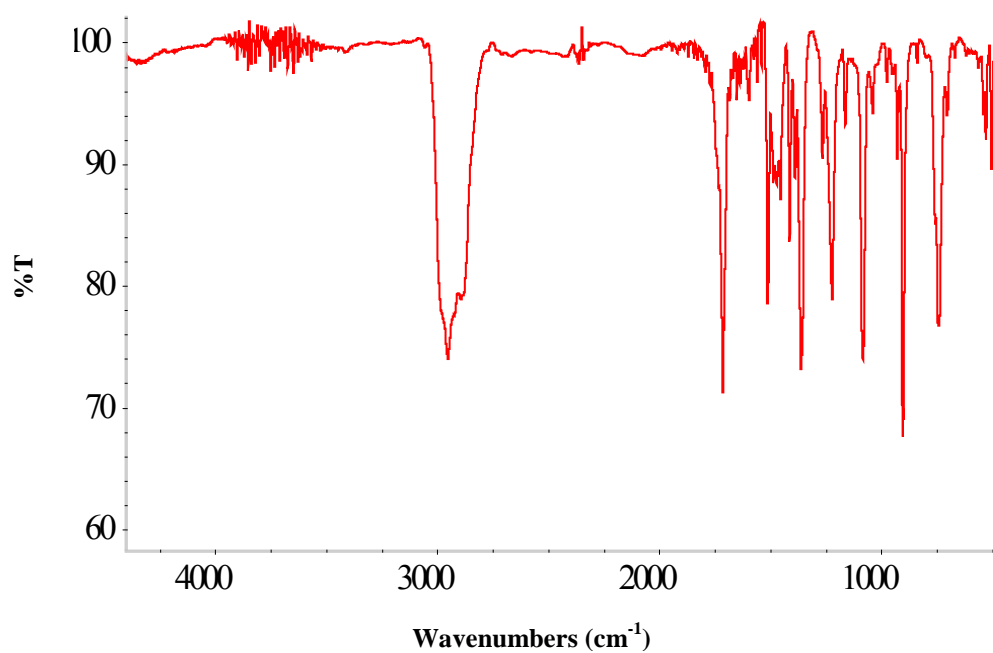
Figure A.62 IR spectrum of DBEDOT **2**
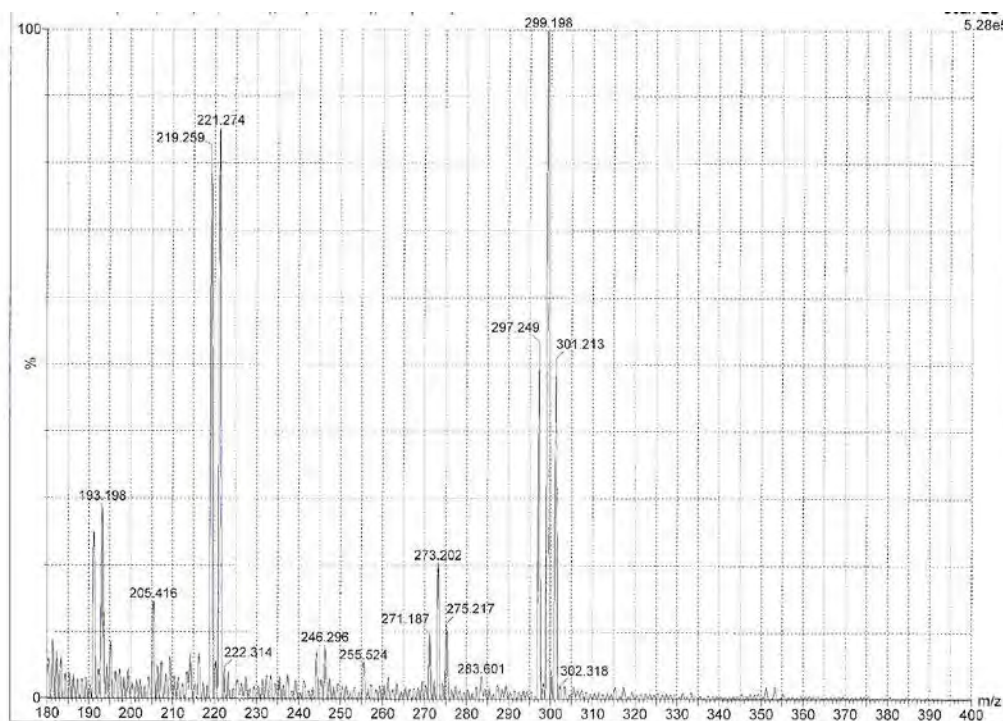
Figure A.63 Mass spectrum of DBEDOT **2**

δ ppm

Figure A.64 ^{1}H-NMR (CDCl$_3$) spectrum of DCEDOT **3**

δ ppm

Figure A.65 ^{13}C-NMR (CDCl$_3$) spectrum of DCEDOT **3**
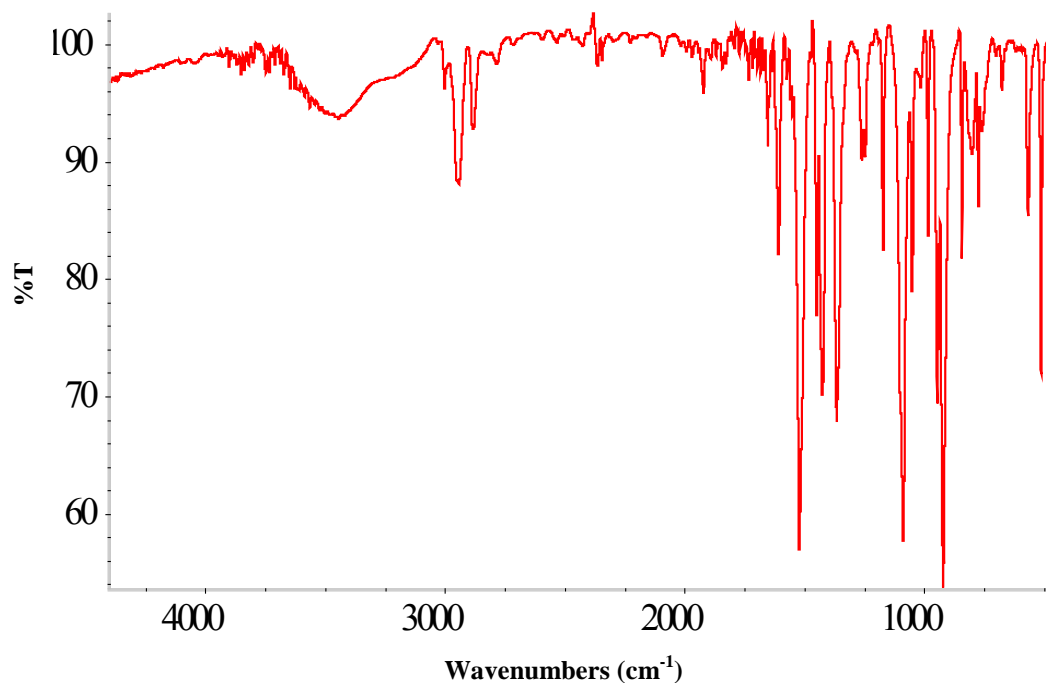
Figure A.66 IR spectrum of DCEDOT **3**
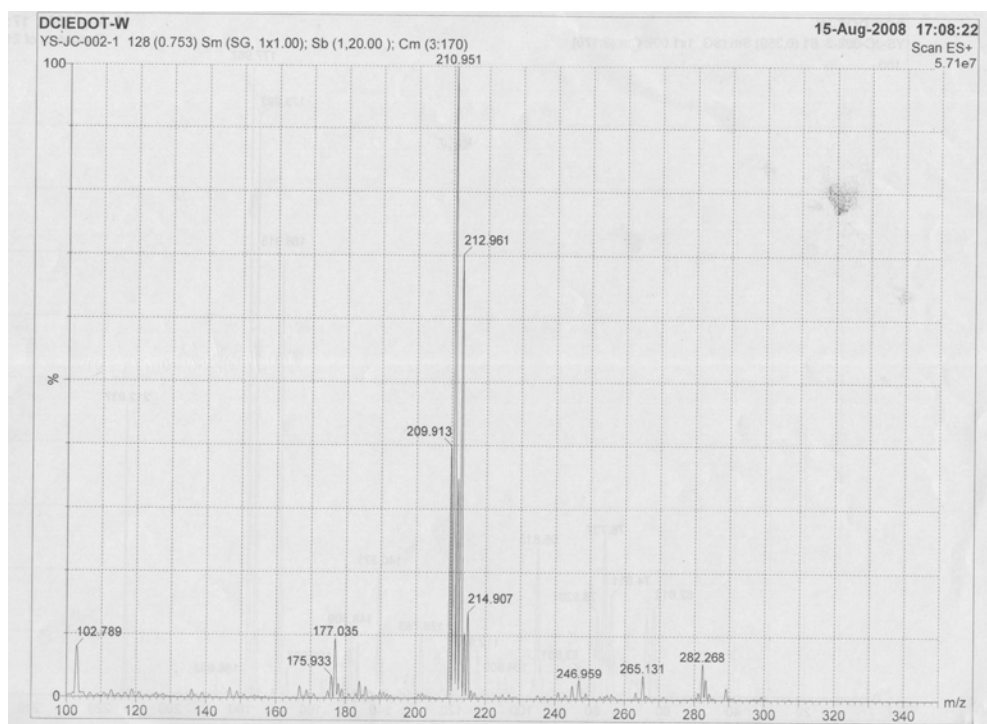
Figure A.67 Mass spectrum of DCEDOT **3**

δ ppm

Figure A.68 ^{1}H-NMR (CDCl[3]) spectrum of DBCDOT **26**

δ ppm

Figure A.69 ^{13}C-NMR (CDCl[3]) spectrum of DBCDOT **26**
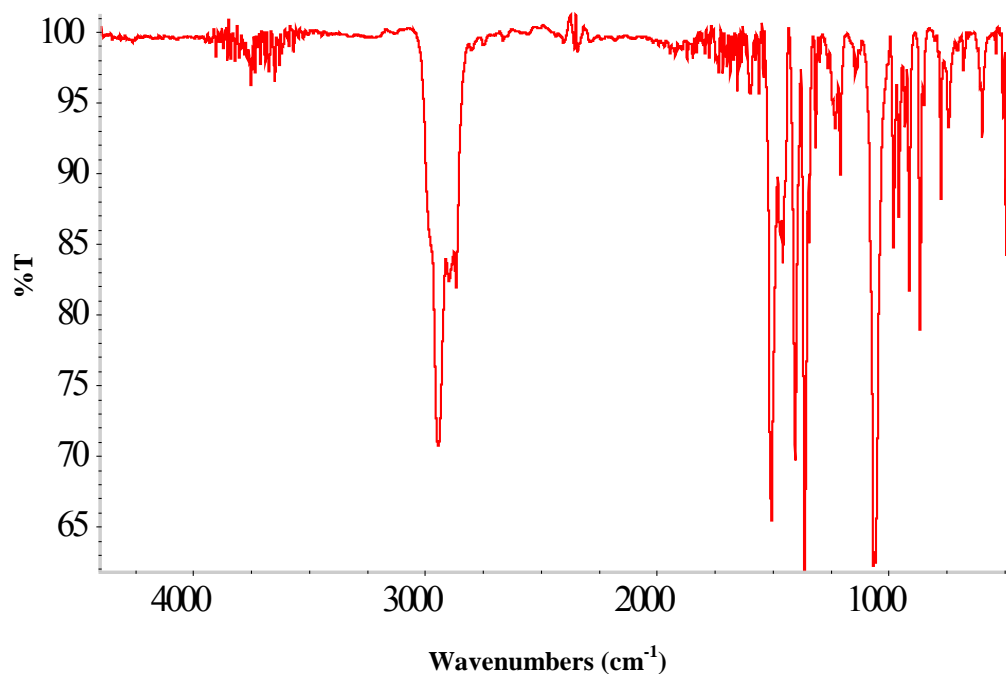
Figure A.70 IR spectrum of DBCDOT

δ ppm

Figure A.71 ^{1}H-NMR (CDCl$_3$) spectrum of DBCDOT **26**

δ ppm

Figure A.72 ^{13}C-NMR (CDCl$_3$) spectrum of DBCDOT **26**
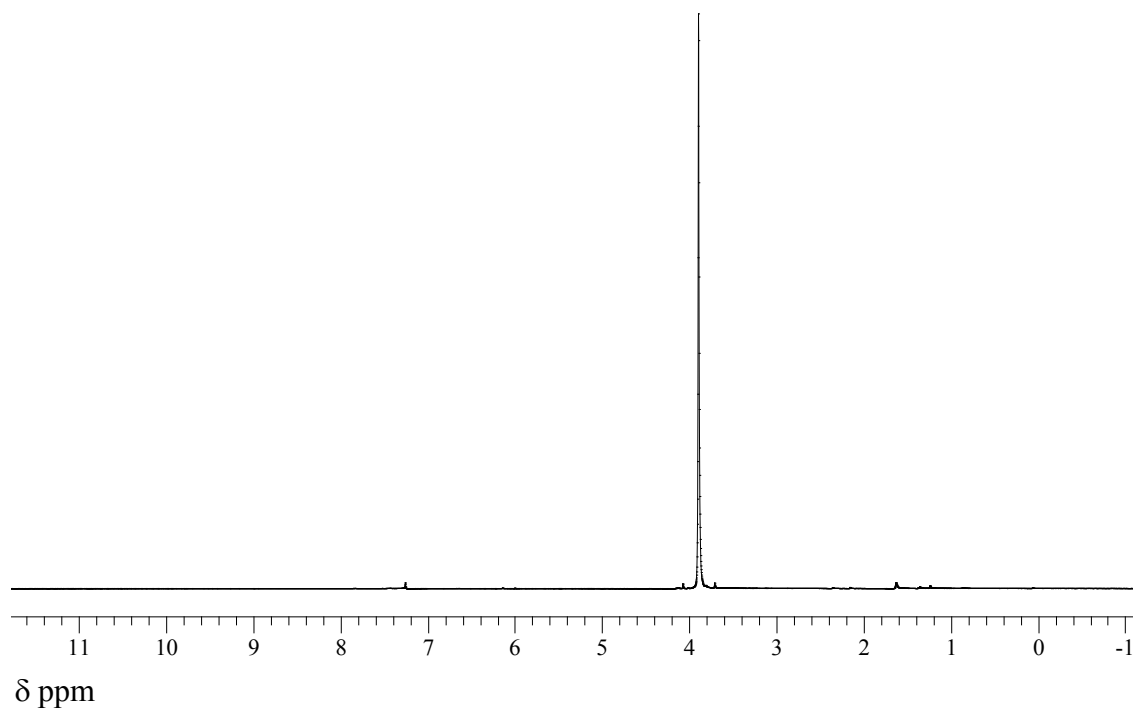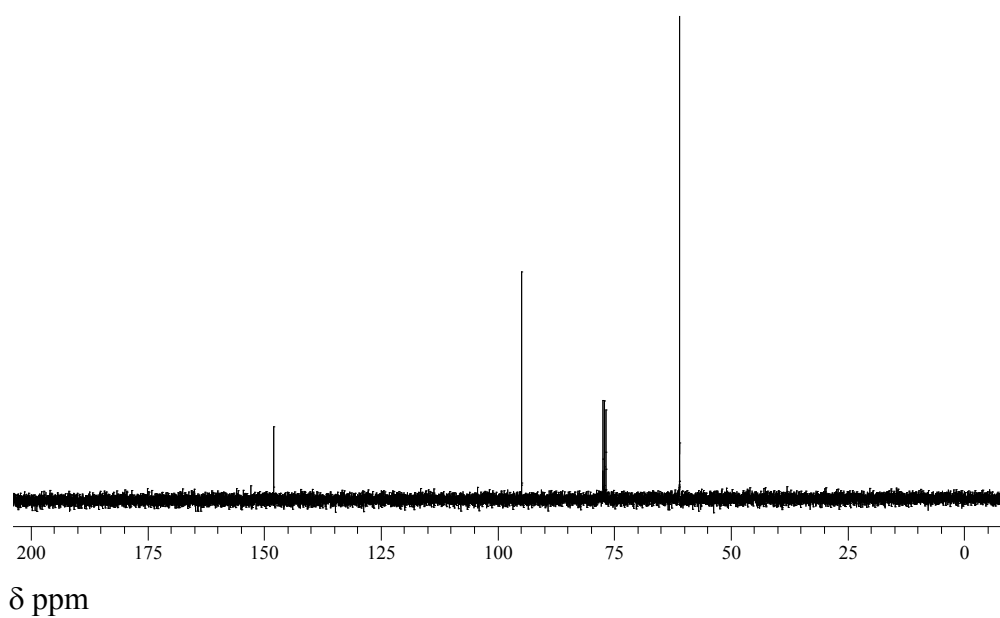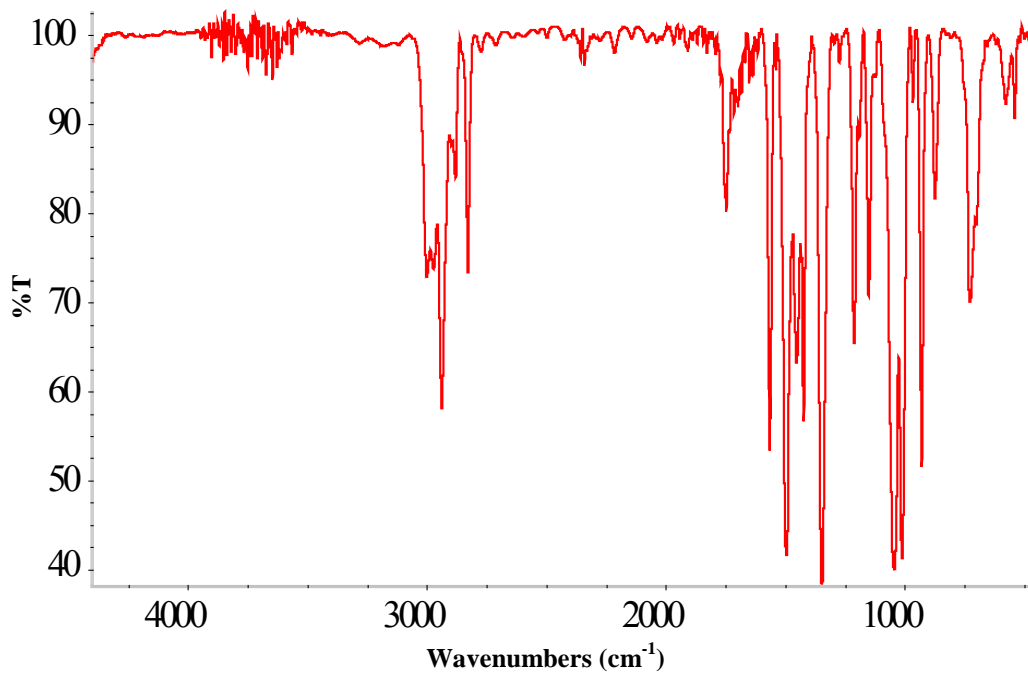
Figure A.73 IR spectrum of DBDMT **27**
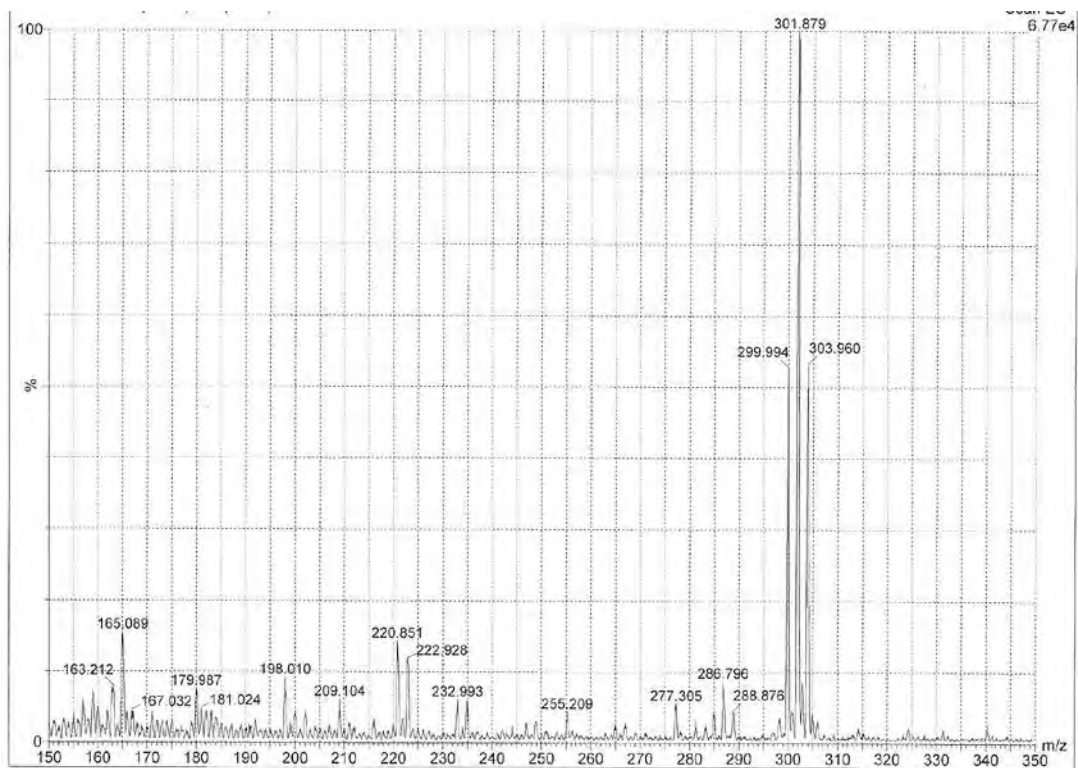
Figure A.76 Mass spectrum of DBDMT **27**

APPENDIX B

The Four-point Probe Method for Electrical Conductivity Measurement [85-87]

Four tiny electrodes are arranged in straight line separated at exactly equal distance (d) and touched the surface of the sample to be measured. Then the electrodes are further connected with an electrical circuit equipped with an Amp meter (A) and a Voltmeter (V) **(Figure B.1)** Contacts between the 4 electrodes and the sample surface must be equal. During the measurement, the current (I) is applied through electrode contact 1 to 4, and the potential difference (ΔV) across electrode contacts 2 and 3 is measured. The resistivity and conductivity of the sample can be calculated from the equation **B-1** and **B-2**, respectively.

The conductivity is determined by the equation below:

Resistivity ($\Omega \cdot cm$); $\rho = (\pi t/\ln 2)(V/I) = 4.53(R \cdot t)$…………………….**(B-1)**

Conductivity (S/cm) $\sigma = 1/\rho$…………………………………………….**(B-2)**

Where I is current (A)

V is voltage (volt)

R is resistant (Ω)

t is film thickness (cm)

Figure B.1 Conductivity measurement by Four-point probe method

I-V Graph

Figure B.2 Example of an I&V curve obtained from four point probe technique
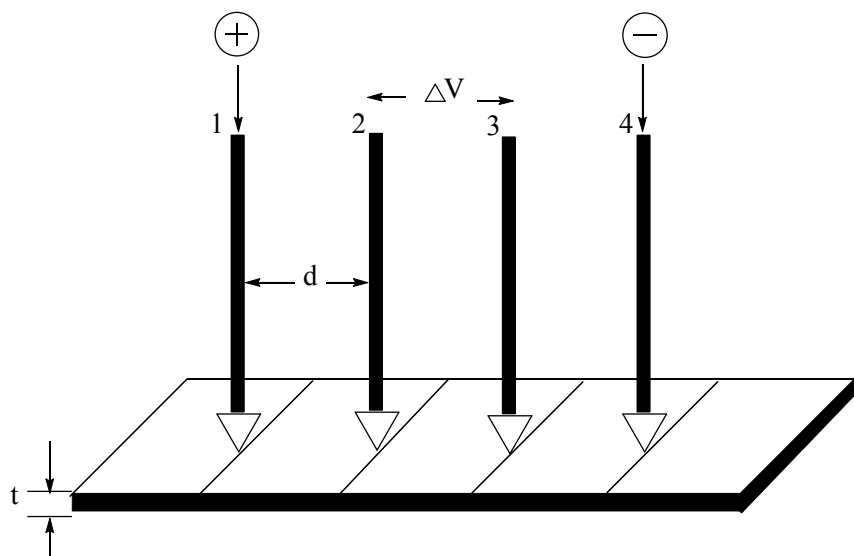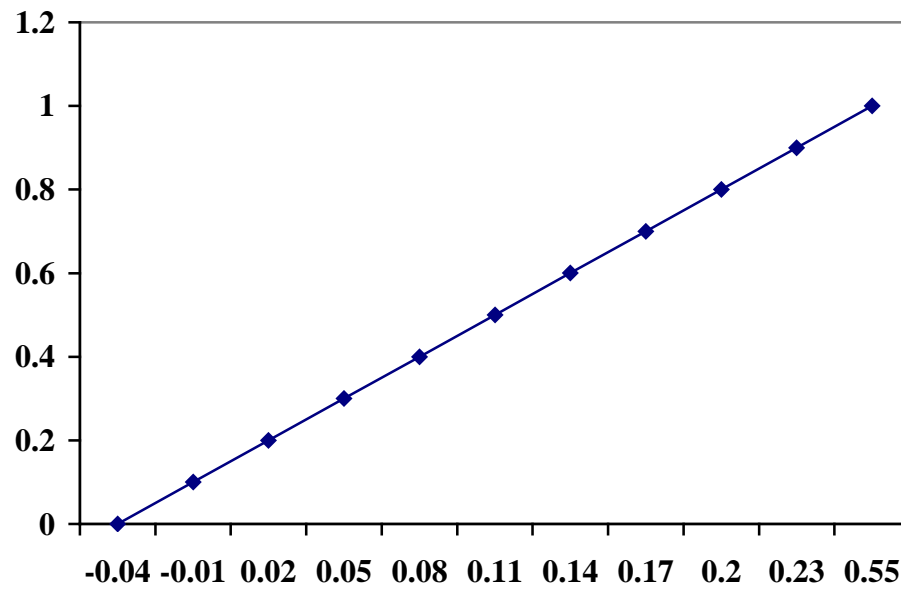
Table B.1 The calculations of PCDOT-conductivity [a]

Entry	Samples	t_{av} (cm)	R (Ω)	σ_{rt} (S/cm)	SD	%SD
1	FeCl$_3$-polymerized PCDOT as-synthesized	0.038	1.201×10^3	4.84×10^{-3}	0.24×10^{-3}	5.26
			1.288×10^3	4.51×10^{-3}		
			1.330×10^3	4.37×10^{-3}		
			Average	4.57×10^{-3}		
2	FeCl$_3$-polymerized PCDOT I$_2$ doped	0.039	2.727×10^2	2.08×10^{-2}	0.11×10^{-2}	5.75
			2.856×10^2	1.98×10^{-2}		
			3.059×10^2	1.85×10^{-2}		
			Average	1.97×10^{-2}		
3	FeCl$_3$-polymerized PCDOT as-synthesized and stored at RT for 2 weeks	0.066	4.643×10^3	0.720	0.038	5.40
			4.507×10^3	0.742		
			5.010×10^3	0.668		
			Average	0.710		
4	SSP- PCDOT heated at 70 °C: as-synthesized	0.024	1.222	7.53×10^{-3}	1.87×10^{-3}	19.9
			0.9755	9.43×10^{-3}		
			0.8158	11.3×10^{-3}		
			Average	9.41×10^{-3}		
5	SSP- PCDOT heated at 70 °C: I$_2$ doped	0.023	618.4	1.55×10^{-2}	0.26×10^{-2}	14.4
			464.6	2.07×10^{-2}		
			542.8	1.77×10^{-2}		
			Average	1.80×10^{-2}		

Table B.1 Continued

Entry	Samples	t_{av} (cm)	R (Ω)	σ_{rt} (S/cm)	SD	%SD
6	SSP- PCDOT heated at 70 ºC: as-synthesized and stored at RT for 2 weeks	0.018	11.22	1.09	0.191	21.5
			17.16	0.715		
			14.28	0.859		
			Average	0.889		
7	SSP- PCDOT heated at 100 ºC: as-synthesized	0.029	1.451	5.25	0.73	14.3
			1.339	5.69		
			1.784	4.27		
			Average	5.07		
8	SSP- PCDOT heated at 100 ºC: I_2 doped	0.025	0.7347	12.0	1.1	9.40
			0.8586	10.3		
			0.7192	12.3		
			Average	11.5		
9	SSP- PCDOT heated at 100 ºC: as-synthesized and stored at RT for 2 weeks	0.024	0.1379	66.7	12.1	22.1
			0.2164	42.5		
			0.1664	55.3		
			Average	54.8		
10	SSP- PCDOT heated at 120 ºC: as-synthesized	0.041	0.6357	8.47	0.59	7.38
			0.6489	8.30		
			0.7309	7.37		
			Average	8.04		

Table B.1 Continued

Entry	Samples	t_{av} (cm)	R (Ω)	σ_{rt} (S/cm)	SD	%SD
11	SSP- PCDOT heated at 120 ºC: I_2 doped	0.023	0.2426	39.6	4.0	9.94
			0.2126	45.1		
			0.2574	37.3		
			Average	40.7		
12	SSP- PCDOT heated at 120 ºC: as-synthesized and stored at rt for 2 weeks	0.041	3.340×10^{-2}	161	30	23.0
			4.161×10^{-2}	129		
			5.326×10^{-2}	101		
			Average	131		

[a] The measurements were carried out using current between 0.1-1 mA

t_{av} = thickness average

Table B.2 diffraction peaks of DBCDOT observed from XRD

No.	2θ	d(Å)	No.	2θ	d(Å)
1	9.443	9.3575	19	29.900	2.9858
2	10.839	8.1554	20	30.556	2.9232
3	15.444	5.7326	21	31.381	2.8482
4	16.284	5.4387	22	32.465	2.7556
5	18.001	4.9236	23	33.134	2.7015
6	18.920	4.6866	24	33.778	2.6514
7	19.507	4.5468	25	34.222	2.6180
8	21.102	4.2067	26	35.375	2.5353
9	21.792	4.0750	27	36.130	2.4840
10	22.518	3.9451	28	36.438	2.4637
11	23.151	3.8388	29	36.995	2,4279
12	23.902	3.7199	30	38.599	2.3306
13	25.055	3.5511	31	39.455	2.2820
14	25.738	3.4584	32	40.779	2.2109
15	26.785	3.3256	33	41.724	2.1630
16	27.420	3.2500	34	42.680	2.1167
17	28.342	3.1464	35	43.117	2.0963
18	29.428	3.0327	36	44.758	2.0231

¹H-NMR spectroscopy of PCDOT

The ^{1}H-NMR spectroscopic studied was perform the establish the structure of partial soluble polymer PCDOT (oligomer) from oxidative polymerization **(Figure B.3)**. The ^{1}H-NMR spectrum of PCDOT disappeared α-proton of thiophene and the other peaks showed broad signals.
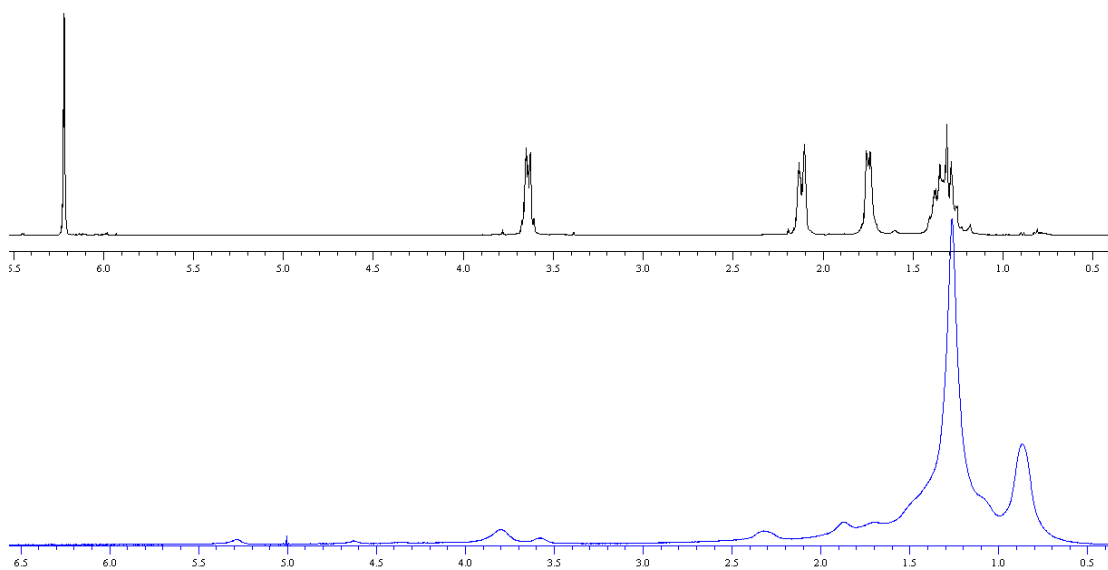

Figure B.3 ^{1}H-NMR spectra of (a) monomer **25** and (b) PCDOT partially soluble in CHCl$_3$ as prepared by FeCl$_3$ oxidation.
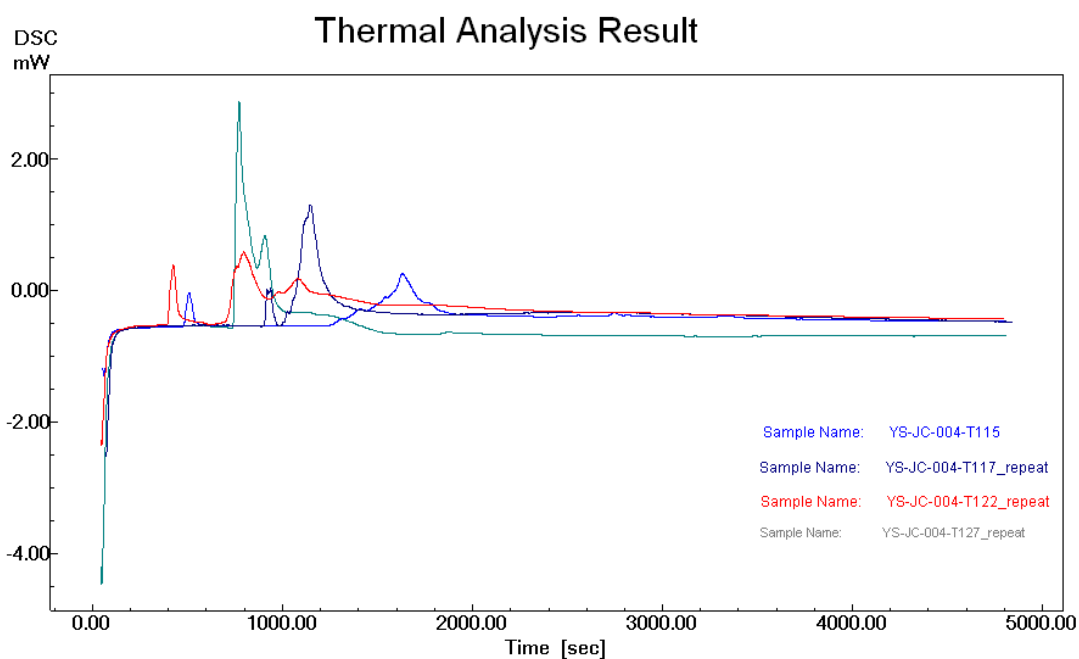
Figure B.4 Isothermal DSC curves of the DBCDOT crystals heated at different temperatures.
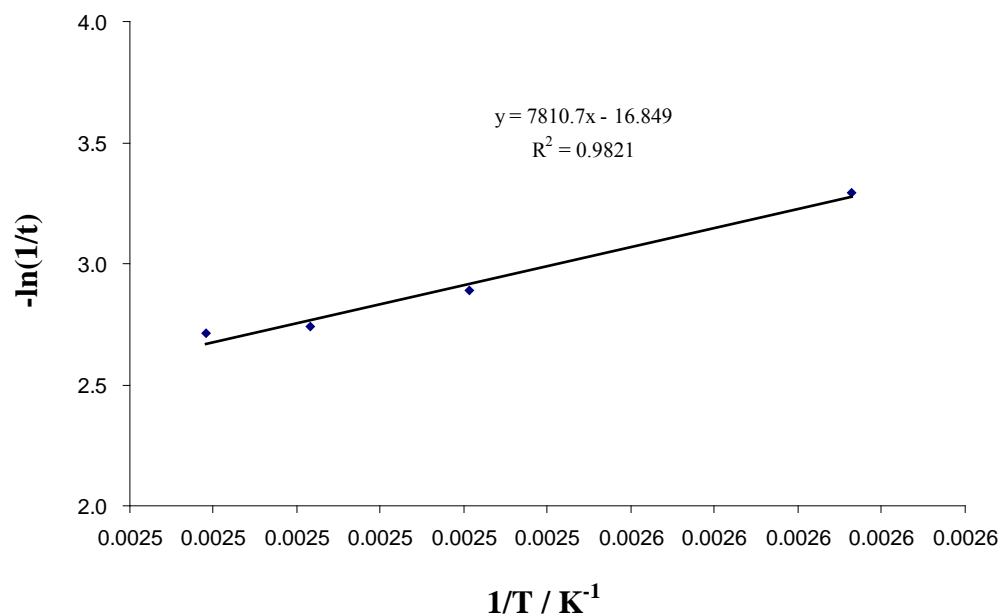

Figure B.5 Arrhenius dependence solid state polymerization of DBCDOT by DSC measurement.

VITA

Mr. Jirasak Chapromma was born on March 19, 1985 in Khonkaen, Thailand. He received a Bachelor,s degree of science from Department of Chemistry, Faculty of Science, Chulalongkorn University, Thailand in 2006. He was admitted to a Master's Degree Program in Chemistry, Faculty of Science, Chulalongkorn University and completed the program in 2009. His address is 281 Moo 6 , Tambol Tungluylai, Amphor Consan, Chaiyaphum 36180.